Dimethyl ether and diethyl ether for enhanced oil recovery from conventional and fractured reservoirs

Chahardowli, Mohammad

DOI
10.4233/uuid:4888c865-bf19-4132-a079-a87db6111916

Publication date
2016

Document Version
Final published version

Citation (APA)
Chahardowli, M. (2016). *Dimethyl ether and diethyl ether for enhanced oil recovery from conventional and fractured reservoirs*. [Dissertation (TU Delft), Delft University of Technology].
https://doi.org/10.4233/uuid:4888c865-bf19-4132-a079-a87db6111916

Important note
To cite this publication, please use the final published version (if applicable).
Please check the document version above.

Dimethyl Ether and Diethyl Ether for Enhanced Oil Recovery from Conventional and Fractured Reservoirs

Mohammad CHAHARDOWLI

ازدیاد برداشت نفت از مخازن شکافدار و غیر شکافدار با استفاده از دی متیل اتر و دی اتیل اتر

محمد چهاردولی

Dimethyl Ether and Diethyl Ether for Enhanced Oil Recovery from Conventional and Fractured Reservoirs

Proefschrift

ter verkrijging van de graad van doctor
aan de Technische Universiteit Delft,
op gezag van de Rector Magnificus prof. ir. K.C.A.M. Luyben,
voorzitter van het College voor Promoties,
in het openbaar te verdedigen op

woensdag 4 mei 2016 om 10.00 uur

door **Mohammad CHAHARDOWLI**

Master of Science in Reservoir Engineering
Sahand University of Technology, Iran
geboren te Malayer, Iran.

This dissertation has been approved by the
Promotor: Prof. dr. J. Bruining
Copromotor: Dr. ir. R. Farajzadeh

Composition of the doctoral committee:

Rector Magnificus,	chairman
Prof. dr. J. Bruining,	Delft University of Technology
Dr. ir. R. Farajzadeh,	Delft University of Technology

Independent members:

Prof. dr. R. Krastev	University of Reutlingen
Prof. dr. W. R. Rossen	Delft University of Technology
Prof. dr. P. L. J. Zitha	Delft University of Technology
Dr. D. Boersma	Shell Global Solutions International
Dr. H. Mahani	Shell Global Solutions International
Prof. dr. ir. E. C. Slob	Delft University of Technology, reserve member

Mohammad Chahardowli,
Dimethyl Ether and Diethyl Ether for Enhanced Oil Recovery from Conventional and Fractured Reservoirs,
Ph.D. Thesis Delft University of Technology,

Keywords: Chemical EOR, dimethyl ether, spontaneous imbibition, mobility control, hybrid EOR, polymer, partition coefficient, oil swelling, viscosity reduction, molecular diffusion, capillary imbibition, mutually soluble solvents, water-wet, mixed-wet.

The work described in this thesis was performed in the department of Geoscience and Engineering, Delft University of Technology, the Netherlands. This research was financially supported by the Ministry of Science, Research, and Technology, Iran; experiments were partly sponsored by Shell Global Solutions International. The last year financial support of this research was based on authors own budget.

Published and distributed by: Mohammad Chahardowli (chahardowli@gmail.com)

ISBN 978-94-6186-641-7
Cover design by M. Chahardowli, M. A. Najafi & S. Najafi

The clear eyes of the wise,
Beholds in every green tree, in every leaf;
A book of the wisdom of God.
Saadi (Persian poet), Diwan (Ghazal no. 296)

To تقدیم به

My parents, پدر و مادرم

My dear wife & my beloved daughter, همسر عزیز و دخترم

My sisters and brothers خواهران و برادرانم

Contents

Chapter

1

Introduction

1.1 World oil demand and supply

About 82% of the world's energy demand is supplied by fossil fuels [1]. The contribution of oil, according to World Energy Outlook 2015, is 32%(see Fig. 1.1) [2]. Oil production reached 92.1 Million barrels per day ($MMbbl/d$) by the end of 2014 [3]. In addition, the global oil demand shows an increasing trend, mostly due to the increasing demand in developing countries. The annual increase of the oil demand is expected to be 1.1 $MMbbl/d$ [2, 3]. Currently, there is a societal debate on the future contribution of fossil fuels, and we refer the interested reader to author MacKay, who gives a scope of renewable energies based on physical principles [4]. Nevertheless, a projection of the importance of the renewable energies is outside of the scope of this thesis.

However, the current view within the oil industry is that oil will continue to play an important role in the energy supply, which will be discussed below.

The chance of new oil discoveries is getting smaller, i.e. the discovery and development of new oil reservoirs will not be enough to supply the increasing global oil demand [5]. Therefore, an additional oil supply that can be obtained by enhanced oil recovery methods, may provide a possible alleviating effect.

1

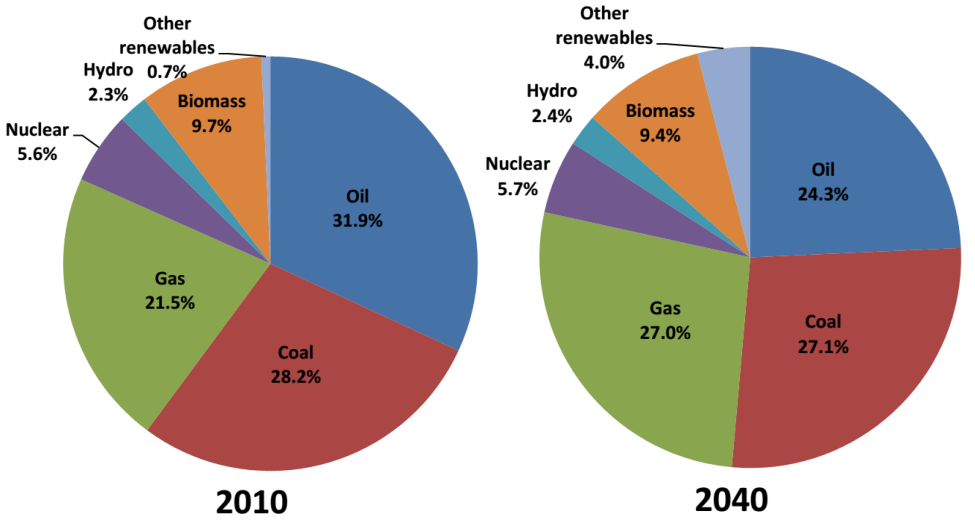

(a) (b)

Figure 1.1: World primary energy consumption, in (a) 2010, and (b) 2040 (expected) [1].

Enhanced oil recovery (EOR) seeks to extract the remaining oil left behind after primary (natural reservoir drive) and after secondary (e.g. water flooding) recovery methods, as conventional recovery methods. Conventional recovery to displace oil to the surface, depends on the properties of the oil, the rock, the aquifer and the gas cap. For instance, the recovery efficiency is typically $30-50\%$ of the oil initially in-place (see Fig. 1.2) [6]. Therefore, $70-50\%$ of the oil remains in the reservoir, which corresponds worldwide to approximately 2.0×10^{12} barrels of unproduced light and intermediate oil. In addition, approximately 5.0×10^{12} barrels of heavy oil are also left behind [7].

This residual or remaining light, medium and viscous oil, trapped by capillary forces is one target of EOR. Other mechanisms, that cause so much oil to be left behind in the reservoir, are the poor displacement efficiency and the poor sweep efficiency (bypassing). Both the sweep efficiency and the displacement efficiency are mainly affected by gravity forces and viscous forces. Bypassing is severely affected by the mobility ratio, defined by the ratio of the mobility of the displacing phase, divided by the mobility of the displaced phase ($M = \frac{\lambda_{water}}{\lambda_{oil}}$) [8].

In the so-called tertiary recovery method (EOR process), the reservoir is flooded by fluids like partially miscible gas, polymer solutions, surfactant solutions, steam, etc. In this stage, the improvement strategies are mainly focused on possible conditions that are considered conducive to a better oil recovery: the reduction of the water-oil interfacial tension, the reduction of the oil viscosity, the improvement of

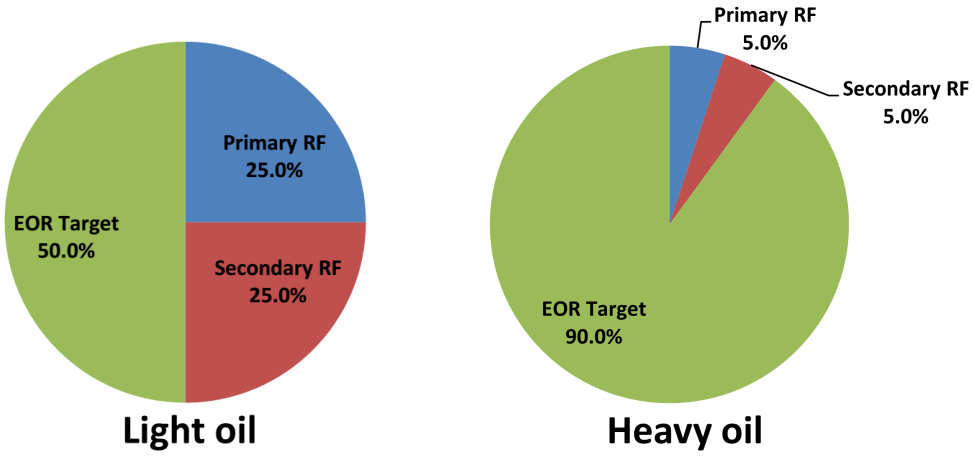

(a) (b)

Figure 1.2: (a) EOR target light oil. (b) EOR target heavy oil [6, 7].

the mobility ratio to obtain a better sweep efficiency, etc. Based on the selected strategy, EOR processes can be classified as (1) thermal EOR, e.g. steam injection or in-situ combustion, (2) (im)miscible gas EOR, e.g. CO_2, natural gas or N_2 injection, and (3) chemical EOR, e.g. polymer, DME injection, etc.; or, (4) other EOR (quaternary) methods like microbial, electrical, etc. Moreover, research for combined EOR processes, e.g. ASP, surfactant-polymer or thermal-(im)miscible gas get more attention. For reasons of easy reference, the worldwide EOR recovery rates and the number of commercial projects are given in Table 1.1 [6].

Table 1.1: The oil rate by EOR and the number of the commercial projects [6].

EOR class	EOR oil rate $Mbbl/d$	Projects
Thermal	2000	> 100
HC EOR	350	< 25
CO_2 EOR	350	> 100
Chemical EOR	350	< 5
Others	100	< 5

As to the cost, chemical EOR methods are classified as the most expensive. Only a limited number of commercial chemical EOR processes are performed at the field scale. However, the evaluations [9] show that chemical EOR is the fastest growing technology and is suitable for a large number of conventional or fractured reservoirs offshore and onshore.

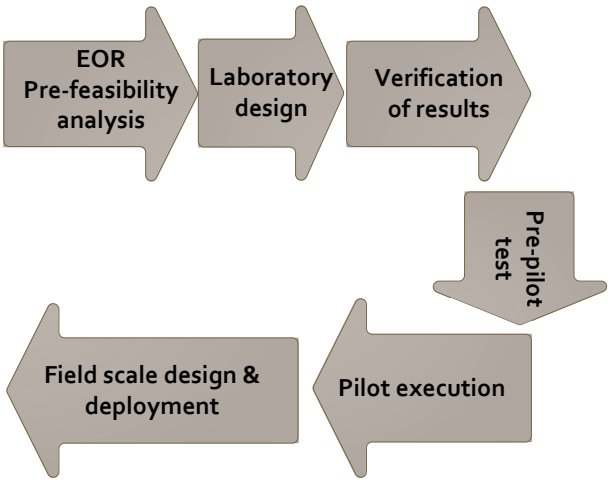

Figure 1.3: Usual necessary steps for EOR design [10].

To develop a successful EOR method, several necessary steps have to be followed, which are summarized in Fig. 1.3 [10]. The first step is to perform a pre-feasibility study. The second step is performing the laboratory tests, which is the focus of this study. The laboratory test will help to determine the technical feasibility. The next steps, i.e. the feasibility of the EOR process from the reservoir engineering point of view, the single well pilot tests and/or inter-well pilot tests and a full field application, are outside the scope of this study.
Mutually soluble solvents can enhance oil recovery. The most successful mutually soluble solvent to date is carbonated water [11–13]. Carbonated water (CW) is sometimes preferred over gaseous carbon dioxide injection, because CW has a higher viscosity. The more favorable viscosity ratio leads to a higher vertical and areal sweep efficiency [14]. Carbon dioxide only partially dissolves in brine (less at high salinities), but depending on its concentration in water, which depends on the pH, it can completely dissolve in brine. Another mutually soluble solvent is alcohol. Alcohols, e.g. isopropyl alcohol (IPA), partially dissolve in brine and partially dissolve in oil. In the Society of Petroleum Engineers (SPE) literature there is no research article describing the use of alcohols for enhanced oil recovery in a field application. To the best of our knowledge, there is very little published work on solvents with an intermediate boiling point, e.g. dimethyl ether (DME) and diethyl ether (DEE) [15–22]. Using DME as an EOR agent is a Shell proprietary technology [23]. DEE and DME are not in all proportions soluble in water, however, they mix in all proportions with oil. The application of DME and DEE as an EOR method can be classified as a mutually soluble solvent method (immiscible), which is a subset of

chemical EOR methods.
In summary, the advantage of ethers (especially DME) is that the solubility in the aqueous phase is higher than the solubility of carbon dioxide; therefore it is easier to transfer them to regions in sufficient quantities of unrecovered oil [15, 24]. Ethers are soluble in all proportions in oil. By releasing the pressure, it is possible to recover large amounts of ether at the end of the EOR process, both from the aqueous and the oleic phase. In this respect, ethers are more suitable than alcohols, because the high boiling point of alcohols makes it more difficult to recover the alcohols after the EOR process.
In this thesis the viability of DEE- and DME-enhanced oil recovery in conventional and in fractured reservoirs is experimentally tested in the laboratory. The results for fractured reservoirs are interpreted and can be used to suggest optimal conditions for enhanced recovery with DME and DEE.
In the next sections, we will describe the DME properties and availability, followed by the physical rationale behind the DME-enhanced oil recovery (DME-EOR). It is expected that DME-EOR is governed by the same mechanisms as DEE-enhanced oil (DEE-EOR). We performed DEE-EOR recovery experiments because they can be performed at atmospheric pressure as opposed to DME, which requires high pressure. We also performed experiments combining hydrolyzed polyacrylamide (HPAM) polymer with DME to optimize the enhanced oil recovery process.

1.2 DME properties and availability

During recent years, DME has been received attention as a new energy source. DME is the simplest ether with two methyl units connected to an oxygen atom. DME is in a gaseous state at atmospheric conditions, and can be liquefied by increasing the pressure ($> 5.1\ bar$) at ambient temperature, or cooling ($< -25^oC$) at atmospheric pressure. Furthermore, it has a low viscosity in the liquid state, a low density and a high solubility in water (17.6 $mol\%$) at room temperature and pressures above 5.1 $bars$ [25]. DME has a very low toxicity, has no effect on ozone depletion and does not form peroxides. In the case of spillage, it has a small environmental footprint [26, 27]. Moreover, the global warming potential (GWP) index of DME is one order of magnitude lower than of CO_2 [28]. These advantages of DME show its significant possibilities to be considered as a multi-source and multi-purpose chemical component [29].
DME is mostly manufactured in two ways: (1) dehydration of methanol and (2) direct synthesis. The facilities for the synthesis of methanol from coal gasification plants can be converted to DME manufacturing facilities by adding a dehydration step to the methanol plant. This method is the most efficient way of manufacturing DME in large quantities [30]. The chemical reaction is shown below.
$2CO + 4H_2 \rightarrow 2CH_3OH$ (methanol synthesis)

1

$2CH_3OH \rightarrow CH_3OCH_3 + H_2O$ (Hydration)
Consequently, the DME price is a function of the methanol price, which is assumed to be stable [31]. The largest DME producers are China, Japan, Tobago, North America, Indonesia; Uzbekistan has recently installed plants to produce DME, while Sweden has installed the first bio-DME plant [31].
Considering storage and transportation, DME is easier to store and to transport in comparison to LPG and LNG. In addition, with small improvements, the existing LPG technologies are usable for DME transport. Therefore, the development of the transportation and the injection technology of DME can benefit from the existing infrastructure [32].

1.3 The basics of DEE- and DME-enhanced oil recovery

The remaining oil appears in the form of disconnected oil ganglia [33], or, in regions non-invaded by the displacing fluids (areal and vertical sweep efficiency), in porous media. With the injection of the aqueous phase, e.g. DME (DEE)/brine or DME/polymer, DME (DEE) partitions between the aqueous phase and the oleic phase. It is proposed to inject DME (DEE) in the form of slugs of dissolved DME (DEE) in brine or polymer. With the displacement of DME (DEE)-assisted flooding into the pore space and the partitioning of DME (DEE) in the oleic phase, DME (DEE) dilutes (swells) the oil and lowers the oil viscosity [15]. The DME (DEE)-rich oil is displaced towards the producing well by a polymer (brine) chase phase injection (see Fig. 1.4).
DME (DEE)-EOR in fractured reservoirs. One of the main recovery mechanisms in fractured reservoirs is spontaneous imbibition. In reservoirs with low permeable matrix blocks, oil-wet matrix blocks and highly viscous oils, the transfer rate between fractures and matrix by spontaneous imbibition is slow, and, consequently, the amount of oil remaining behind is considerable. Literature data are inconclusive whether DME and DEE can accelerate or enhance the matrix-fracture transfer rate as well as reduce the amount of residual oil in the matrix [15]. It is expected that laboratory experiments can elucidate the relevant mechanisms.
Mobility control of DME-enhanced water flooding. In the presence of large-scale heterogeneities in the reservoir, or in the case of a high mobility ratio, i.e. $M \geq 5$, the displacement efficiency is low and large amounts of oil are left unproduced in the reservoir [34]. Therefore, performing DME/polymer flooding could improve the displacement efficiency by lowering the mobility ratio [8, 34]. DME lowers the viscosity of the oleic phase, which further lowers the mobility ratio. Moreover, DME dilutes the oil (swelling effect) and therefore it contributes to the reduction of the residual oil.

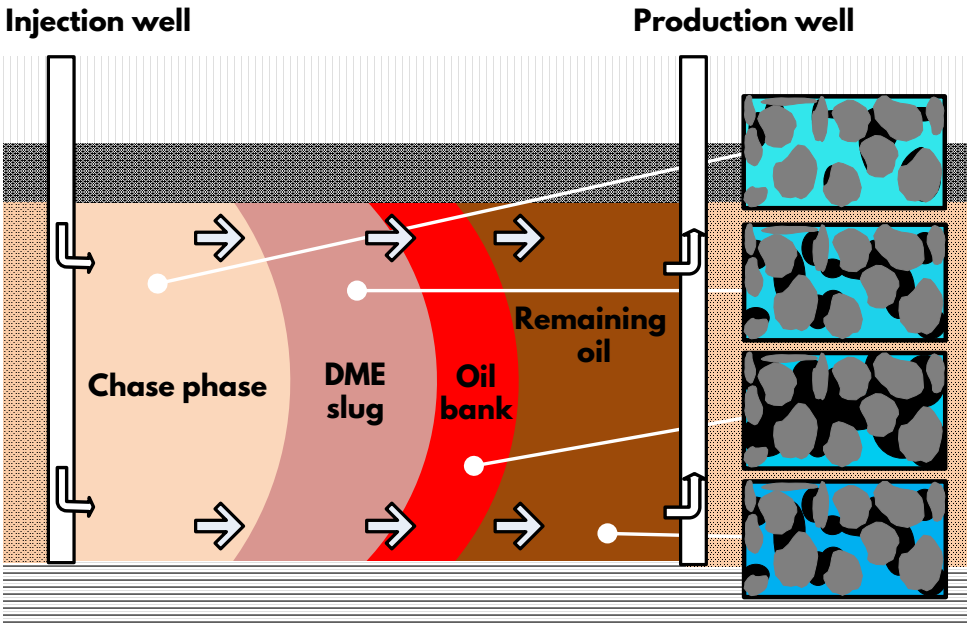

Figure 1.4: Schematics of DME-enhanced EOR.

1.4 Objectives of the thesis

The principal objective of this thesis is to obtain more insight in oil recovery by mutually soluble solvents, especially dimethyl ether (DME). The main research question is how does DME (DEE) enhance the oil recovery from conventional and fractured reservoirs? In order to answer the research question, we performed systematic bulk and porous media laboratory studies. The objectives of this thesis are as follows:

- To obtain experimental values for the partition coefficient of a few mutually soluble solvents, and to quantify the effect of the initial solvent concentration, of the presence of salt, and of the oil type on the partition coefficient for different aqueous/oleic systems.
- To demonstrate the potential of DME and DEE to improve oil recovery from sandstone and carbonate rocks. To find experimental evidence whether DME and DEE can enhance the spontaneous imbibition process.
- To describe and to understand the oil recovery enhancement mechanisms in the spontaneous imbibition of DME/brine (DEE/brine) into a single oil-filled matrix by numerical modeling.

- To develop mobility control experiments for DME-enhanced water flooding in the laboratory.

1.5 Outline of the thesis

This thesis is based on four inter-related experimental and numerical research papers using ethers as mutually soluble solvents for EOR that we completed at the TU Delft.
Chapter 2 presents an experimental study to obtain the partition coefficient of diethyl ether (DEE) and tetrahydrofuran (THF) in brine/oil and in water/oil systems. The chapter investigates the effect of the presence of salt, solvent concentration and model oil type (hexadecane, Ondina 919 and Ondina 933) on the partition coefficient of THF and DEE between the oleic and the aqueous phases. The results of this study were used for the estimation of the order of magnitude of the partition coefficient used in the simulations in chapter 3 to interpret DEE/brine spontaneous imbibition experiments. The experiments were conducted in Amott cells, where both oil saturated mixed-wet (aged) Berea and water-wet Berea cores and oil saturated mixed-wet (aged) dolomite cores were exposed to brine (3 w/w% NaCl in demi-water) with or without 7 v/v% DEE. The recovery factor and the recovery rate were monitored by reading the measuring tube that was mounted on top of the Amott cell. Afterwards, we combined mass conservation of the components and Darcy's law with a simplified (constant partition coefficient) phase behavior of the DEE-brine-crude oil system to develop a numerical model for DEE/brine spontaneous imbibition. Comparison between the experimental and numerical results shows which mechanisms are responsible for the oil recovery. Based on the results of this chapter, we designed the experimental and the numerical studies for chapter 4. Chapter 4 describes the enhancement of oil recovery by spontaneous imbibition by adding dimethyl ether (DME) to the imbibing brine. We designed a high pressure modified Amott cell to be able to study the effect of liquid DME. In this study, we tested compatibility of brine solutions and DME as well as the mixing procedure. We also investigated the compatibility of DME with the material used in the modified Amott cell and in transport vessels. Then, we carried out two-stage spontaneous imbibition experiments with brine and with DME/brine mixtures in water-wet and in mixed-wet cores. We adapted our numerical model to interpret DME/brine spontaneous imbibition experiments. These experiments and the comparison to numerical simulations gave us more insight for the design and the execution of mobility control of DME-enhanced water flooding experiments in chapter 5. This chapter investigates the improvements of recovery of intermediate viscous oil in core flooding experiments (non-fractured cores) by adding DME and polymer to the displacing aqueous phase. For this we used co-injection of a mixture of 10 ± 0.2 mol% DME in a polymer solution of 1500 ppm HPAM in brine (3 w/w%). The enhancement of the oil recovery by the displacement of the

injected DME/brine or DME/polymer slug by chase polymer or chase brine was also studied. The thesis will end with the main conclusions in chapter 6.

Bibliography

[1] British Petroleum, "BP Statistical Review of World Energy 2015," available at http://on.bp.com/1ScHRK8.

[2] OPEC, "World Oil Outlook 2015," available at http://bit.ly/1moJatT.

[3] IEA, "World energy outlook special report 2015: Energy and climate change," available at http://bit.ly/1fJIufF.

[4] D. MacKay, *Sustainable Energy-Without the Hot Air*. UIT Cambridge, 2008.

[5] V. Alvarado and E. Manrique, "Enhanced Oil Recovery: an Update Review," *Energies*, vol. 3, no. 9, pp. 1529–1575, 2010.

[6] S. Kokal and A. Al-Kaabi, "Enhanced Oil Recovery: Challenges & Opportunities," *World Petroleum Council: Official Publication*, pp. 64–68, 2010.

[7] S. Thomas, "Enhanced Oil Recovery-an Overview," *Oil & Gas Science and Technology-Revue de l'IFP*, vol. 63, no. 1, pp. 9–19, 2008.

[8] L. W. Lake, R. Johns, B. Rossen, and G. Pope, *Fundamentals of Enhanced Oil Recovery*. Society of Petroleum Engineers, 2014.

[9] "Enhanced Oil Recovery Market by Technology (Thermal, Gas, Chemical, Microbial and Seismic) and by Applications (Onshore and Offshore) - Global Trend & Forecast to 2019," http://prn.to/1S1yOib, accessed: 11-Feb.-2015.

[10] A. Satter, J. E. Varnon, and M. T. Hoang, "Integrated Reservoir Management," *Journal of Petroleum Technology*, vol. 46, no. 12, pp. 1–057, 1994.

[11] R. Christensen, "Carbonated Waterflood Results–Texas and Oklahoma," in *Annual Meeting of Rocky Mountain Petroleum Engineers of AIME*. Society of Petroleum Engineers, 1961.

[12] H. Ramsay Jr, "Case Histories of Carbonated Waterfloods in Dewey-Bartlesville Field," in *SPE Secondary Recovery Symposium*. Society of Petroleum Engineers, May, 1962.

[13] J. Scott, and C. Forrester, "Performance of Domes Unit Carbonated Waterflood-First Stage," *Journal of Petroleum Technology*, vol. 17, no. 12, pp. 1–379, 1965.

[14] M. Sohrabi and A. Emadi, "Novel Insights into the Pore-Scale Mechanisms of Enhanced Oil Recovery by CO_2 Injection," in *Proceedings of SPE Europec/EAGE Annual Conference*, Society of Petroleum Engineers, jun 2012.

[15] M. Chahardowli, A. Zholdybayeva, R. Farajzadeh, and H. Bruining, "Solvent-enhanced Spontaneous Imbibition in Fractured Reservoirs," in *Proceedings of 75th EAGE Conference & Exhibition incorporating SPE EUROPEC 2013*. Society of Petroleum Engineers, Jul. 2013.

[16] M. Chahardowli, R. Farajzadeh, and H. Bruining, "Numerical Simulation of Mutually Soluble Solvent-Aided Spontaneous Imbibition in Fractured Reservoirs," in *14th European Conference on the Mathematics of Oil Recovery*, Catania, Sep. 2014.

[17] A. Chernetsky, S. Masalmeh, D. Eikmans, P. D. Boerrigter, C. Parsons, A. Parker, D. Boersma, J. Cui, B. Dindoruk, P. te Riele, A. Kindi, and N. Azri, "Experimental Results and Modelling Workflow of the DME Enhanced Waterflood Technology," in *The Abu Dhabi International Petroleum Exhibition and Conference, ADIPEC*. Society of Petroleum Engineers, 2015.

[18] M. Chahardowli, R. Farajzadeh, and H. Bruining, "Experimental Investigation of the Use of the Dimethyl Ether/Polymer Hybrid as a Novel Enhanced Oil Recovery Method," *submitted to Journal of Industrial and Engineering Chemistry*.

[19] M. Chahardowli, R. Farajzadeh, and H. Bruining, "Experimental Investigation of the Use of Dimethyl Ether/Polymer Hybrid as an Enhanced Oil Recovery Method," in *SPE EOR Conference at Oil and Gas West Asia*, 2016.

[20] J. Groot, A. Chernetsky, P. Te Riele, B. Dindoruk, J. Cui, L. Wilson, and R. Ratnakar, "Representation of Phase Behavior and PVT Workflow for DME Enhanced Water-Flooding," in *SPE EOR Conference at Oil and Gas West Asia*. Society of Petroleum Engineers, 2016.

[21] P. t. Riele, C. Parsons, P. Boerrigter, J. Plantenberg, B. Suijkerbuijk, J. Burggraaf, A. Chernetsky, D. Boersma, and R. Broos, "Implementing a Water Soluble Solvent Based Enhanced Oil Recovery Technology-Aspects of Field Development Planning," in *SPE EOR Conference at Oil and Gas West Asia*. Society of Petroleum Engineers, 2016.

[22] A. Alkindi, N. Al-Azri, D. Said, K. AlShuaili, and P. Te Riele, "Persistence in EOR-Design of a Field Trial in a Carbonate Reservoir Using Solvent-Based Water-Flood Process," in *SPE EOR Conference at Oil and Gas West Asia*. Society of Petroleum Engineers, 2016.

[23] C. Blom, R. Hedden, A. Matzakos, and E. Uehara-Nagamine, "Oil Recovery Process," Jun. 27 2013, wO Patent App. PCT/US2012/070,093.

[24] Z. Duan and R. Sun, "An improved Model Calculating CO_2 Solubility in Pure Water and Aqueous NaCl Solutions from 273 to 533 K and from 0 to 2000 bar," *Chemical geology*, vol. 193, no. 3, pp. 257–271, 2003.

[25] K. Fujimoto and Y. Ohno, "DME Handbook," in *Japan DME Forum, Ohmsha, Tokyo*, 2007.

[26] T. Fleisch, A. Basu, M. Gradassi, and J. Masin, "Dimethyl Ether: a Fuel for the 21st Century," *studies in surface science and catalysis*, vol. 107, pp. 117–125, 1997.

[27] T. a. Semelsberger, R. L. Borup, and H. L. Greene, "Dimethyl Ether (DME) as an Alternative Fuel," *Journal of Power Sources*, vol. 156, pp. 497–511, 2006.

[28] D. A. Lashof and D. R. Ahuja, "Relative Contributions of Greenhouse Gas Emissions to Global Warming," *Nature Publishing Group*, 1990.

[29] H. Erdener, A. Arinan, and S. Orman, "Future Fossil Fuel Alternative; Dimethyl Ether (DME) a Review," *Int. J. Ren. Ener. Res*, vol. 1, no. 4, pp. 252–258, 2011.

[30] T. H. Fleisch, a. Basu, and R. a. Sills, "Introduction and Advancement of a New Clean Global Fuel: The Status of DME Developments in China and Beyond," *Journal of Natural Gas Science and Engineering*, vol. 9, pp. 94–107, 2012.

[31] "Where is DME Being Produced?" available at http://www.aboutdme.org/index.asp?sid=97.

[32] I. M. Sivebaek and J. r. Jakobsen, "The Effect of Gasses on the Viscosity of Dimethyl Ether," *Tribology International*, vol. 41, pp. 839–843, 2008.

[33] F. Dullien, *Porous Media: Fluid Transport and Pore Structure*. Academic Press, 1979.

[34] K. Sorbie, *Polymer-Improved Oil Recovery*. Blackie, 1991.

Chapter

2

Measurement of the partition coefficient of diethyl ether and tetrahydrofuran in oil / water + NaCl systems

2.1 Summary

The partition coefficients of diethyl ether (DEE) and tetrahydrofuran (THF) were measured in different water/oil systems. We used different oil types, i.e. hexadecane, Ondina 919 and Ondina 933, different initial solvent concentrations in the aqueous phase and performed the experiments with and without the presence of NaCl in the aqueous phase. To validate the results, we measured the partition coefficient of diethyl ether in demi-water/C_{16} with two methods, viz., with refractive index and with density measurements. The results in terms of the logarithm of the partition coefficient of DEE, $Log_{10}(K_{oa}^{DEE})$, differed maximally 0.1 in demi-water/C_{16} and 0.17 in brine/C_{16}. We did not find the partition coefficients measured in salt solutions in the literature. However, our measured values for water/C_{16} system were different from the data in the literature by a factor of about 3.5 in terms of the partition coefficient, K_{oa}^{DEE}, and we were not able to explain the discrepancy. Given the fact that the solutions were shaken for 24 hours, and with the estimation of the evaporation

rate, it was unlikely that these mechanisms could explain the discrepancies. We also compared our measured values with the proposed correlations for the prediction of the partition coefficient. It was observed that our K_{oa}^{DEE} was closer to values derived from the Meyer and Maurer's correlation (approximately by a factor of 1.2) than the values obtained from the Abraham's correlation (approximately by a factor of 3.5). Nevertheless, as stated by the correlation developers, both correlations are not suitable for the prediction of the partition coefficient of THF and thus both correlations predict a very different values for the partition coefficient than our values. Moreover, added salt increased the DEE and THF partition coefficients in systems with different oil types. In addition, the result showed that the partition coefficient was a weak function of the initial solvent concentration, but considering the experimental error it was more or less constant. It was also observed that the partition coefficient of DEE was higher than the partition coefficient of THF.

2.2 Introduction

Oil recovery by mutually soluble solvents (solvent-enhanced oil recovery) can be described as a two-phase flow problem involving mass transfer between the oleic phase and the aqueous phase. The partitioning of the mutually soluble solvents between the oleic phase and the aqueous phase is beneficial for reducing the residual oil in spontaneous/forced oil displacement processes both in conventional and in fractured oil reservoirs [1–8].

We use the mutually soluble solvent (MSS) diethyl ether (DEE) and tetrahydrofuran (THF) to study the recovery mechanisms of solvent-enhanced oil recovery. In practice, the MSS is dissolved in the aqueous phase before it is injected. After injection, it moves in the reservoir and, upon contact with the oleic phase, the MSS partitions between the oleic phase and the aqueous phase. The MSS contributes partly to the mobilizing trapped oil in the reservoir because of a number of mechanisms such as oil swelling and oil viscosity reduction [1–3]. The partitioning of the solvent between the phases can be quantified with the partition coefficient, which is the ratio between the concentration of MSS in the oleic phase divided by the concentration in the aqueous phase [9–11]. The partition coefficient is a measure of the lipophilicity or hydrophobicity of the solvent, which both indicate the preference of the solvent to be in the oleic phase with respect to being in the aqueous phase at equilibrium conditions (see Fig. 2.1) [12]. Moreover, from a microscopic point of view, the partition coefficient provides information about the intermolecular forces between the solvent in the oleic phase and in the aqueous phase at equilibrium conditions [13]. The thermodynamic condition for the partition coefficient (distribution coefficient, equilibrium ratio) of a solvent between the oleic phase and the aqueous phase at a

constant temperature can be defined by:

$$c_s^o = K_{oa} c_s^a \tag{2.1}$$

where c_s^o and c_s^a are the solvent concentration in the oleic phase and the solvent concentration in the aqueous phase respectively; the unit of the concentration could be mol/L, mol/kg, mole fraction or volume fraction, and K_{oa} is the partition coefficient, which is a weak function of the MSS concentration [14–16]. The partition coefficient has an important impact on the recovery factor for solvent-enhanced oil recovery processes [2, 3, 17, 18]. Several parameters affect the partition coefficient. Firstly, it is a strong function of temperature, for instance, with an increase of temperature, the partition coefficient increases [19, 20]. Another very important parameter affecting the partition coefficient is salinity; increasing the salt concentration increases the partition coefficient (and decreases the solubility in the aqueous phase). This effect can be explained by the salting out effect [21–25]. The existence of divalent ions in the aqueous phase also affects the partition coefficient more than the presence of monovalent ions [26]. Indeed, the ionic composition of the aqueous phase, the type of electrolyte and the pH of the aqueous phase influences the partition coefficient [27–30]. The composition of the oil can also affect the partition coefficient [31, 32]. Only limited experimental data on the solubility of DEE in brine and of DEE in oil (hexadecane) exist and, to our knowledge, no experimental data of the partition coefficient of DEE between brine and hexadecane is available. However, a few reports appeared in the literature on the partition coefficient of DEE between water and hexadecane [33, 34]. Therefore, a systematic study was performed to measure the partition coefficient of DEE and THF between an aqueous phase and model oils, e.g. hexadecane, Ondina 919 and Ondina 933. The effect of the initial DEE or THF concentrations in the aqueous phase, of oil type and of the presence of NaCl in the aqueous phase were investigated. The structure of the chapter is organized as follows: section 2.3 describes the experimental procedure and materials. The validation of the experimental results and a comparison with the literature are described in section 2.4. Experimental results are discussed in section 2.5. Conclusions are drawn at the final section.

2.3 Experimental study

2.3.1 Outline

The purpose of the experiments was to obtain the partition coefficients of DEE and THF in oil/water systems. Following the shake-flask protocol [35–37], a certain initial number of moles of the aqueous phase (n_a^i) with an initial solvent mole fraction of $x_{a,s}^i$ was prepared in a test tube. Then, an approximately equal volume of hydrocarbon

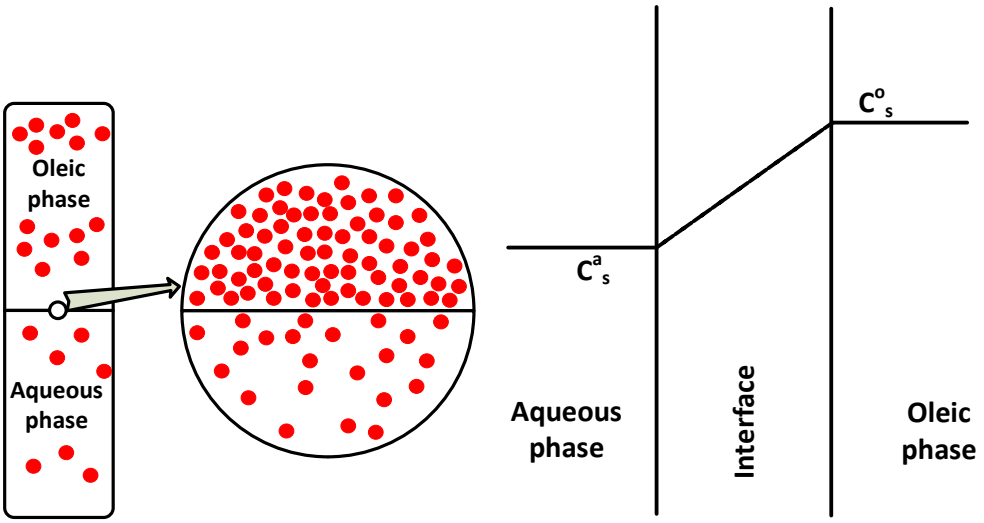

(a) (b)

Figure 2.1: (a) Schematic of a test tube, where the aqueous phase and the oleic phase are in equilibrium across the interface. Due to the oil preference of the solvent, the concentration of the solvent in the oleic phase is higher than in the aqueous phase. (b) Schematic of Fickean diffusion of solvent through a monolayer in the interface. The partition coefficient correlates the mole fraction of the solvent in the oleic phase (c_s^o) with the solvent mole fraction in the aqueous phase (c_s^a). The coefficients at various concentrations are determined experimentally.

corresponding to $n_{o,h}^i$ of oil was added to the test tube. The tube was shaken in a controlled temperature environment of $23°C$ for a period of about 24 $hours$, after which we assumed that equilibrium was attained. For DEE in water/C_{16} systems, we also obtained the calibration curves from density measurements using a Paar density-meter. By using the density measurements it was possible to determine the DEE mole fractions, both in the oleic phase and in the aqueous phase. We also determined the mole fractions of DEE or THF in the oleic phase using a refractometer, and calibration curves were obtained with an Abbe refractometer. From the refractive index measurements it was only possible to assess the composition of DEE in the oleic phase, because the refractive index of DEE and water/brine are very similar. By subtracting the total number of moles of DEE in the oleic phase from the total number of DEE initially added, we could obtain the number of moles of DEE in the aqueous phase. However, it was possible to determine the concentration of THF from refractive index measurements both in the aqueous phase and in the oleic phase. Now, the partition coefficient of DEE or THF could be determined as the ratio of the respective mole fraction in the oleic phase divided by the mole fraction in the

aqueous phase (see Eq. (2.1)). In this study, we assumed that the effect of the mutual solubility of water in oil and oil in water was negligible and, consequently, did not affect the measurements [26].

2.3.2 Materials and methods

2.3.2.1 Chemicals

DEE and THF (purity> 99.9%, Sigma-Aldrich) were chosen as solvent. Hexadecane ($C_{16}H_{34}$, purity> 99.9%) was purchased from Sigma-Aldrich, Germany. Ondina 933 and Ondina 919 consist of saturated paraffinic and saturated cyclo-paraffinic components. They are highly refined, non-stabilized, free of smell, taste, and color mineral oils. They are used as the basic oil for pharmaceutical products [38].
Demi-water was prepared by flowing water from a semi permeable column to remove the minerals ($pH = 6.8 \pm 0.1$, resistivity= 18.2 $M\Omega.cm$, conductivity= 0.056 $\mu S/cm$) at 23°C. Table 2.1 summarizes the physical properties of the chemical liquids. Moreover, some aqueous solutions were prepared by adding 0.5 mol/L sodium chloride (NaCl, Merck) to the demineralized water (brine).

2.3.3 Preparation of the aqueous solutions

The aqueous solutions of 0.9, 1.1 and 1.3 $mol\%$ (mole of solvent divided by total mole of mixture) DEE in demi-water or in brine (0.5 molar) were prepared by mixing appropriate amounts of demi-water or brine and DEE in a flask. Then, the solutions were shaken for a few hours, so that a homogenous mixture was obtained. Similarly, mixtures of 1.1, 2.4, 3.8 and 5.3 $mol\%$ of THF/demi-water and THF/brine (0.5 molar) were prepared. After shaking, the weight of the sample was measured to verify that volatilization did not occur in the mixture. Next, the equivalent volume of oil (hexadecane, Ondina 919 or Ondina 933) was added to the test tube. Then, the total weight was measured again. The flask was shaken for a period of about 24 $hours$. In order to accelerate the separation of the two immiscible phases, subsequently, the test tube was centrifuged for about 5 $mins$ under a centrifugal acceleration of 1000 g. Afterwards, the total weight of the test tube and liquids were measured to confirm there was no mass loss due to evaporation.

Table 2.1: Physical properties of the species at temperature 20°C [38–41].

Name	Density kg/m^3	Viscosity $Pa.s$	MW $kg/kmol$	RI n_D	Solubility in water, kg/m^3
Hexadecane	773	3.3×10^{-3}	226.44	1.4335	3.04×10^{-7}
Ondina 919	856	4.35×10^{-2}	360	1.4694	negligible
Ondina 933	886	2.12×10^{-1}	415	1.4800	negligible
Diethyl ether	714.5	2.35×10^{-4}	74.12	1.3523	69
Tetrahydrofuran	889.2	5.5×10^{-4}	72.11	1.4070	miscible

2.3.4 Determination of the DEE partition coefficient in oil/ water system

2.3.4.1 Measurements with the refractometer

For the determination of the partition coefficient, we need to obtain calibration curves. Therefore, we considered the DEE/demi-water mixture, the DEE/brine mixture and the DEE/oil mixture separately. To calibrate the DEE/oil mixture, we mixed an amount (weight) of oil, water or brine with DEE, carefully avoiding evaporation of the components. After mixing, the test tube was shaken in an IKA KS250 Basic shaker for a few hours. Then, the total weight was measured to verify that the MSS had not vaporized from the mixture. The measured weight showed that the maximum vaporization that occurred in the mixture with the highest DEE concentration, i.e. 1.3 $mol\%$, was less than -2% of the initial DEE weight. Because DEE is a highly volatile component, we assumed that the mass loss during the test, was due to evaporation of DEE. Thus, the evaporated DEE was deducted from the initial DEE amount and the DEE concentration in the mixture was corrected. Subsequently, we measured the refractive index of the mixture. Thus, we obtained a calibration curve, i.e. the composition of the DEE/oil mixture versus the refractive index. However, the contrast between the refractive index (RI) of brine and the refractive index of the mixture of DEE/brine is very small; it was not possible to use the Abbe refractometer to precisely characterize the DEE concentration in water.
The same procedure could, however, be used for the determination of the calibration curves for the THF/brine mixture and the THF/demi-water mixture. The AR4 Abbe refractometer (KRÜSS) was calibrated before measurements, by obtaining the refractive index of demi-water at ($23°C$). The refractive index measurement was used to determine the partition coefficient, i.e. the ratio of mole fractions of THF in oil and in water. With THF, there was enough difference between the refractive indices of all pure components and the mixtures of different amounts of THF in the oleic or in the aqueous phase. The calibration curves are shown in Figs. A.1-A.2. We used the "Eureqa" package [42] to obtain a regression curve that expresses the refractive index as a function of the mole fraction of MSS in the oleic phase or in

the aqueous phase. This allowed us to obtain the partition coefficient, being the ratio between the mole fraction in the oleic phase and the mole fraction in the aqueous phase, as a function of the measured refractive indices in the oleic and the aqueous phases respectively. However, for DEE only a calibration curve in the oleic phase was obtained. The composition in the aqueous phase was obtained from mass conservation considerations. The derivations can be found in A.3.

2.3.4.2 Measurements with the density-meter

To obtain the calibration curves using the density-meter, we followed the following procedure: first, we put a certain amount of demi-water, brine or hexadecane in a test tube. Afterwards, we added a certain amount of DEE to the tube. Subsequently, we measured the weight of the mixture and we put the tube in a shaker. After shaking for about 3 hours, we weighed the mixture; and we deducted the mass loss from the initial weight of DEE. Then, we measured the density of each mixture separately with a DAM 4100M Anton Paar density-meter. Then, we obtained the calibration plot of the mole fraction of DEE in the mixture versus the density of the mixture (see page 136). After establishing the calibration curves, we shaken different proportions of DEE/brine (e.g. 0.49, 0.75, 1.00, 1.27 and 1.52 $mol\%$) or DEE/demi-water (e.g. 0.25, 0.50, 0.76 and 1.01 $mol\%$) in a test tube for a few hours. Moreover, weighing the mixture before and after mixing verified that DEE evaporation was negligible. Then, we added the corresponding mass of hexadecane to the mixture of DEE/brine or DEE/demi-water. The mixture was again weighed and it was shaken for a period of 24 hours in the shaker. Then, we controlled the mass conservation and we assumed any loss in mass occurred due to DEE evaporation. Consequently, we deducted the volume of evaporated mass from the mass of DEE in the mixture. The mass loss was however negligible. Subsequently, we measured the density of the aqueous phase and the density of the oleic phase. Afterwards, using the calibration curves, we determined the DEE mole fraction in the aqueous phase and in the oleic phase. The contrast between the density of DEE and hexadecane is however small and the uncertainty of the density measurement with the DAM $4100M$ density-meter in the hexadecane/DEE mixture is ± 0.164 $mol\%$ as infers from the least significant digit. Finally, we obtained the partition coefficient from Eq. (2.1) by dividing the DEE mole fraction in the oleic phase by the DEE mole fraction in the aqueous phase.

2.3.5 Estimation of the uncertainties

Second order polynomials were regressed to the measured values for the calibration curves. Then, the uncertainties in the measurements were obtained by the regression

polynomial. For instance, the uncertainty was calculated by:

$$\Delta c = \frac{\Delta n}{\partial_n f(n)}, \tag{2.2}$$

where Δc is the uncertainty in the estimation of concentration from the refractive index measurements, Δn is the uncertainty in the measurement of refractive index by refractometer, and $\partial_n f(n)$ is the first order derivation of the tuned polynomial to the reference curves with respect to refractive index. Moreover, the uncertainty in estimation of the concentration in the aqueous phase is determined from the uncertainty in mass conservation. Afterwards, the relative uncertainty error of the partition coefficient measurement was calculated by adding the uncertainties in mole fractions in both phases [43–45]:

$$\frac{\Delta K_{oa}}{K_{oa}} = \sqrt{\left(\frac{\Delta c_s^o}{c_s^o}\right)^2 + \left(\frac{\Delta c_s^a}{c_s^a}\right)^2}, \tag{2.3}$$

where ΔK_{oa} is the uncertainty in the measurement of the partition coefficient, c_s^o and Δc_s^o are the concentration and the uncertainty in the concentration of MSS in the oleic phase respectively; c_s^o was obtained from the calibration curves and the refractive index of the sample, c_s^a is the concentration of MSS in the aqueous phase, and Δc_s^a is the uncertainty in the MSS concentration in the aqueous phase.
For the density measurements we followed the same procedure, except we used the partial molar volume versus mole fraction for the calibration curve. The molar volume is the inverse of molar density. The molar density is the mass density divided by the mole fraction averaged molecular weight. The advantage of this method is that the calibration curve of the molar volume versus the mole fraction is a more or less straight line. In order to determine the composition of the solution we proceed as follows: first, we need to convert the mass density measured at a composition to the molar density as a function of the composition. Therefore, we need to estimate the composition. Using the calibration curve, we get a calculated composition. We have to minimize the difference between the calculated and the measured compositions. To accomplish this we used Excel solver.

2.4 Validation of experimental results

The experimental results allowed to obtain the effect of the presence of NaCl, the solvent concentration in the aqueous phase and the oil type on the partition coefficient of solvent (DEE or THF) in different oil/water systems. We will discuss the experimental results consecutively for DEE and THF.

2.4.1 Comparison between K_{oa}^{DEE} from the density-meter and the refractometer measurements

As stated before, we separately measured the partition coefficient of DEE between hexadecane and water/brine with both the density-meter and the refractometer at $23°C$. Fig. 2.2 shows the partition coefficient, $\log_{10} K_{oa}^{DEE}$, for the demi-water/C_{16} system (left) and the brine/C_{16} system (right) as a function of the initial concentration of DEE in the aqueous phase in mole fractions. The partition coefficient is defined as the ratio between the mole fraction of DEE in the aqueous phase and the mole fraction of DEE in the aqueous phase. The result shows that our measured K_{oa}^{DEE} values (in mole fraction units), from both the refractive index measurement and the density-meter measurement, were in agreement within the experimental error. For example, a $\log_{10} K_{oa}^{DEE}$ of $1.45-1.62\pm0.13$ in demi-water/C_{16} was obtained from the refractive index measurements and from the density measurements, a $\log_{10} K_{oa}^{DEE}$ of $1.30-1.64\pm0.15$ in demi-water/C_{16} system was obtained. Moreover, in the brine/C_{16} system, $\log_{10} K_{oa}^{DEE}$ from the refractive index measurement was $1.78 - 1.86 \pm 0.14$, and $\log_{10} K_{oa}^{DEE}$ from the density measurement was $1.73 - 1.95 \pm 0.22$.

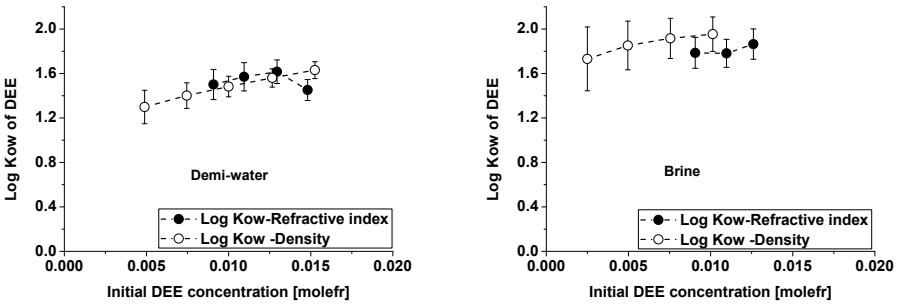

(a) (b)

Figure 2.2: (a) $\log_{10} K_{oa}^{DEE}$ for demi-water/C_{16} system (b) $\log_{10} K_{oa}^{DEE}$ for brine/C_{16} system, both in mole fraction units and as a function of the initial concentration of DEE in the aqueous phase in mole fractions. The result shows that measured $\log_{10} K_{oa}^{DEE}$ values from both the refractive index measurements and the density measurements reasonably coincide via the experimental error.

2.5 Comparison of the test results to the literature

There is relatively little data on the solubility of DEE in water or brine, and on ether in alkanes or mineral oils [46, 47]. There is even less experimental data on the partition coefficient of DEE between water and hexadecane. In the literature, a

partition coefficient for DEE in terms of the $\log_{10} K_{oa}^{DEE}$ between water and C_{16} at $298.15K$ was reported as 0.89 and 0.85, both expressed in mole per liter DEE in C_{16} divided by mole per liter DEE in water [33, 34].

The free energy values in the Abraham's paper [33] are given in $kcal/mole$ and we multiplied these values by 4.184 to convert them to $kJ/mole$. We subsequently added $RT \ln(\overline{V}_w/\overline{V}_h) = 6.8961 kJ/mole$, where $\overline{V}_w$ and $\overline{V}_h$ are partial molar volumes of water and hexadecane, to the quoted free energy of transfer of $\Delta\widehat{G_{tr}^0} = -12.0081\ kJ/mole$, when one mole of DEE was transferred from the aqueous phase to the oleic phase. Therefore, new free energy of transfer was obtained, i.e. $\Delta G_{tr}^0 = -5.1120\ kJ/mole$. In this way, we were able to reproduce the value of 0.89 in the molar ratio for the $\log_{10} K_{oa}^{DEE}$ between water and C_{16} in their table. However, the obtained $\log_{10} K_{oa}^{DEE}$ of $1.45 - 1.62$ in the mole fraction ratio of the refractive index measurements would correspond to a $\log_{10} K_{oa}^{DEE}$ of $0.25 - 0.42$ in the molar ratio. The reason for the discrepancy is still not clear to us. Nevertheless, one possible reason can be a slow establishment of the partition equilibrium. In addition, some correlations have been proposed to predict the partition coefficient of species between two phases, e.g. Meyer and Maurer's correlation [48] and Abraham's correlation [34]. Both correlations predict the partition coefficient of DEE between water/hexadecane systems in moles per liter units. For instance, $\log_{10}(K_{oa}) = 0.86$ was obtained from Abraham's correlation and $\log_{10}(K_{oa}) = 0.24$ was obtained from Meyer and Maurer's correlation.

By considering the solubility in brine ($0.5M\ NaCl$) solutions, we can determine the activity coefficient of DEE for various temperatures. We use the Davies [49] or Setchenow coefficient [50–54]:

$$\gamma_{DEE}(I) = \exp(K_s I), \tag{2.4}$$

where I is the ionic strength and K_s is Setchenow coefficient. Fig. 2.3 plots the logarithm of the solubility reported in reference [46] versus the ionic strength I at 25^oC and 15^oC; from the plot we concluded that $K_s = 0.215\ L/mol$ at 25^oC and $K_s = 0.220\ L/mol$ at $15°C$, which for all practical purposes are the same.

Using the estimated salting out coefficient and Eq. (2.5), it was possible to take into account the salinity effect on the partition coefficient. For brine of 0.5 molar NaCl in demi-water, the ionic strength was equal to $I = 0.5$, therefore, we obtain

$$\log_{10} K_{ob}^{DEE} = \log_{10} K_{ow}^{DEE} + 0.107, \tag{2.5}$$

where $\log_{10} K_{ob}^{DEE}$ is the logarithm of the partition coefficient of DEE between brine and hexadecane and $\log_{10} K_{ow}^{DEE}$ is the logarithm of the partition coefficient of DEE between demi-water and hexadecane. Comparing the experimental results of the partition coefficient of DEE in demi-water/C_{16} to the partition coefficient of DEE in brine/C_{16} (Figs. 2.2a and 2.2b) showed that the presence of NaCl in the

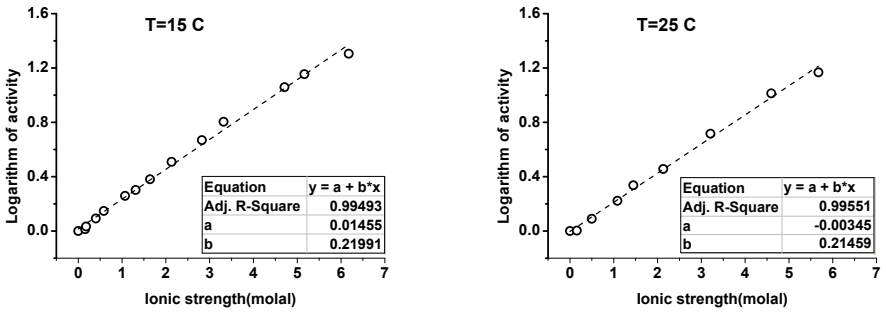

(a) (b)

Figure 2.3: Calculation of Setchenow coefficient from literature. The logarithm of the activity was a more or less linear function of the ionic strength. The slope is called Setchenow coefficient, which is, to an excellent approximation, independent of the ionic strength.

aqueous phase increases the partition coefficient. For instance, for the refractive index measurements, $\log_{10} K_{oa}^{DEE}$ in brine/C_{16} and demi-water/C_{16} differs between $0.24 - 0.28$, which could be expected considering the experimental errors. Moreover, for the density measurement, $\log_{10} K_{oa}^{DEE}$ in brine/C_{16} and demi-water/C_{16} differed between $0.47 - 0.55$, which was larger than for the refractive index measurements but could be expected considering the experimental errors.

2.6 Results and discussion

2.6.1 The partition coefficient of DEE

Here, we discuss the experimental results for two different oils, i.e. Ondina 919 ($O19$) and Ondina 933 ($O33$). To the best of our knowledge, there are no measured data on the partition coefficient of DEE in the brine/Ondina oil systems or in the demi-water/Ondina oil systems. We only measured the partition coefficient using the refractive index procedure. Figs. 2.4a and 2.4b show the $\log_{10} K_{oa}^{DEE}$ versus the initial DEE concentration in the aqueous phase for $O19$ and $O33$ respectively. The graphs with the black squares denote the measured values for brine and the white squares show the values for demi-water. The values of $\log_{10} K_{oa}^{DEE}$ varied between $1.77 - 1.96 \pm 0.11$ for the brine/$O19$ system and showed a decreasing trend with an increasing initial DEE concentration in the aqueous phase. In view of error bars, the decrease was not significant. Moreover, in the demi-water/$O19$ system, the same small decreasing trend, which was also not significant within experimental error, was observed. A partition coefficient in terms of $\log_{10} K_{oa}^{DEE}$ of $1.41 - 1.60 \pm 0.11$

was obtained. Furthermore, it was observed that $\log_{10} K_{oa}^{DEE}$ in brine/$O19$ was $0.36 - 0.40 \pm 0.11$ bigger than that of demi-water/O19, which appeared to be larger than experimental error. Besides, in the demi-water/$O33$ system, $\log_{10} K_{oa}^{DEE}$ was $1.32 - 1.45 \pm 0.11$ and for the brine/$O33$ system, the measured values were $1.66 - 1.90 \pm 0.11$. In addition, the presence of salt increased the $\log_{10} K_{oa}^{DEE}$ of $0.21 - 0.49 \pm 0.11$, which showed the right trend for the salting out effect.

The effect of the initial concentration: It appears that the initial DEE concentration influenced the $\log_{10} K_{oa}^{DEE}$ very slightly but not significantly for all systems (see Figs. 2.2 and 2.4).

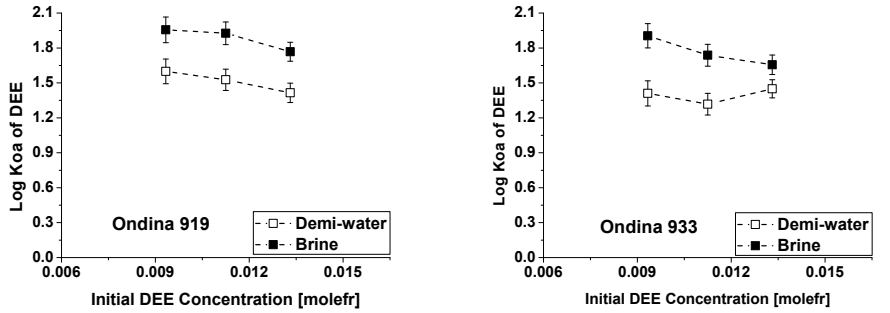

(a) (b)

Figure 2.4: A comparison between the partition coefficient of DEE between demi-water and brine (0.5 molar NaCl in demi-water) is shown for Ondina 919 (a) and Ondina 933 (b).

The effect of oil type: Fig. 2.5 shows the bar-charts that depict $\log_{10} K_{oa}^{DEE}$ between brine/demi-water and different oils, i.e. C_{16}, $O19$ and $O33$, and in the different initial DEE concentrations of 0.9 $mol\%$ (Fig. 2.5a), 1.1 $mol\%$ (Fig. 2.5b) and 1.3 $mol\%$ (Fig. 2.5c). The oil type is shown on the x-axis, and the y-axis shows $\log_{10} K_{oa}^{DEE}$. Moreover, the white bars depict the $\log_{10} K_{oa}^{DEE}$ in demi-water/oil systems and the shadowed bars represent the $\log_{10} K_{oa}^{DEE}$ in brine/oil systems. C_{16} is a single component oil, while Ondina oils are multi-component oils. Therefore, we only compared the obtained partition coefficient of DEE for the systems having $O19$ and $O33$. As Fig. 2.5 shows, in all systems containing $O19$ and $O33$, $\log_{10} K_{oa}^{DEE}$ was slightly higher for $O19$ than for $O33$, but can be considered the same within the experimental errors.

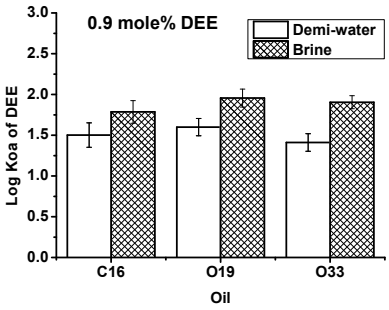

(a)

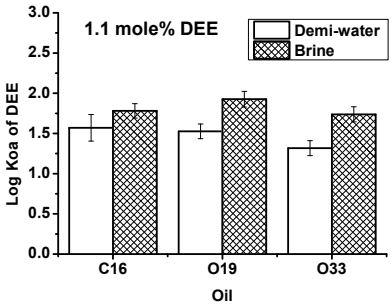

(b)

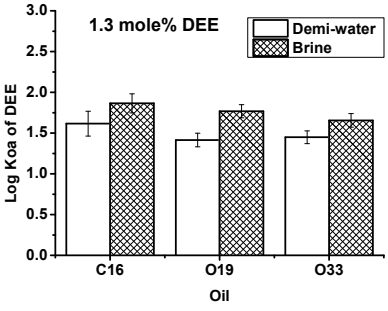

(c)

Figure 2.5: The partition coefficient of DEE in terms of its logarithm is shown for demi-water/oil and brine/oil systems for three different initial DEE concentrations, viz., 0.9 mol% (a), 1.1 mol% (b) and 1.3 mol% (c).

2.6.2 The partition coefficient of THF

Fig. 2.6 shows the logarithm of the partition coefficient of THF, i.e. $\log_{10} K_{oa}^{THF}$ in different oils. The x-axis denotes the initial THF concentration in the aqueous phase and the y-axis shows the $\log_{10} K_{oa}^{THF}$. There are two separate graphs in all sub-figures, i.e. a plot with black squares for the brine/oil system and a plot with white squares showing the water/oil system, both representing the measured values. In the brine/oil systems, $\log_{10} K_{oa}^{THF}$ was measured in the mixtures with an initial THF concentration of 1.1 *mol*%, 2.4 *mol*%, 3.8 *mol*% and 5.3 *mol*%, respectively. Moreover, in the demi-water/oil systems was only measured for the mixtures initially with 2.4 *mol*%, 3.8 *mol*% THF.

Fig. 2.6a shows the results for demi-water/C_{16} and brine/C_{16} systems. For the demi-water/C_{16} system, the $\log_{10} K_{oa}^{THF}$ was $0.84 - 0.96 \pm 0.26$. However, to the best

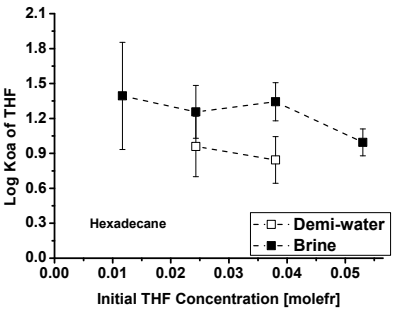

(a)

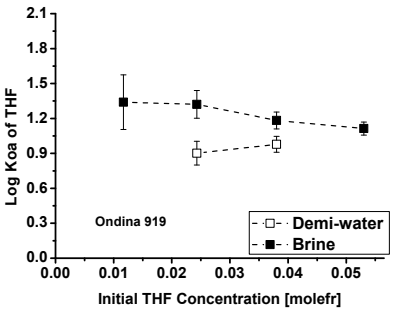

(b)

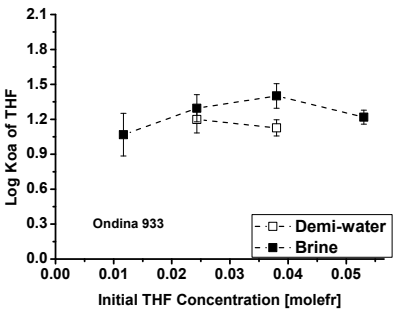

(c)

Figure 2.6: The partition coefficient of THF in term of its logarithm is shown for C_{16} (a), $O19$ (b) and $O33$ (c) as a function of the initial mole fraction of THF in the aqueous phase. The presence of NaCl in the aqueous phase increases the THF partition coefficient in the oil (salting out effect).

of our knowledge, the only measured values for the logarithm of partition coefficient of THF between hexadecane and water are reported as $\log_{10} K_{oa}^{THF} = -0.02$ [34] and $\log_{10} K_{oa}^{THF} = 0.09$ [33], both in the molar ratio. This corresponds to 1.18 and 1.29 in the mole fraction ratios respectively. We are not able to explain the difference between our values and the reported values in the literature. In addition, it is stated in Meyer and Maurer's paper [48] and in Abraham's paper [33] that the the presented correlations for the prediction of the partition coefficient of solvents do not predict the $\log_{10} K_{oa}^{THF}$ accurately. For example, the logarithm of the partition coefficient of THF between demi-water and hexadecane, $\log_{10} K_{oa}^{THF}$, is -0.14 in Abraham's correlation and 2.36 in Meyer and Maurer's correlation, both calculated in molar ratios. The presence of salt increased the partition coefficient in terms of $\log_{10} K_{oa}^{THF}$ of $0.3 - 0.5 \pm 0.26$ for the brine/C_{16} system.

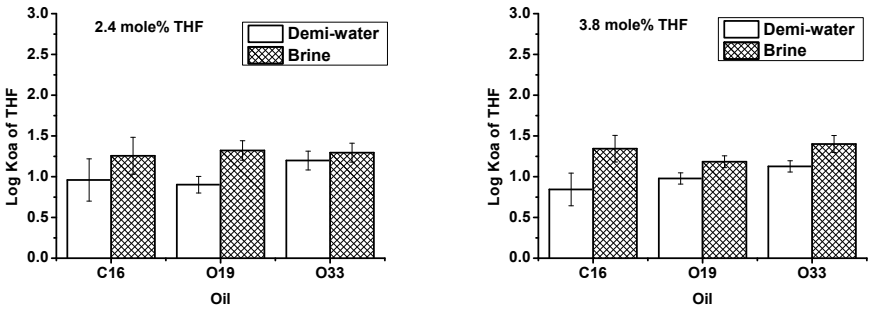

(a) (b)

Figure 2.7: The effect of the oil type on the THF partition coefficient is shown. The salting out effect leads to a higher partition coefficient.

In the brine/$O19$ system, the partition coefficient in terms of $\log_{10} K_{oa}^{THF}$ was $1.11-1.34\pm0.23$ with an insignificant decreasing trend within the experimental error. Moreover, the partition coefficient in terms of $\log_{10} K_{oa}^{THF}$ was $0.90-0.98\pm0.10$ for the demi-water/$O19$ system. Therefore, the salt increased the partition coefficient in terms of $\log_{10} K_{oa}^{THF}$ of $0.20-0.42\pm0.12$. Furthermore, the logarithm of the partition coefficient of THF in brine/$O33$ was $1.07-1.40\pm0.18$ and it was $1.13-1.20\pm0.18$ in demi-water/O33, which showed an increase of $0.1-0.27\pm0.12$ due to the salting out effect. The improvements of $\log_{10} K_{oa}^{THF}$ with the presence of salt differed in different oils, this may be attributed to the fact that the equilibrium was not attained in all systems.

The effect of oil type: We only compared the results for $O19$ and $O33$ mineral oils. Although, in the system of initially 2.4% of THF in brine, the partition coefficient was more or less the same for both $O19$ and $O33$ oils. The general trend appeared to be a higher partition coefficient of THF in Ondina 933 than in Ondina 919, in both brine/oil and demi-water/oil systems.

The effect of solvent type: Fig. 2.8a shows the comparison between the partition coefficient of THF and DEE between brine and different oil types. Here, the initial solvent concentration was 1.1 $mol\%$ in brine. Considering the experimental error, the partition coefficient in terms of $\log_{10} K_{oa}^{DEE}$ was higher than $\log_{10} K_{oa}^{THF}$in all oil types. The difference between Ondina 919 and 933 was considerable, but for C_{16} it was insignificant within experimental error. It seems that the different molecular structure of THF or DEE influenced the partitioning of THF and DEE in different oils. For instance, the DEE molecule is an open chain (one oxygen atom at the center with two ether chains from sides), but the THF molecule is a five-membered aromatic ring with four carbon atoms and one oxygen atom (see Fig. 2.8b and 2.8c).

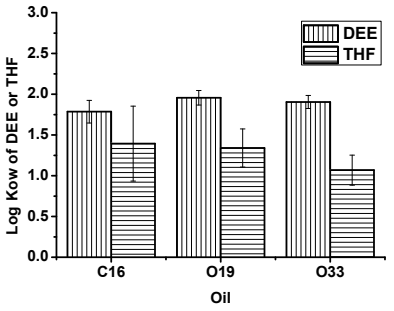

(a)

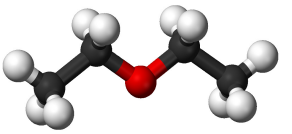

(b) DEE molecule

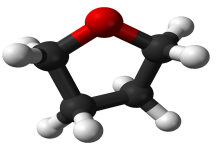

(c) THF molecule

Figure 2.8: (a) The Comparison between the partition coefficient of DME and THF in the brine/oil systems is shown. In the same operating condition, DEE partitions more effectively in all oil types than THF. A reason could be the difference between the molecular structures of the solvents (b and c). The DEE molecule is an open chain of one oxygen atom at the center with two ether chains in both sides (b). The THF molecule is a five-membered aromatic ring with four carbon atoms and one oxygen atom (c).

2.7 Concluding remarks

We measured the partition coefficient of diethyl ether (DEE) and tetrahydrofuran (THF) in brine/oil and in demi-water/oil systems. We investigated the effect of the presence of salt, of the initial solvent concentration in the aqueous phase, and of oil type (hexadecane, Ondina 919 and Ondina 933) on the partition coefficient of DEE or THF between the aqueous and oleic phase. The partition coefficient can be measured using either a refractometer or a density-meter. Added salt increases the partition coefficient (due to lower solubility in the aqueous phase). It appears that the partition coefficients of DEE and of THF are weak functions of the initial solvent concentration in the aqueous phase. It was observed that the partition coefficient of DEE in brine/oil systems was higher than the partition coefficient of THF.

Bibliography

[1] M. Chahardowli, A. Zholdybayeva, R. Farajzadeh, and H. Bruining, "Solvent-Enhanced Spontaneous Imbibition in Fractured Reservoirs," in *Proceedings of 75th EAGE Conference & Exhibition incorporating SPE EUROPEC 2013*. Society of Petroleum Engineers, Jul. 2013.

[2] M. Chahardowli, R. Farajzadeh, and H. Bruining, "Numerical Simulation of Mutually Soluble Solvent-Aided Spontaneous Imbibition in Fractured Reservoirs," in *14th European Conference on the Mathematics of Oil Recovery*, Catania, Sep. 2014.

[3] A. Chernetsky, S. Masalmeh, D. Eikmans, P. D. Boerrigter, C. Parsons, A. Parker, D. Boersma, J. Cui, B. Dindoruk, P. te Riele, A. Kindi, and N. Azri, "Experimental Results and Modelling Workflow of the DME Enhanced Waterflood Technology," in *The Abu Dhabi International Petroleum Exhibition and Conference, ADIPEC*. Society of Petroleum Engineers, 2015.

[4] M. Chahardowli, R. Farajzadeh, and H. Bruining, "Experimental Investigation of the Use of the Dimethyl Ether/Polymer Hybrid as a Novel Enhanced Oil Recovery Method," *accepted for publication in Journal of Industrial and Engineering Chemistry*, DOI:10.1016/j.jiec.2016.04.008.

[5] J. Groot, A. Chernetsky, P. Te Riele, B. Dindoruk, J. Cui, L. Wilson, and R. Ratnakar, "Representation of Phase Behavior and PVT Workflow for DME Enhanced Water-Flooding," in *SPE EOR Conference at Oil and Gas West Asia*. Society of Petroleum Engineers, 2016.

[6] P. t. Riele, C. Parsons, P. Boerrigter, J. Plantenberg, B. Suijkerbuijk, J. Burggraaf, A. Chernetsky, D. Boersma, and R. Broos, "Implementing a Water Soluble Solvent Based Enhanced Oil Recovery Technology-Aspects of Field Development Planning," in *SPE EOR Conference at Oil and Gas West Asia*. Society of Petroleum Engineers, 2016.

[7] A. Alkindi, N. Al-Azri, D. Said, K. AlShuaili, and P. Te Riele, "Persistence in EOR-Design of a Field Trial in a Carbonate Reservoir Using Solvent-Based Water-Flood Process," in *SPE EOR Conference at Oil and Gas West Asia*. Society of Petroleum Engineers, 2016.

[8] M. Chahardowli, R. Farajzadeh, and H. Bruining, "Experimental Investigation of the Use of Dimethyl Ether/Polymer Hybrid as an Enhanced Oil Recovery Method," in *SPE EOR Conference at Oil and Gas West Asia*, 2016.

[9] K. Aly and E. Esmail, "Refractive Index of Salt Water: Effect of Temperature," *Optical Materials*, vol. 2, pp. 195–199, 1993.

[10] A. Martin, P. Sinko, and Y. Singh, *Martin's Physical Pharmacy and Pharmaceutical Sciences: Physical Chemical and Biopharmaceutical Principles in the Pharmaceutical Sciences*, ser. International edition. Lippincott Williams & Wilkins, 2011.

[11] S. Srebrenik and S. Cohen, "Theoretical Derivation of Partition Coefficient from Solubility Parameters," *The Journal of Physical Chemistry*, vol. 80, no. 9, pp. 996–999, Apr. 1976.

[12] S. Standal, J. Haavik, a.M. Blokhus, and a. Skauge, "Effect of Polar Organic Components on Wettability as Studied by Adsorption and Contact Angles," *Journal of Petroleum Science and Engineering*, vol. 24, no. 2-4, pp. 131–144, Dec. 1999.

[13] W. J. Lambert, "Modeling Oil-water Partitioning and Membrane Permeation Using Reversed-phase Chromatography," *Journal of Chromatography A*, vol. 656, no. 1 - 2, pp. 469 – 484, 1993.

[14] C. T. Chiou, "Partition Coefficient and Water Solubility in Environmental Chemistry," *Hazard Assessment of Chemicals: Current Departments*, vol. 1, p. 117, 2012.

[15] J. T. Davies, *Interfacial Phenomena*. Elsevier, 2012.

[16] E. Dumont, G. Darracq, and A. Couvert, "Determination of Partition Coefficients of Three Volatile Organic Compounds (Dimethylsulphide, Dimethyldisulphide and Toluene) in Water/Silicone Oil Mixtures," *Chemical Engineering Journal*, vol. 162, no. 3, pp. 927–934, Sep. 2010.

[17] V. Dwarakanath, T. Chaturvedi, A. Jackson, T. Malik, A. A. Siregar, and P. Zhao, "Using Co-Solvents to Provide Gradients and Improve Oil Recovery During Chemical Flooding in a Light Oil Reservoir," in *SPE Symposium on Improved Oil Recovery*. Society of Petroleum Engineers, 2008.

[18] G. Ren, H. Zhang, and Q. Nguyen, "Effect of Surfactant Partitioning on Mobility Control During Carbon-Dioxide Flooding," *SPE Journal*, vol. 18, no. 04, pp. 752–765, 2013.

[19] F. Ravera, M. Ferrari, L. Liggieri, R. Miller, and A. Passerone, "Measurement of the partition coefficient of surfactants in water/oil systems," *Langmuir*, vol. 13, no. 18, pp. 4817–4820, 1997.

[20] J.-L. Salager, N. Marquez, A. Graciaa, and J. Lachaise, "Partitioning of ethoxylated octylphenol surfactants in microemulsion-oil-water systems: Influence of temperature and relation between partitioning coefficient and physicochemical formulation," *Langmuir*, vol. 16, no. 13, pp. 5534–5539, 2000.

[21] G. M. Anderson and D. A. Crerar, *Thermodynamics in Geochemistry: the Equilibrium Model*. Oxford University Press, USA, 1993.

[22] C.-C. Chen, H. I. Britt, J. F. Boston, and L. B. Evans, "Extension and application of the pitzer equation for vapor-liquid equilibrium of aqueous electrolyte systems with molecular solutes," *AIChE Journal*, vol. 25, no. 5, pp. 820–831, 1979.

[23] M. Randall and C. F. Failey, "The activity coefficient of non-electrolytes in aqueous salt solutions from solubility measurements. the salting-out order of the ions." *Chemical Reviews*, vol. 4, no. 3, pp. 285–290, 1927.

[24] A. Solheim, "Partition of alcohol between excess oil and aqueous phases in surfactant flooding processes," Society of Petroleum Engineers, 1990.

[25] S. H. Standal, A. M. Blokhus, J. Haavik, A. Skauge, and T. Barth, "Partition coefficients and interfacial activity for polar components in oil/water model systems," *Journal of colloid and interface science*, vol. 212, no. 1, pp. 33–41, 1999.

[26] C. T. C. Jafvert, J. C. J. Westall, E. Grieder, and R. P. Schwarzenbach, "Distribution of Hydrophobic Ionogenic Organic Compounds Between Octanol and Water: Organic Acids," *Environmental science & technology*, vol. 24, no. 12, pp. 1795–1803, Dec. 1990.

[27] S. Endo, A. Pfennigsdorff, and K.-U. Goss, "Salting-out effect in aqueous nacl solutions: Trends with size and polarity of solute molecules," *Environmental science & technology*, vol. 46, no. 3, pp. 1496–1503, 2012.

[28] T. A. Gebrehiwet, G. D. Redden, Y. Fujita, M. S. Beig, and R. W. Smith, "The effect of the CO_3^{2-} to Ca^{2+} ion activity ratio on calcite precipitation kinetics and Sr^{2+} partitioning," *Geochem. Trans*, vol. 13, no. 1, pp. 1–11, 2012.

[29] C. Reichardt and T. Welton, *Solvents and Solvent Effects in Organic Chemistry*. John Wiley & Sons, 2011.

[30] S. Wille, M. Buggert, L. Mokrushina, W. Arlt, and I. Smirnova, "Effect of electrolytes on octanol-water partition coefficients: Calculations with cosmo-rs," *Chemical Engineering & Technology*, vol. 33, no. 7, pp. 1075–1082, 2010.

[31] B. Bennett, B. Bowler, and S. Larter, "Determination of C0-C3 Alkylphenols in Crude Oils and Waters," *Analytical chemistry*, vol. 68, no. 20, pp. 3697–3702, 1996.

[32] O. F.M. and M. Silva, "Effect of Oil Composition on Minimum Miscibility Pressure-Part 2: Correlation," *SPE Reservoir Engineering*, vol. 2, no. 4, 1987.

[33] M. H. Abraham, H. S. Chadha, G. S. Whiting, and R. C. Mitchell, "Hydrogen-Bonding .32. an Analysis of Water-Octanol and Water- Alkane Partitioning and the Delta-Log-P Parameter of Seiler." *Journal of Pharmaceutical Sciences*, vol. 83, no. 8, pp. 1085–1100., 1994.

[34] M. H. Abraham, G. S. Whiting, R. Fuchs, and E. J. Chambers, "Thermodynamics of Solute Transfer from Water to Hexadecane," *Journal of the Chemical Society, Perkin Transactions 2*, no. 2, p. 291, 1990.

[35] "Test No. 107: Partition Coefficient (N-Octanol/Water): Shake Flask Method," Jul. 1995.

[36] M. Ioppolo-Armanios, R. Alexander, and R. I. Kagi, "Geosynthesis of organic compounds: I. alkylphenols," *Geochimica et cosmochimica acta*, vol. 59, no. 14, pp. 3017–3027, 1995.

[37] P. Taylor, S. Larter, M. Jones, J. Dale, and I. Horstad, "The effect of oil-water-rock partitioning on the occurrence of alkylphenols in petroleum systems," *Geochimica et cosmochimica acta*, vol. 61, no. 9, pp. 1899–1910, 1997.

[38] S. N. V. B.V., *Shell Smeermiddelen Voor Industrie En Scheepvaart*. Shell Nederland Verkoopmaatschappij B.V, 1992.

[39] S. Budavari, M. O'Neil, A. Smith, and P. Heckelman, "The merck index-encyclopedia of chemicals, drugs and biologicals. rahway, nj: Merck and co," *Inc*, vol. 512, p. 754, 1989.

[40] X. Meng, P. Zheng, J. Wu, and Z. Liu, "Density and viscosity measurements of diethyl ether from 243 to 373k and up to 20mpa," *Fluid Phase Equilibria*, vol. 271, no. 1, pp. 1–5, 2008.

[41] D. G. Shaw and A. Maczynski, "Iupac-Nist Solubility Data Series. 81. Hydrocarbons With Water and Seawater-Revised and Updated. Part 11. C13-C16 Hydrocarbons With Water," *Journal of Physical and Chemical Reference Data*, vol. 35, no. 2, p. 687, 2006.

[42] R. Ehrenberg, "Software scientist: With a little data, eureqa generates fundamental laws of nature," *Science News*, vol. 181, no. 1, pp. 20–21, 2012.

[43] M. Ferrari, L. Liggieri, F. Ravera, C. Amodio, and R. Miller, "Adsorption Kinetics of Alkylphosphine Oxides at Water/Hexane Interface," *Journal of Colloid and Interface Science*, vol. 186, no. 1, pp. 40–45, Feb. 1997.

[44] F. Ravera, M. Ferrari, and L. Liggieri, "Adsorption and partitioning of surfactants in liquid-liquid systems," *Advances in Colloid and Interface Science*, vol. 88, no. 1-2, pp. 129 – 177, 2000, beijing Conference, May 1999.

[45] J. Taylor, *An Introduction to Error Analysis- the Study of Uncertainties in Physical Measurements*, second edi ed. Sausalito: University Science Books, 1977.

[46] P. C. L. Thorne, "The Solubility of Ethyl Ether in Solutions of Sodium Chloride," p. 262, 1921.

[47] A. E. Hill, "The mutual solubility of liquids. i. the mutual solubility of ethyl ether and water. ii. the solubility of water in benzene," *Journal of the American Chemical Society*, vol. 45, no. 5, pp. 1143–1155, 1923.

[48] P. Meyer and G. Maurer, "Correlation and Prediction of Partition Coefficients of Organic Solutes Between Water and an Organic Solvent With a Generalized Form of the Linear Solvation Energy Relationship," *Industrial & Engineering Chemistry Research*, vol. 34, no. 1, pp. 373–381, 1995.

[49] C. W. Davies, "The extent of dissociation of salts in water. part viii. an equation for the mean ionic activity coefficient of an electrolyte in water, and a revision of the dissociation constants of some sulphates," *Journal of the Chemical Society (Resumed)*, pp. 2093–2098, 1938.

[50] R. Battino, T. R. Rettich, and T. Tominaga, "The solubility of oxygen and ozone in liquids," *Journal of physical and chemical reference data*, vol. 12, no. 2, pp. 163–178, 1983.

[51] H. L. Clever, "Setchenov Salt-Effect Parameter," *Journal of Chemical & Engineering Data*, vol. 28, no. 3, pp. 340–343, Jul. 1983.

[52] L. Copolovici and Ü. Niinemets, "Salting-in and salting-out effects of ionic and neutral osmotica on limonene and linalool henry Òş law constants and octanol/water partition coefficients," *Chemosphere*, vol. 69, no. 4, pp. 621–629, 2007.

[53] F. A. Long and W. F. McDevit, "Activity Coefficients of Nonelectrolyte Solutes in Aqueous Salt Solutions." *Chemical Reviews*, vol. 51, no. 1, pp. 119–169, Aug. 1952.

[54] T. Solomon, "The Definition and Unit of Ionic Strength," *Journal of Chemical Education*, vol. 78, no. 12, p. 1691, Dec. 2001.

Chapter

3

Numerical and experimental evaluation of diethyl ether-enhanced spontaneous imbibition in water-wet and mixed-wet rocks

3.1 Summary

Indicators of a successful recovery from fractured reservoirs are the amount and the rate with which oil is displaced out of the matrix blocks. In favorable circumstances substantial amounts of oil can be recovered at high rates. In less favorable situations recovery is slow, due to a low permeability of the matrix, a high viscosity of the oil, or is small due to adverse wetting conditions. In this chapter we investigate the possibility of increasing the recovery factor and enhancing the recovery rate by the addition of solvents, e.g. di-alkylether to brine. Experiments were conducted in Amott cells, where both mixed-wet and water-wet Berea sandstone and mixed-wet dolomite cores were exposed to brine (3 w/w% NaCl) with or without 7 v/v% diethyl ether (DEE). The recovery factor and the recovery rate could be monitored by reading a graded cylinder, which is mounted on top of the Amott cell. In water-wet Berea, the primary recovery from the matrix block exposed to pure brine, was $46 - 67$% of the oil initially in-place (OIIP), and additional secondary recovery, after exposure to

brine with dissolved DEE, was $1-11\%$ of the OIIP. One-stage ultimate recovery using a DEE/brine mixture was approximately the same as the obtained ultimate recovery from two-stage ultimate recovery, but the imbibition rate was faster. For mixed-wet Berea, the primary and secondary recoveries were $49-50\%$ and $29-37\%$ of the OIIP respectively, and the ultimate primary recovery was $79-86\%$ of the OIIP. For the mixed-wet dolomite the primary and secondary recoveries were $6-8\%$ and $27-29\%$ of the OIIP respectively; the ultimate primary recovery was 35% of the OIIP. We developed a model to describe the DEE/brine imbibition into an oil-filled core. We used relative permeabilities and capillary pressure that are characteristic of water-wet and mixed-wet cores. Model equations were solved using a commercial finite element package (COMSOL). Interfacial tensions were obtained from separate laboratory experiments. We optimized the correspondence between experiment and theory by modifying the sorting factor and the relative permeability end-points. Oil viscosities were obtained from an empirical relation (quarter-power law); the ideal mixing law (partial molar volumes independent of composition) was used as an equation of state (EOS). Solubility characteristics were taken from the literature. For the diffusion coefficient in the liquid we used the Wilke-Chang relation. A good agreement between experiment and theory was obtained.

3.2 Introduction

Naturally fractured reservoirs contain about 20% of the world's oil reserves and production [1]. From the engineering point of view, reservoirs with naturally occurring fractures that significantly affect the fluid flow, are considered fractured reservoirs [2]. Production from fractured reservoirs depends on the matrix-fracture interaction [3]. In reservoirs with low permeable matrix blocks, oil-wet matrix blocks and viscous oils, the transfer rate between fractures and matrix is slow and, consequently, the recovery is low. When a strongly water-wet matrix or a mixed-wet matrix is surrounded by an immiscible wetting phase in the fracture, spontaneous imbibition is the most important production mechanism [4, 5]. Since the spontaneous imbibition process is largely dominated by capillary diffusion, the parameters that control the capillary diffusion, will affect the spontaneous imbibition process, i.e. the wetting properties of the matrix-fluid [6–11], the relative permeability and the capillary pressure functions [12, 13], the matrix permeability [14, 15], the viscosities of the phases [16–18], the initial water saturation [19–21], and the boundary conditions [16, 22, 23]. Mutually soluble solvents (MSS) can accelerate and enhance the matrix-fracture transfer rate [24–32].

This study focuses on the solvent diethyl ether (DEE), which is mutually soluble in water and in oil. In fractured reservoirs, the solvent is transported by imbibition of the aqueous phase into the matrix block. Upon contact with oil, the solvent

composition at the boundary between the aqueous and the oleic phase is determined by Henry's Law. Subsequently, the solvent diffuses into the oleic phase until the system is in equilibrium. The distribution of the solvent between the oleic phase and the aqueous phase can be quantified by the partition coefficient. The partition coefficient is defined as the equilibrium concentration of the solvent in the oleic phase divided by the equilibrium concentration in the aqueous phase. A higher partition coefficient leads to a higher solvent concentration in the oleic phase [33]. Due to the migration of the solvent from the aqueous phase into the oleic phase, both the oil properties and/or rock-oil interactions are modified. For instance the oil mobility (permeability/viscosity) may increase and this may enhance the ultimate recovery and the imbibition rate in the fractured reservoirs [34–37]. An additional contributor to enhanced recovery is oil swelling (dilution); when a solvent diffuses in the oleic phase, the volume of the oil in the porous medium increases. The oil swelling improves oil recovery in two ways: first, when remaining oil swells, it occupies more pore space. Consequently, the oil saturation increases leading to a higher oil relative permeability [38]. Secondly, after introducing the solvent into the core, the residual oil is not pure oil anymore, but contains the solvent and, for a given residual oil saturation, less pure oil will stay behind. In addition, because of the difference between the partial molar volumes of DEE in the aqueous phase and in the oleic phase, the amount of transported DEE has a larger volume in the oleic phase than in the aqueous phase [39], which leads to further oil recovery. Another mechanism affecting recovery is alteration of the oil-water interfacial tension [32, 40]. However, DEE will not sufficiently reduce interfacial tension (IFT) for a significant increase in recovery, as shown in the capillary de-saturation curve [41]. Most current literature treats imbibition of solvent free wetting phases with an emphasis on scaling up functions. Therefore, it is advantageous to carry out solvent-enhanced spontaneous imbibition experiments (e.g. in an Amott cell) and to interpret the results with a transport model to elucidate the recovery mechanisms of solvent-enhanced imbibition.

A series of static imbibition experiments with mutually soluble solvents was performed using an Amott imbibition cell. The effects of the matrix permeability, the oil viscosity, the DEE concentration, the wettability of the surface, both in the primary and in the secondary mode, were studied. The chapter is organized as follows: first, the experimental procedure is explained in section 3.3. In section 3.4, the results of the DEE/brine spontaneous imbibition process is presented and discussed. Section 3.5 introduces a theory of DEE/brine enhanced imbibition and derives the ensuing model equations; the numerical model results are compared with the experimental results. Conclusions are drawn at the final section.

3.3 Experimental study

The purpose of the experiments was to elucidate the recovery mechanism of diethyl ether (DEE)/brine in fractured reservoirs. The design of the experiments consisted of an Amott imbibition cell (see Fig. 3.1a), in which an oil-filled core was immersed in a DEE/brine mixture. DEE dissolves both in brine and in oil. The oil produced from the core sample was collected in the top graded part and measured as a function of time. Only at the end of the experiment, the concentration of DEE in oil and in brine was measured. At the end of the experiment, diffusion completely mixed the oleic fluids.

3.3.1 Rock and fluid properties

The experiments used different oils, different concentrations of DEE, and core samples with different permeabilities and wetting properties, i.e. mixed-wet and water-wet core samples. The core samples were drilled from cubic meter blocks of Bentheimer sandstone, Berea sandstone, Red Felser sandstone and Silurian dolomite and then sawn to the desired size using a water-cooled diamond saw. Afterwards, they were dried in an oven at $55°C$ for about 24 $hours$. All core samples had a diameter of 3.00 ± 0.01 cm and a length of 5.00 ± 0.01 cm. For spontaneous imbibition experiments in water-wet cores, three different core types were selected, i.e. Berea sandstone, Bentheimer sandstone and Red Felser sandstone. Originally, all the sandstones are water-wet. Berea sandstone (BRS) is a layered heterogeneous sandstone, and all core samples were drilled perpendicular to the layer direction ($\varphi \cong 21 \pm 1\%$, $k = 87 - 125\ mD$). Red Felser sandstone (RFS) is also a heterogeneous rock, with a porosity of $\varphi \cong 21 \pm 1\%$ and a permeability of $k = 200 - 600\ mD$. Finally, Bentheimer sandstone (BTS) is a consolidated, nearly homogeneous, highly permeable sandstone, consisting of 91.7 $w/w\%$ quartz, 2.7 $w/w\%$ clay (kaolinite and montmorillonite) and 4.9 $w/w\%$ feldspar, 0.4 w/w% carbonate minerals and 0.3 $w/w\%$ oxide minerals ($\varphi \cong 23 \pm 1\%, k = 1000 - 2000\ mD$) [42]. All water-wet core samples were saturated with oil, without connate water saturation.

In order to carry out spontaneous imbibition in mixed-wet cores, Berea sandstone ($\varphi \cong 20 \pm 1\%, k = 160 - 171\ mD$) and Silurian dolomite ($\varphi \cong 20 \pm 1\%, k = 139 - 289\ mD$) cores were aged with crude oil B at $60°C$ and 55 $bars$ for 6 weeks. The initial water saturation in mixed-wet cores varied between 0.106 ± 0.001 and 0.195 ± 0.001. The water-wet core samples were saturated with three different oils viz.: crude oil A, Ondina 933 and hexadecane (industrial grade). Ondina 933 consists of saturated paraffinic and saturated cyclo-paraffinic components. Ondina oils are highly refined, non-stabilized, free of smell, taste and color, mineral oils, and are used as the basic oil for pharmaceutical products [43]. All mixed-wet cores were saturated with crude oil B. The properties of the oils used in this study are summarized in

Table 3.1. Brine with a composition of 0.5 M sodium chloride (NaCl, Merck) in demineralized water ($pH = 6.8 \pm 1$) was used as the aqueous phase. Two aqueous phase solutions were prepared by dissolving 5 $v/v\%$ or 7 $v/v\%$ of DEE ($(C2H5)_2O$, Sigma Aldrich, purity> 99.9%) in brine and by stirring for about $1 - 2$ $hours$. The physical properties of DEE are shown in Table 3.2. Weighing was used as the basis for the preparation of all mixtures.

Table 3.1: Physical properties of oils at temperature 20°C.

Name	Density (kg/m^3)	Viscosity ($Pa.s$)
Hexadecane (C16)	773	3.3×10^{-3}
Ondina 933 (O33)	886	2.12×10^{-1}
Crude oil A	850	8.0×10^{-2}
Crude oil B	901	8×10^{-3}

Table 3.2: Physical properties of DEE at temperature 20°C [44, 45].

Property	Value
Viscosity, ($mPa.s$)	0.235
Density, (kg/m^3)	714.5
Boiling point at atmospheric pressure, ($^\circ C$)	34.5
Solubility in water, (kg/m^3)	69

3.3.2 Amott imbibition cell

Figure 3.1a shows a schematic of the Amott imbibition cell, which was used to conduct the spontaneous imbibition experiments for both water-wet and mixed-wet cores. The Amott imbibition cell consists of two glassware parts, i.e. a tube with a diameter of 5.5 ± 0.1 cm and a length of 8.0 ± 0.1 cm, that is closed on one side and open on the other side. It is connected to a smaller diameter ($1 \pm 0.1cm$) graded tube with a length of 12.8 ± 0.1 cm and a volume of about 10.0 ± 0.1 cm^3, which is open at both ends, but which can be closed at one end by a stopper. The parts are attached together with clamps. Between the tubes, a glass cone is mounted to ensure a smooth transition between the tubes (see Fig. 3.1a).

3.3.3 Core cleaning procedure

For most experiments, we used a new core, without any prior cleaning. For a few experiments, we reused the core; the used cores were placed in a Soxhlet extractor

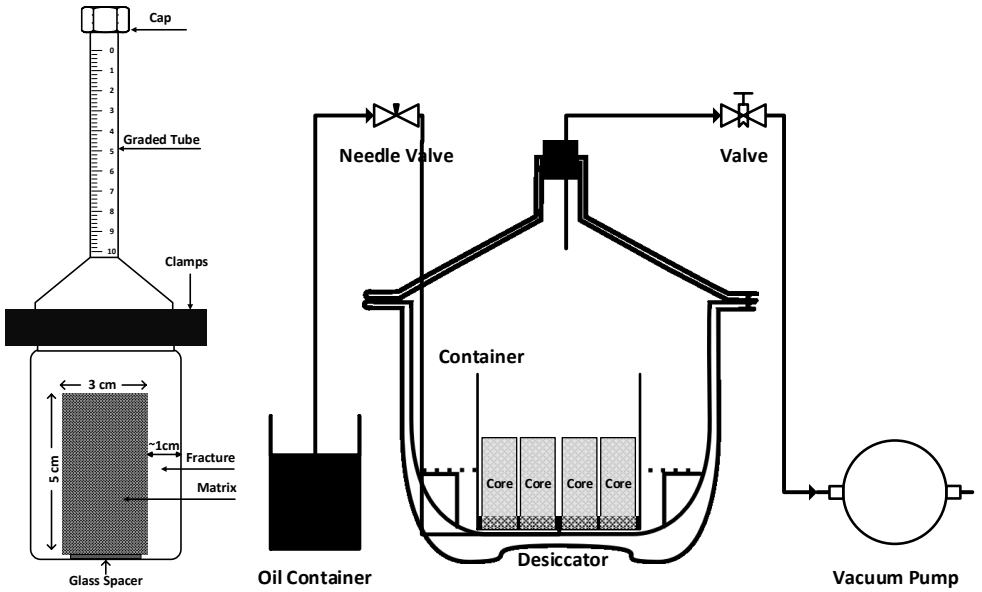

(a) Amott cell (b) Desiccator

Figure 3.1: (a) Schematic drawing of an Amott imbibition cell. An oil-filled core is placed in the middle of the lower part. The upper part is attached to the lower part with clamps. The Amott cell is gradually filled with an aqueous phase from the top until it reaches the zero level in the graded cylinder; then the cap is closed. (b) Schematic drawing of the vacuum saturation set-up; core samples are placed in a desiccator. The vacuum valve to the vacuum pump is switched on for a few hours. After evacuation, the vacuum valve is switched off and a needle valve is switched on to an oil container to allow saturation of the cores at a very low flow rate (Desiccator picture was taken from: www.clker.com/clipart-desiccator.html).

apparatus. First, the used core was cleaned by rinsing it continuously with 20 PV toluene for about 24 *hours*. Subsequently, the core was flushed with methanol for about 3 *hours* in the same apparatus. After cleaning, the core was dried in an oven at 60°C for about 24 *hours*. In all cases that we reused a core, we started with a spontaneous imbibition test with 7 $v/v\%$ of DEE and, after cleaning, the test was conducted with an aqueous phase of 5 $v/v\%$ DEE in brine.

3.3.4 Saturation procedure

First, trapped air in all core samples was removed by the evacuation method. An evacuation set-up, which consists of a desiccator and a vacuum pump, is drawn schematically in Fig. 3.1b. To evacuate the core sample, it was located in a container inside the desiccator. Then, the evacuation valve was switched on to the vacuum

pump for about $3-4$ *hours*. Next, the vessel was opened to allow flow through a needle valve, where cores were saturated under a very low flow rate.

3.3.5 Porosity and permeability measurement

The porosity measurement was carried out as follows. First, the bulk volume of the core was determined from the radius and its length. Secondly, the weight of the dry sample was measured; then the sample was saturated with crude oil and weighed again. The porosity was calculated using the density of the filling liquid and the core bulk volume. As already stated before, the porosity of the samples varied between $20 \pm 1\%$ and $23 \pm 1\%$, depending on the rock type. The permeability of the water-wet (WW) core samples was measured with a Ruska permeameter, whereas the permeability of the mixed-wet (MW) cores was determined from the application of Darcy's equation to fluid flow experiments.

3.3.6 Experimental procedure

After saturating, the core was brought into an Amott imbibition cell, which was subsequently filled with brine with or without DEE, to perform spontaneous imbibition experiments. The core sample was placed vertically on a small glass spacer at the bottom of the Amott cell (see Fig. 3.1a). The upper and the lower part of the Amott cell were attached together with clamps. A pure brine solution was gradually poured into the Amott cell and the core was exposed to brine without DEE. Brine imbibition experiments were conducted as the base case for all core types and the production was read from the graded cylinder versus time. After that, production effectively stopped and the core was moved to another Amott imbibition cell, which was subsequently filled with a mixture of DEE in brine (DEE/brine). The experiments, in which the sample is first exposed to brine and then to a DEE/brine mixture, are called two-stage imbibition experiments. Another type of experiment was the one-stage imbibition experiment; in the one-stage experiments, the core was exposed directly to the DEE/brine mixture and the production of the oleic phase was recorded versus time. All experiments were conducted at ambient pressures and temperatures. For the water-wet core samples, the production rate was initially very fast; at the beginning the production data were recorded every minute; then the data were gathered hourly, and afterwards daily, until production effectively stopped. For the mixed-wet samples, the data were gathered hourly at the beginning, and then daily. During the one-stage or the two-stage imbibition experiments, many oil drops were not released from the external surface of the core. Therefore, at the end of the experiments, the Amott imbibition cell was shaken to detach the oil drops from the core. This causes a sudden jump in the production curve at the end of each imbibition stage. In the experiments with a mixture of DEE/brine, the DEE

concentration in the oleic phase was quantified using two methods, viz.: a refractive index measurement, and a conductivity meter measurement. An Abbe refractometer was implemented to quantify the DEE concentration in the transparent oils (Ondina 933 and hexadecane). Crude oils A and B were completely opaque; therefore, it was not possible to measure the DEE concentration with the Abbe refractometer. However, we could determine the DEE concentration from a calibration curve that related the DEE concentration and the conductivity.

3.4 Experimental results

The purpose of the experiments was to elucidate the oil recovery mechanisms by adding DEE to the imbibing aqueous phase. DEE is soluble both in the aqueous and in the oleic phase. We will discuss the experimental results consecutively for the water-wet and the mixed-wet cores.

3.4.1 Experiments in water-wet cores

Water-wet cores with different permeabilities were saturated with three different oils (see Table 3.1). As discussed before (see page 38), several samples were exposed to the one-stage spontaneous imbibition test and several to the two-stage spontaneous imbibition test. Results on BRS, BTS and RFS samples are shown in Fig. 3.2; salient features are summarized in Table 3.3. Fig. 3.2 shows the two-stage spontaneous imbibition recoveries in various water-wet core samples. The permeability of oil-filled samples for all core types was between 87 and 2014 mD, and in total 46% to 67% of the Oil Initially In-Place (OIIP) was produced during the primary production process (see Table 3.3). The larger part of the OIIP was produced during the primary imbibition (without DEE). However, the solvent could reduce the remaining oil and, thus, improve the ultimate oil recovery. For instance, in water-wet core samples, the incremental recovery due to the secondary imbibition by DEE/brine varied between 3% and 21% of the remaining oil (see Fig. 3.2b). Moreover, the ultimate recovery for different water-wet core samples varied between 57% to 68% of the OIIP.

In general, it was observed that a saturated core with the same oil had higher primary and ultimate recoveries and a lower incremental recovery, if the permeability increased. For instance, $BTCW4$ with a permeability of 2014 mD was saturated with crude oil A, and after primary imbibition the remaining oil saturation, was $40 \pm 3\%$ of the OIIP corresponding to a recovery of 60% of the OIIP. Subsequently, the secondary imbibition, with 7 $v/v\%$ DEE in brine, obtained an ultimate recovery of $65 \pm 3\%$ of the OIIP, which corresponds to an additional secondary recovery of $5\% \pm 3\%$ of the OIIP. However, in $RFCW3$ with a permeability of 377 mD, the primary imbibition and the secondary imbibition yielded $53 \pm 3\%$ and $8 \pm 3\%$ of the OIIP respectively, leading to an ultimate recovery of 61% of the OIIP. Finally,

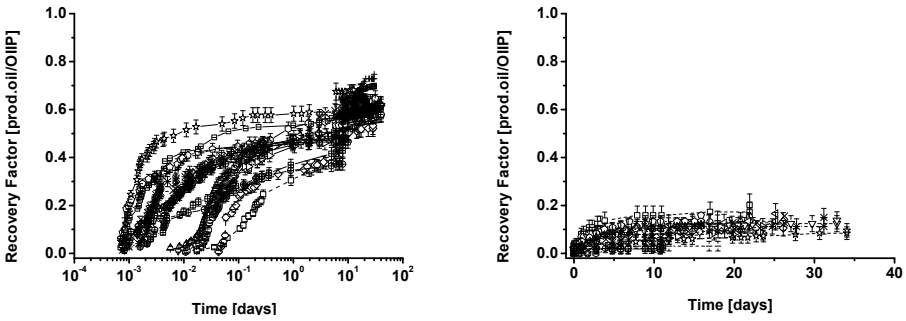

(a) (b)

Figure 3.2: (a) Recovery factor from water-wet core samples by brine (primary stage 10 *days*) and a mixture of 7 $v/v\%$ DEE/brine imbibition. A jump in the recorded oil production can be observed beyond one day. It is caused by shaking the Amott cell (see experimental procedure). After shaking, the sample was transferred to another Amott cell and exposed to brine with DEE, where secondary recovery occurs. The secondary recovery was added to the primary recovery. All core samples were saturated with different oils (see Table 3.1). Production from cores that were filled with crude oil occurred after a delay of an hour, as opposed to recovery with other model-oil filled cores, where the production started immediately. (b) Incremental recovery from DEE/brine imbibition. Time zero corresponds to the beginning of the secondary imbibition process, after primary imbibition. The final incremental recovery was obtained after shaking the Amott cell.

for $BRCW4$ with a permeability of 87 mD, the ultimate recovery after secondary production was $57 \pm 3\%$ of the OIIP, which was smaller than the UR obtained from samples $RFCW3$ and $BTCW4$. Comparison between $BTOW1$ and $RFOW9$, which were saturated with the same oil supported this observation. The minimum value of the inverse Bond number ($1/N_B = \sigma\sqrt{\frac{\varphi}{k}}/(\Delta\rho g H)$) for the primary imbibition and the secondary imbibition was 105 ± 1 and 28 ± 1 respectively. This indicates that in water-wet core samples, capillary forces are the main driving forces for penetration of the aqueous phase into the porous medium. In addition, the capillary diffusion coefficient is proportional to the square root of the permeability of the core, so a higher permeability leads to a higher Peclet number, which describes the capillary forces divided by viscous forces. A higher permeability leads to a higher gravity number (gravity forces divided by viscous forces). Indeed, recovery of extra oil with the solvent indicates that (an)other oil recovery mechanism(s) exist(s). However, it appears that the incremental recovery from water-wet cores strongly depends on the remaining oil saturation (ROS). This means that during the secondary imbibition by the DEE/brine mixture, the maximum incremental recovery with DEE was attained in the case of the maximum remaining oil. Nevertheless, a significant correlation

between the incremental recovery and the permeability or the oil type (and as a result viscosity, density or IFT) was not observed. A higher oil recovery in case of a higher remaining oil may indicate that the swelling mechanism is more effective than other mechanisms, like viscosity reduction. Moreover, it was observed that a faster oil recovery was obtained from the core samples, which were saturated with an oil of a lower viscosity than the samples which were saturated with an oil of a higher viscosity. In other words, higher oil viscosity leads to a slower imbibition rate (see Fig. 3.3).

The normalized recovery factor is plotted versus dimensionless time in Fig. 3.3

Table 3.3: Two-stage recovery from water-wet oil-filled core samples with different permeabilities.

Rock type	K $[mD]$	Oil	$1/NB$ brine	$1/NB$ DEE	RF brine $[v/v]$	UR $[v/v]$
$BTCW4$	2014	COA	111 ± 1	28 ± 1	0.60 ± 0.03	0.65 ± 0.03
$BTOW1$	1687	$O33$	288 ± 1	148 ± 1	0.65 ± 0.03	0.66 ± 0.03
$BTHW8$	1436	C_{16}	105 ± 1	93 ± 1	0.67 ± 0.04	0.68 ± 0.04
$RFCW3$	377	COA	244 ± 1	61 ± 1	0.53 ± 0.03	0.61 ± 0.03
$RFOW9$	166	$O33$	858 ± 1	442 ± 1	0.57 ± 0.03	0.61 ± 0.03
$RFHW2$	295	C_{16}	222 ± 1	198 ± 1	0.56 ± 0.03	0.63 ± 0.03
$BRCW4$	87	COA	510 ± 1	127 ± 1	0.46 ± 0.03	0.57 ± 0.03

for the brine imbibition stage. We transformed the time to a dimensionless time as proposed by Ma et al. (1995), to correct for the viscosity of the phases, the permeability and the dimension of the core sample, viz.:

$$t_D = t\sqrt{\frac{k}{\varphi}}\frac{\sigma}{\sqrt{\mu_o\mu_a}}\frac{1}{L_c^2}, \tag{3.1}$$

where μ_o and μ_a are the viscosity of the oleic phase and of the aqueous phase respectively, σ is the interfacial tension, and φ and k are the porosity and the permeability of the core. L_c is a characteristic length, which is approximately the same for all our experiments and it is defined as:

$$L_c = \sqrt{\frac{V_b}{\sum_{i+1}^{n} A_i/l_{Ai}}}, \tag{3.2}$$

where V_b is the bulk volume of the matrix, A_i is the area open to imbibition with respect to i^{th} direction, and l_{Ai} is the distance that the imbibition front travels from the inlet to the outer boundary. The characteristics length for a core with all boundaries open to imbibition fluid is calculated in Appendix A.4. In addition, the

normalized production is defined as the recovery factor at different time incrementals divided by the ultimate recovery factor at the end of the primary imbibition stage. Even then there is convergence of the curves; there is still a large variation, as has already been observed by previous authors [46–50]. A consistent observation is that the brine imbibition into crude oil-filled cores takes a longer time (see Fig. 3.3b), which can possibly be attributed to the wetting properties of crude oil. However, the contact time between crude oil and the rock was insufficient to change the wettability of the rock. In all cases we observe that the normalized recovery factor (which is by definition 100% at long times) tends to reach a limit and that longer times are not increasing the recovery (see Fig. 3.3).
The addition of DEE does lead to an additional recovery. This may be attributed to a swelling effect, as the DEE dissolves in the oil and increases the saturation. Therefore, it is suggested that the saturation increases beyond the residual saturation and further recovery is possible. In view of the form of the capillary de-saturation curve [51] it is unlikely that any change in surface tension will be responsible for the additional recovery of oil.

3.4.1.1 One-stage imbibition versus two-stage imbibition

Figure 3.4 compares the one-stage imbibition with the two-stage imbibition in both RFS and BRS cores. When $BRCW2$ was surrounded directly with 7 $v/v\%$ DEE/brine in primary recovery, the production reached a plateau of $57 \pm 4\%$ of the OIIP after 164 *hours*. In contrast, after exposing $BRCW4$ and $BRCW5$ to brine and then to a 7 $v/v\%$ DEE/brine mixture, the ultimate recoveries after 690 *hours* were $57 \pm 3\%$ of the OIIP, and $53 \pm 3\%$ of the OIIP, respectively (Fig. 3.4a). Moreover, for the $RFCW6$, $RFCW7$, $RFCW2$, and $RFCW3$ cores, both the one-stage imbibition and the two-stage imbibition had approximately the same ultimate recovery of about $62 \pm 3\%$ of the OIIP. However, like BRS core samples, the production plateau time for RFS in the one-stage imbibition was shorter than the two-stage imbibition (see Fig. 3.4b). This suggests that for the water-wet core samples, the one-stage imbibition has a higher production rate than a two-stage imbibition, but that the ultimate recovery is more or less the same. Production data from the one-stage and the two-stage experiments are summarized in Table 3.5.

3.4.1.2 Effect of the DEE concentration on the oil recovery from water-wet cores

Figure 3.5 shows the two-stage imbibition production curve from a single core with different DEE concentrations. First, the $BRCW5$ core was subjected to a two-stage imbibition experiment, using a brine mixture and subsequently a 7 $v/v\%$ DEE/brine mixture. We observed a primary recovery of $45 \pm 3\%$ of the OIIP, and an ultimate

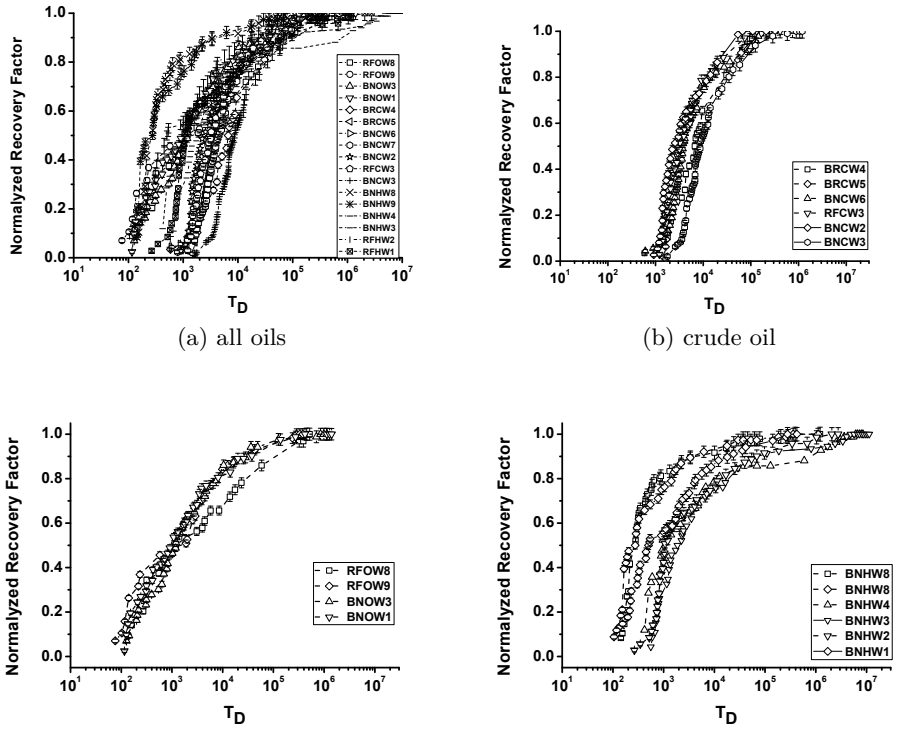

(a) all oils (b) crude oil

(c) Ondina 933 (d) hexadecane

Figure 3.3: (a) Normalized oil recovery from water-wet core samples by brine (primary stage) versus dimensionless time [16]. All core samples were saturated with different oils (see Table 3.1). Although there is a convergence, there is still a large variation between results. The results have collapsed on a single curve for crude oil A (b) and Ondina 933 (c), however, for hexadecane (d), they remained dispersed.

recovery of $53 \pm 3\%$ of the OIIP. After the cleaning process (see page 39), another two-stage imbibition experiment was performed. This time we used a mixture of 5 $v/v\%$ DEE/brine in the second stage. We obtained a primary recovery of $51 \pm 3\%$ of the OIIP and an ultimate recovery of $57 \pm 3\%$ of the OIIP. We also performed two-stage imbibition experiments in two other cores ($RFCW2$ and $RFCW3$) with 7 $v/v\%$ and 5 $v/v\%$ DEE/brine. The results revealed that two dissimilar DEE concentrations (5 $v/v\%$ and 7 $v/v\%$) roughly led to the same ultimate recovery. Indeed, the incremental recovery is still low, because the primary recovery by brine is high. Results for all cores are summarized in Table 3.5.

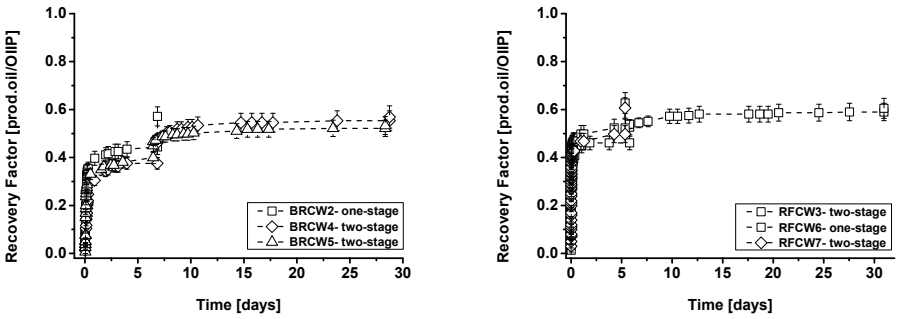

(a) (b)

Figure 3.4: (a) Comparison between oil recovery from water-wet Berea core samples by 7 $v/v\%$ DEE/brine mixture from the one-stage imbibition and from the two-stage imbibition with brine (primary stage; 10 *days*) and 7 $v/v\%$ DEE/brine mixture, after the jump. The jump is caused by shaking the Amott cell at the end of each stage. All core samples were saturated with crude oil A (see Table 1). (b) Comparison between oil recovery from water-wet Red Felser core samples by 7 $v/v\%$ DEE/brine one-stage imbibition and two-stage imbibition with brine (primary stage; 10 *days*) and 7 $v/v\%$ DEE/brine, after the jump.

Table 3.4: Comparison between oil recovery from the one-stage imbibition and the two-stage imbibition with the mixture of 7 $v/v\%$ DEE/brine in water-wet cores.

Rock type	PV $[ml]$	$1/NB$ brine	$1/NB$ DEE	RF brine $[v/v]$	UR $[v/v]$
$RFCW6$	7.52 ± 0.03		57 ± 1		0.63 ± 0.04
$RFCW7$	7.54 ± 0.03		62 ± 1		0.61 ± 0.04
$RFCW2$	7.55 ± 0.04	348 ± 1	87 ± 1	0.56 ± 0.04	0.62 ± 0.03
$RFCW3$	7.60 ± 0.03	243 ± 1	61 ± 1	0.53 ± 0.03	0.61 ± 0.03
$BRCW2$	7.62 ± 0.03		119 ± 1		0.57 ± 0.04
$BRCW4$	7.72 ± 0.03	510 ± 1	127 ± 1	0.46 ± 0.03	0.57 ± 0.03
$BRCW5$	8.01 ± 0.03	489 ± 1	122 ± 1	0.45 ± 0.03	0.53 ± 0.03

3.4.2 Experiments in mixed-wet cores

The mixed-wet core samples, as opposed to the water-wet cores, had an initial water saturation. They were exposed to both one-stage and two-stage imbibition processes. The procedure of making the samples mixed-wet has already been described before (see page 38). This procedure modified the samples from water-wet to mixed-wet. Therefore, once they were immersed in the aqueous solution, the spontaneous imbibition started in all core samples. In contrast to the water-wet cores, all oil drops

Table 3.5: Oil recovery from water-wet samples after two-stage imbibition with 5 and 7 $v/v\%$ DEE in the aqueous phase.

Rock type	Oil	PV $[ml]$	DEE Conc. $[v/v\%]$	RF brine $[v/v]$	UR $[v/v]$
RFCW2	COA	8.66 ± 0.03	5%	0.62 ± 0.04	0.65 ± 0.03
			7%	0.56 ± 0.03	0.62 ± 0.03
RFCW3	COA	8.83 ± 0.03	5%	0.57 ± 0.03	0.61 ± 0.03
			7%	0.53 ± 0.03	0.61 ± 0.03
BRCW5	COA	8.15 ± 0.04	5%	0.51 ± 0.04	0.57 ± 0.04
			7%	0.45 ± 0.03	0.53 ± 0.03

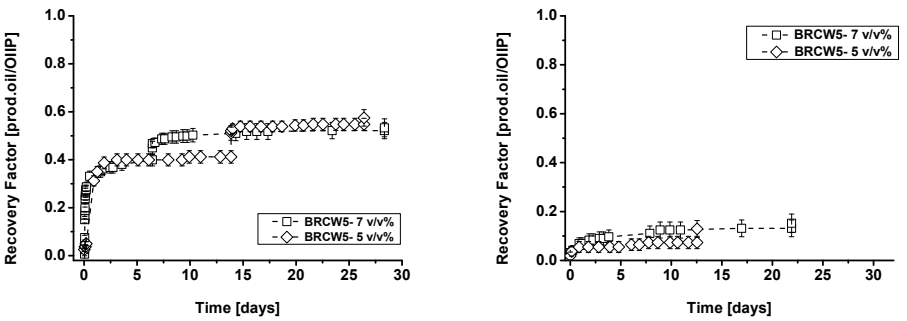

(a) (b)

Figure 3.5: Comparison between two-stage oil recovery from a water-wet core sample by a mixture of 7 $v/v\%$ DEE/brine and a mixture of 5 $v/v\%$ DEE/brine after the jump. Both experiments were performed on the same core, $BRCW5$ (see Table 3.5). In both experiments the primary imbibition was carried out by brine. The jump is caused due to detachment of the oil droplets from the rock surface by shaking the Amott cell. The core samples were saturated with crude oil A. The ultimate recovery for primary and secondary imbibition is the recovery obtained after shaking. (b) Comparison between incremental recoveries from 5 $v/v\%$ and from 7 $v/v\%$ DEE/brine mixture. The mixture of 7 $v/v\%$ DEE/brine led to a higher incremental recovery.

were released from the surface of the core at the end of the primary or secondary imbibition; there was no jump in the production curves. Similar to water-wet core samples, the imbibition process was capillary dominated, because the minimum inverse Bond number for the spontaneous imbibition in the mixed-wet cores was 97 ± 1.

3.4.2.1 One-stage imbibition versus two-stage imbibition

Figure 3.6 compares the one-stage imbibition versus the two-stage imbibition for mixed-wet Berea sandstone, $BRSM$, (see Fig. 3.6a), and for mixed-wet Silurian dolomite, $SLDM$, (see Fig. 3.6b). For both rock types, the ultimate recovery after the one-stage imbibition was approximately the same as the ultimate recovery after the two-stage imbibition process. The final recovery was $80 \pm 4\%$ of the OIIP for $BRSM5$ and was $35 \pm 3\%$ of the OIIP for $SLDM6$; the one-stage imbibition in mixed-wet dolomite cores led to a slightly lower ultimate recovery than the two-stage ultimate recovery. However, similar to water-wet samples, application of DEE/brine imbibition as a secondary method (one-stage) causes an accelerated oil recovery and a higher imbibition rate than a tertiary method (two-stage). The results are summarized in Table 3.6.

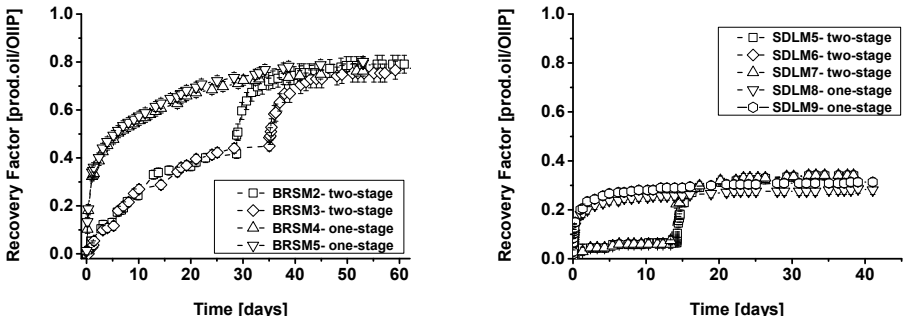

(a) (b)

Figure 3.6: (a) Comparison between the oil recovery from mixed-wet Berea core samples ($BRSM$) by a 7 $v/v\%$ DEE/brine mixture from the one-stage imbibition and from the two-stage imbibition with brine (primary stage; $30 - 40$ *days*) and a 7 $v/v\%$ DEE/brine mixture. In contrast to the behavior of the water-wet cores, all oil drops were released from the surface of the core at the end of the primary or secondary imbibition; there was no jump in the production curves. All core samples were saturated with crude oil B. The ultimate recovery was approximately the same for both the one-stage and the two-stage imbibition. (b) Comparison between oil recovery from mixed-wet dolomite core samples ($SLDM$) by a 7 $v/v\%$ DEE/brine mixture from the one-stage imbibition and from the two-stage imbibition with brine (primary stage; 15 *days*) and a 7 $v/v\%$ DEE/brine mixture. All core samples were saturated with crude oil B. The ultimate recovery was approximately the same both for the one-stage and for the two-stage imbibition.

Table 3.6: Oil recovery by the one-stage imbibition and the two-stage imbibition from mixed-wet core samples.

Rock type	DEE conc. $[v/v]$	S_{wc}	RF brine	Incr. RF	UR $[v/v]$
$BRSM2$	7%	0.164	0.50 ± 0.02	0.59 ± 0.04	0.79 ± 0.02
$BRSM3$	7%	0.193	0.49 ± 0.02	0.74 ± 0.04	0.86 ± 0.02
$BRSM4$	7%	0.173			0.76 ± 0.02
$BRSM5$	7%	0.195			0.80 ± 0.02
$BRSM6$	5%	0.173	0.49 ± 0.02	0.52 ± 0.03	0.75 ± 0.02
$BRSM7$	5%	0.171	0.46 ± 0.02	0.47 ± 0.03	0.73 ± 0.02
$SLDM5$	7%	0.120	0.07 ± 0.02	0.29 ± 0.02	0.34 ± 0.02
$SLDM6$	7%	0.126	0.06 ± 0.02	0.30 ± 0.02	0.35 ± 0.02
$SLDM7$	7%	0.111	0.08 ± 0.02	0.29 ± 0.02	0.34 ± 0.02
$SLDM8$	7%	0.132			0.34 ± 0.02
$SLDM9$	7%	0.144			0.37 ± 0.02

3.4.2.2 Effect of the DEE concentration on the oil recovery from mixed-wet cores

Contrary to the water-wet core samples, the initial DEE concentration could affect the ultimate recovery from the mixed-wet cores. Primary imbibition was approximately 45% of the OIIP for all cores; but the production rate and the incremental recoveries by 5 v/v% and by 7 v/v% DEE/brine mixtures from $BRSM$ were different (see Fig. 3.7). The 7 v/v% DEE/brine mixture improved both ultimate recovery and the imbibition rate in comparison to the 5 v/v% mixture. For comparison, incremental recovery after imbibition of 7 v/v% and of 5 v/v% mixtures were about 70% of the remaining oil and 50% of the remaining oil respectively, which corresponds to an extra recovery of 30% and 20% of the OIIP respectively. It appears that DEE/brine with a higher DEE concentration was more effective in the mixed-wet Berea cores than in the water-wet sandstone cores. A tentative explanation is as follows. The 7 v/v% mixture caused a higher oil swelling and, as a result, a higher oleic phase saturation. Consequently, the relative permeability of the oleic phase increased and a higher oil mobility was obtained. At the same time, the viscosity reduction contributed to the production, but it was considered less important.

3.4.2.3 Comparison between oil recovery from mixed-wet sandstone and dolomite cores

Figure 3.8 compares the two-stage imbibition process between $BRSM$ and $SLDM$. The permeability of the samples was in the same range, and they were aged by

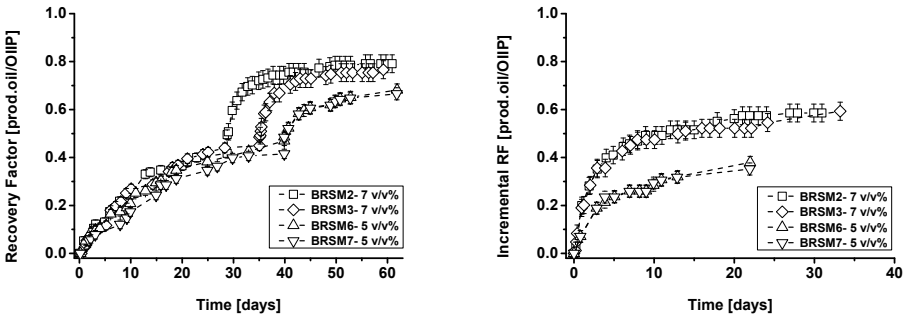

(a) (b)

Figure 3.7: (a) Comparison between oil recovery by two-stage imbibition of brine and 5 $v/v\%$ DEE/brine, and of brine and 7 $v/v\%$ DEE/brine from mixed-wet Berea cores. All core samples were saturated with crude oil B (see Table 3.1). A mixture of 7 $v/v\%$ DEE/brine led to a higher ultimate recovery in comparison to a mixture of 5 $v/v\%$ DEE/brine. (b) Comparison between the incremental recovery by 5 $v/v\%$ and 7 $v/v\%$ DEE/brine mixture from mixed-wet Berea cores. The 7 $v/v\%$ DEE/brine mixture led to a higher incremental recovery and imbibition rate compared to a 5 $v/v\%$ DEE/brine mixture.

the same procedure; however, the connate water saturation was different (see Table 3.6). The primary production, the ultimate recovery, the incremental recovery and the imbibition rate in $BRSM$ cores were higher than those in $SLDM$ cores. As stated before, in the water-wet cores with a higher remaining oil, the DEE/brine imbibition process led to a higher oil recovery during the secondary imbibition stage. Nevertheless, the comparison between the $SLDM$ and $BRSM$ shows a different trend. This possibly implies that another mechanism contributes to the oil recovery in the mixed-wet core samples.

3.4.2.4 Comparison between oil recovery from mixed-wet and water-wet Berea

The two-stage recovery from mixed-wet Berea and water-wet Berea is shown in Fig. 3.9 to emphasize the distinction between the oil recovery. The permeability of the core samples was more or less the same, and the brine imbibition obtained an approximately similar primary recovery. But, with the DEE/brine imbibition, the ultimate recovery, the incremental recovery and the imbibition rate were higher in the mixed-wet cores than in the water-wet cores. Indeed, the viscosities of both crude oils were not the same. However, this large difference between the recoveries cannot be explained by viscosity only.

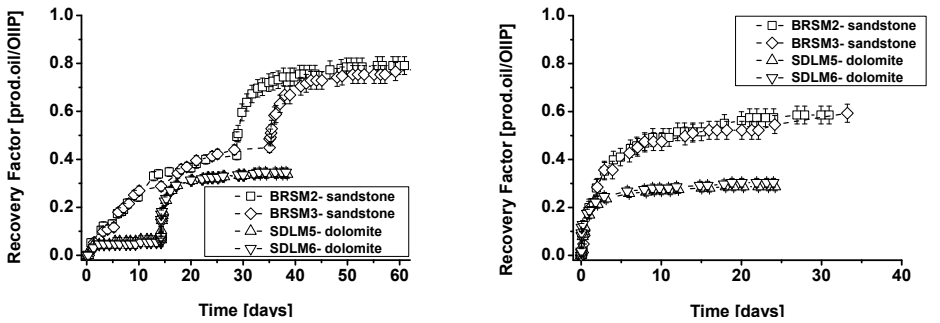

(a) (b)

Figure 3.8: (a) Comparison between oil recovery from mixed-wet Berea core samples and mixed-wet Silurian dolomite core samples during the two-stage imbibition with brine and 7 v/v% DEE/brine. All core samples were saturated with crude oil B. The primary recovery, the ultimate recovery and the imbibition rate in the mixed-wet core ($BRSM$) were higher than in the mixed-wet Silurian dolomite ($SLDM$). (b) Comparison between the incremental recovery of remaining oil from DEE/brine imbibition; the incremental recovery from $BRSM$ was higher than from $SLDM$.

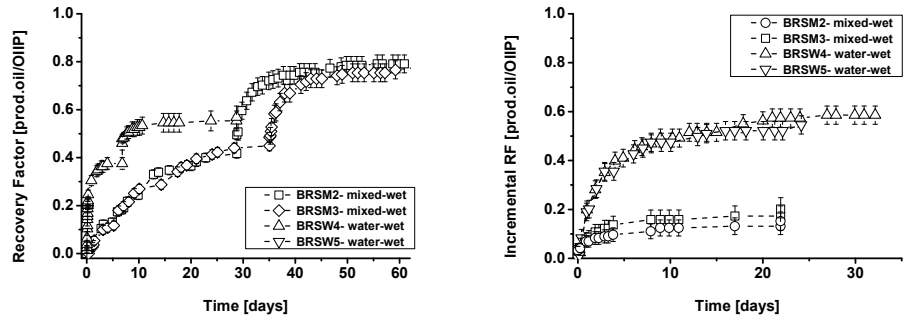

(a) (b)

Figure 3.9: (a) The two-stage spontaneous imbibition in mixed-wet Berea cores versus water-wet Berea cores. Water-wet cores were saturated with crude oil A, while mixed-wet cores were saturated with crude oil B. Primary imbibition was performed using brine, whereas for secondary imbibition a mixture of 7 v/v% DEE/brine was used. (b) Incremental recovery from DEE/brine imbibition in mixed-wet Berea ($BRSM$) vs. water-wet Berea ($BRSW$) is shown. DEE/brine imbibition led to a higher incremental oil recovery in the $BRSM$ core than the recovery in the $BRSW$ core.

3.5 Numerical modeling

The purpose of the numerical modeling was to investigate the mechanisms of the DEE-enhanced spontaneous imbibition into a single matrix, which was surrounded by

fractures. Our experimental observation was, that the DEE/brine imbibition reduced the remaining oil in the core. We combined mass conservation of the components and Darcy's law with a simplified (constant partition coefficient) phase behavior of the DEE-brine-crude oil system to develop a numerical model for DEE/brine spontaneous imbibition. Afterwards, we solved the model equations using a commercial finite element package (COMSOL Multiphysics). In this section, we will describe the details of the ensuing equations and the numerical modeling results of three experiments.

3.5.1 Model description

The imbibition process occurs in a cylindrically symmetric geometry (core). The vertical cross-section of the cylinder is a rectangular plane. We developed a 2-D axially-symmetric, two-phase and three-components model for the DEE/brine spontaneous imbibition in a matrix block that is surrounded by fractures. The initial and the boundary conditions were established assuming capillary-gravity equilibrium. First, we optimized the agreement between the experimental primary recovery (recovery with brine) and the simulation, by modifying the sorting factor, relative permeability end-points and capillary entry pressure. Afterwards, the proper relative permeability and capillary pressure functions were used to model the spontaneous imbibition of a DEE/brine mixture into the core.
The combination of mass conservation for the oil, the brine and the solvent components with Darcy's law reads:

$$\sum_{\alpha=1}^{2}\sum_{c=1}^{3}\Big(\varphi\frac{\partial}{\partial t}(S_\alpha V_{\alpha c})+\nabla.\big(V_{\alpha c}u_\alpha(S_a,V_{aw},P_a)\big)-\nabla.(\varphi D_{sc}S_\alpha\nabla.V_{\alpha c})\Big)=0,$$
$$\alpha=o,a,\qquad c=h,w,s, \quad (3.3)$$

where S_α denotes the saturation of phase α, P_α is the pressure of phase α, $V_{\alpha c}$ is the volume fraction of component c in phase α, i.e. V_{aw} is the volume fraction of the brine component in the aqueous phase, u_α is the Darcy velocity of phase α, which is calculated from Darcy's equation (equation 3.4), D_{sc} is the molecular diffusion coefficient of DEE in the aqueous or in the oleic phase. The subscripts a, o, s, w and h denote the aqueous phase, the oleic phase, the solvent component, the brine component and the hydrocarbon component, respectively. A similar set of equations was used to simulate the spontaneous imbibition of brine into the core.
The Darcy velocity for phase α is defined by:

$$u_\alpha(P_\alpha,V_{aw},S_a)=-\frac{kk_{r\alpha}(S_a)}{\mu_\alpha(V_{aw})}(\nabla P_\alpha+\rho_\alpha(V_{aw})g\mathbf{e}_z), \quad (3.4)$$

where k is the absolute permeability, $k_{r\alpha}$ is the relative permeability of phase α, μ_α is the viscosity of phase α, ρ_α is the density of phase α, g is the acceleration due to

gravity, and z is the upward vertical distance with $z = 0$ at the bottom of the core. The molecular diffusion of DEE in the oleic or in the aqueous phase is calculated from the Wilke-Chang correlation [52]:

$$D_{sc} = 7.4 \times 10^{-8} \Big(\frac{T(\phi_c \, M_c)^{1/2}}{\mu_c \hat{V}_s^{0.6}} \Big), \tag{3.5}$$

where ϕ_c is the association parameter, which is equal to one, both for crude oil and for brine, M_c is the molecular weight of oil or of brine, $\mu_c[mPa.s]$ is the viscosity of oil or of brine, $\hat{V}_s[cm^3/mol]$ is the molar volume of DEE, defined as the volume of a mole of DEE at its normal boiling point, and $T[K]$ is the temperature.
The system of equations is not yet complete, i.e. there are 8 unknowns with 3 equations; therefore, we use five additional auxiliary equations, viz.:

$$\sum V_{ac} = 1, \qquad c = w, s, \tag{3.6}$$

$$\sum V_{oc} = 1, \qquad c = h, s, \tag{3.7}$$

$$\sum S_{\alpha} = 1, \qquad \alpha = o, a, \tag{3.8}$$

$$P_c(S_{\alpha}) = P_a - P_o, \tag{3.9}$$

$$V_{as} = K_{oa} V_{os}, \tag{3.10}$$

where P_c is the capillary pressure function, V_{os} is the volume fraction of DEE in the oleic phase and K_{oa} is the partition coefficient of DEE, which is defined as the volume fraction of DEE in the oleic phase divided by the volume fraction of DEE in the aqueous phase. The capillary pressure function is described by the Brooks-Corey correlation:

$$P_c(S_a) = P_{cb} S_e(S_a)^{(-1/\lambda)}, \tag{3.11}$$

where S_e is the effective saturation, and P_{cb} is the capillary entry pressure, which is defined by:

$$P_{cb} = \gamma \sigma \sqrt{\frac{\varphi}{K}} S_e(0.5)^{(1/\lambda)}, \tag{3.12}$$

where γ is a fitting parameter for the capillary pressure function, σ is the interfacial tension, φ is the porosity of the rock, λ is the sorting factor, S_a is the saturation of the aqueous phase. The effective saturation of the aqueous phase is defined by:

$$S_e(S_a) = \frac{S_a - S_{wc}}{1 - S_{wc} - S_{or}}. \tag{3.13}$$

where S_{wc} is the connate water saturation, S_{or} is the residual oil saturation. The capillary pressure function was extended below the connate water saturation ($S_a < S_{wc}$) in order to avoid instabilities due to infinite capillary pressures near S_{wc}. We disregarded the negative capillary pressure in mixed-wet cores.

The relative permeabilities use the residual oil saturation and the sorting factor as fitting parameters. The relative permeability curves were also described by the Brooks-Corey correlation:

$$k_{ra}(S_a) = k^e_{ra} S_e(S_a)^{(3+2/\lambda)}, \tag{3.14}$$

$$k_{ro}(S_a) = k^e_{ro}(1 - S_e(S_a))^2(1 - S_e(S_a)^{(1+2/\lambda)}), \tag{3.15}$$

where k^e_{ra} and k^e_{ro} are the end-point relative permeability for the aqueous phase and for the oleic phase.

The viscosity of both the oleic and the aqueous phase were obtained from an empirical correlation (quarter-power law):

$$\mu_a = \left(\frac{V_{aw}}{\mu_W^{1/4}} + \frac{V_{as}}{\mu_S^{1/4}} \right)^{-4}, \tag{3.16}$$

$$\mu_o = \left(\frac{V_{oh}}{\mu_H^{1/4}} + \frac{V_{os}}{\mu_S^{1/4}} \right)^{-4}, \tag{3.17}$$

where V_{oh} is the volume fraction of hydrocarbon in the oleic phase, μ_W is the viscosity of pure brine, μ_H is the viscosity of pure hydrocarbon and μ_S is the viscosity of pure DEE. In addition, the densities of the aqueous phase and of the oleic phase were obtained by:

$$\rho_a = \frac{1}{\frac{V_{os}}{\rho_S} + \frac{V_{aw}}{\rho_W}}, \tag{3.18}$$

$$\rho_o = \frac{1}{\frac{V_{os}}{\rho_S} + \frac{V_{oh}}{\rho_H}}, \tag{3.19}$$

where ρ_W, ρ_H and ρ_S are the density of pure brine, of pure oil and of pure DEE respectively.

The initial and boundary conditions were defined by the application of the capillary-gravity equilibrium around the core. The integrated oil production through the whole domain was used to calculate the oil recovery curve. We solved the model equations using a commercial equation based finite element package (COMSOL Multiphysics). The relative correspondence between the experimental results and the numerical model was modified using the matching parameters, e.g. sorting factor, end-points and the capillary entry pressure. Fig. 3.10 shows the distribution of the hydrocarbon in the core, which is obtained from the numerical model at time 4.55×10^6 seconds. Arrows show the upstream hydrocarbon concentration towards the downstream hydrocarbon concentration. The sensitivity of the numerical results to the input parameters is addressed in section 4.5.1.

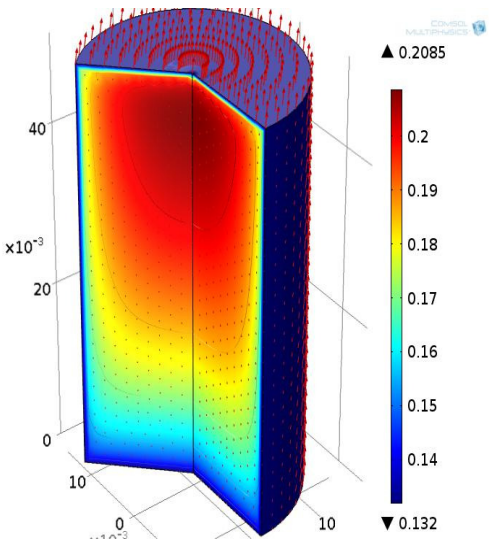

Figure 3.10: A distribution of hydrocarbon in the core is shown. The distribution is obtained form the numerical model at time 4.55×10^6 seconds. Arrows show the upstream hydrocarbon concentration towards the downstream hydrocarbon concentration.

3.5.2 Model results and comparison to experiments

Our hypothesis in this research is that the DEE transport mechanism involves convection and diffusion. We assume that there is instantaneous local thermodynamic equilibrium between the components in the oleic and in the aqueous phases. Capillary forces displace the aqueous phase into the core, gravity forces displace the bulk fluid, and molecular diffusion displaces components comprising the oleic and the aqueous phases. Locally, DEE partitions instantaneously between the oleic and the aqueous phases. As the volume of the aqueous phase is less affected by the presence of DEE than the volume of the oleic phase, the total volume of the fluids increases. Furthermore, with the DEE dissolution in oil, the production rate is increased due to the oil viscosity reduction.

Figure 3.11a depicts numerical modeling of the primary oil recovery by the spontaneous imbibition of brine into an oil-filled Berea core ($BRCW4$). The core was placed in the Amott cell and the cell was filled with brine. The recovery was recorded as a function of time. Our model shows that capillary diffusion causes brine to imbibe into the core. A primary oil recovery of 47% of the OIIP was reproduced by the numerical model. However, there is a poor agreement between the model and the experimental results during $0.4 - 2$ days after exposing the core to a brine solution (see Fig. 3.11a). The observed discrepancy is possibly due to delayed recovery in the experimental results. The possible reasons for the delay in the production curve are

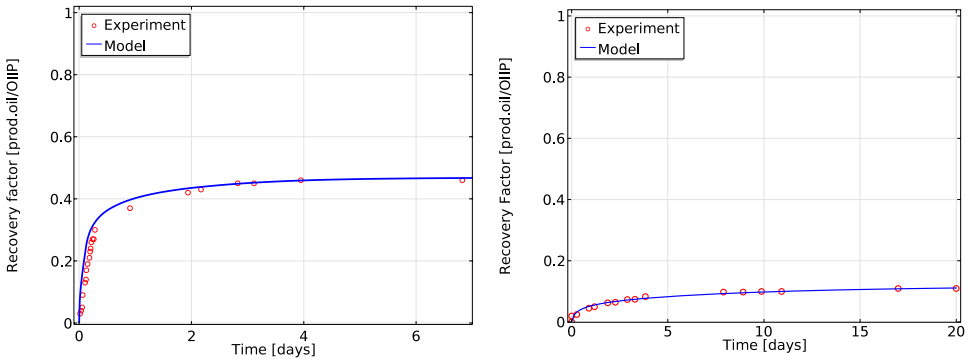

(a) (b)

Figure 3.11: (a) Numerical modeling of the primary oil recovery by spontaneous imbibition of brine into an oil-filled water-wet Berea core ($BRCW4$). The numerical model shows that brine is imbibing into the core due to capillary diffusion. A primary recovery of 46% of the OIIP was reproduced by the numerical model. However, there is a poor agreement between the numerical model and the experimental results during $0.4 - 2$ days after exposing the core to brine. A reason for such a discrepancy is that the drops that were attached to the rock surface caused a delayed recovery in the experimental results. (b) Our numerical model predicts that imbibition of the solvent into the core and the DEE partitioning into the oleic phase induces swelling of the oil and reduces the oil viscosity. Hence, an extra oil recovery of 11% of the OIIP was produced.

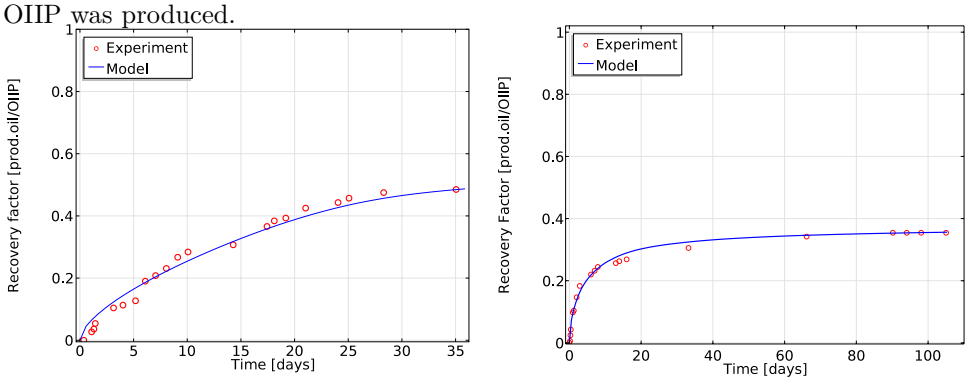

(a) (b)

Figure 3.12: There is good agreement between the numerical model and the spontaneous imbibition in an oil-filled mixed-wet Berea core ($BRSM3$). (a) Numerical modeling of the primary oil recovery by spontaneous imbibition of brine into the ($BRSM3$) core. Our model shows that water imbibes into the core due to capillary diffusion. The primary recovery of 48% of the OIIP was predicted by the numerical model. (b) There is a good agreement between the experimental results and the numerical model in DEE/brine imbibition into the $BRSM3$ core. The model reproduced an extra oil recovery of 35% of the OIIP due to DEE/brine imbibition.

Table 3.7: Model parameters used in the numerical simulations of DEE imbibition.

Parameter	$BRCW4$	$BRSM3$	$SLDM5$
$P_{cb},\ Pa$	2.9×10^4	12.1	5.0
K^e_{ra}	0.3	0.2	0.8
K^e_{ro}	0.85	0.2	0.8
λ	0.5	0.7	1
ROS	0.53	0.52	0.93
K_{oa}	1.7	2.9	2.5
$D_o,\ (m^2/s)$	2.3×10^{-11}	1×10^{-10}	1×10^{-10}
$D_a,\ (m^2/s)$	8×10^{-10}	8×10^{-10}	8×10^{-10}

listed on page 85.

Figure 3.11b shows the numerical modeling of DEE/brine imbibition in $BRCW4$ water-wet core. Our numerical model for the DEE/brine imbibition process (the secondary imbibition stage) includes the DEE transfer from the aqueous phase into the oleic phase, assuming instantaneous thermodynamic equilibrium. The mechanism of the DEE transfer depends on the DEE molecular diffusion both in the aqueous and in the oleic phase. The molecular diffusion of DEE in the oleic phase is slow, but upon dilution of the oleic phase due to DEE dissolution, it is accelerated by a factor of 200 in the extremely diluted oleic phase (crude oil A). The molecular diffusion of DEE in the aqueous phase is however, one order of magnitude faster than the molecular diffusion in the oleic phase. Upon DEE transfer to the oleic phase, the volume of the oleic phase increases (oil swelling). Another mechanism contributing to the oil swelling is that the DEE molecule has a larger volume in the oleic phase than in the aqueous phase, which further improves the swelling effect. Moreover, with the DEE transfer into the oleic phase, the oil viscosity is reduced, which leads to an accelerated oil production. Figure 3.11b shows a good agreement between the experimental results and the numerical model. The model parameters are shown in Table 3.7.

Figure 3.12a shows numerical simulation of the primary oil recovery by spontaneous imbibition from mixed-wet Berea core $BRSM3$; when the core was exposed to a brine mixture. Similar to $BRCW4$, the driving force for the penetration of brine into the core was capillary diffusion. The model predicted a primary oil recovery of 49% of the OIIP, which agreed with the oil recovery in the experiment. The production plateau time in $BRSM3$ was much longer than $BRCW4$, which indicated that the $BRSM3$ core was less water-wet than the $BRCW4$ core. Fig. 3.12b shows the secondary oil recovery by DEE/brine imbibition into $BRSM3$. A good agreement between the numerical model and the experimental result was obtained. The model parameters are shown in Table 3.7.

The prediction of the oil recovery by brine imbibition from $SLDM5$ core is

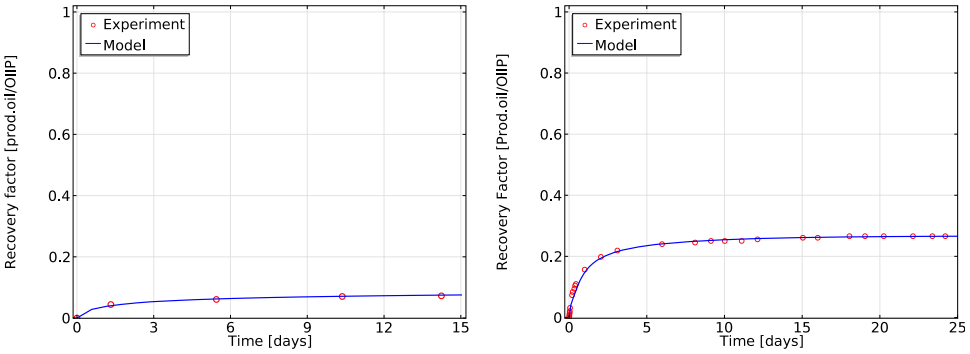

(a) (b)

Figure 3.13: A good agreement between the numerical model and the spontaneous imbibition on the $SLDM5$ core. (a) Numerical modeling of the primary oil recovery by spontaneous imbibition of brine into an oil-filled mixed-wet dolomite core ($SLDM5$). Our model shows that brine imbibes into the core due to capillary diffusion. The primary recovery of 7% of the OIIP was predicted by the numerical model. (b) There is a good agreement between the experimental results and the numerical model in DEE/brine imbibition into $SLDM5$. The model reproduced an extra oil recovery of 27% of the OIIP due to DEE/brine imbibition.

shown in Fig. 3.13a. Similar to previous studies, capillary diffusion led to brine imbibition into the core. However, the oil recovery was very low, i.e. 7% of the OIIP. This indicated that $SLDM5$ core was more hydrophobic than both $BRCW4$ and $BRSM3$ cores. The tuned model and the experimental results of DEE/brine imbibition are presented in Fig. 3.13b, which both show an extra oil recovery of 27% of the OIIP. The model parameters are also shown in Table 3.7.

3.6 Concluding remarks

We investigated the possibility of increasing the recovery factor and enhancing the recovery rate by the addition of diethyl ether to brine. The main oil recovery mechanisms by spontaneous imbibition of DEE/brine can be studied using an Amott cell. The primary recovery with brine from water-wet cores was $46-67\%$ of the OIIP. By adding DEE, the additional oil recovery in water-wet cores was 1-11% of the OIIP. In mixed-wet Berea (mixed-wet dolomite) cores, a primary oil recovery of $49-50\%$ $(6-8\%)$ of the OIIP was produced after brine imbibition. With DEE/brine, an additional oil recovery of $29-37\%$ $(27-29\%)$ of the OIIP was produced from mixed-wet Berea (mixed-wet dolomite) cores, which was higher than the additional recovery from water-wet cores. We developed a model to describe the DEE/brine imbibition into an oil-filled core. The model involves the transport of DEE from the aqueous phase into the oleic phase due to partitioning, molecular diffusion of DEE

from DEE-rich zone into DEE-free zone, oil recovery due to oil swelling (dilution) and oil recovery acceleration due to oil viscosity reduction. The model comprises Darcy's law and the simplified phase behavior of the DEE-brine-crude oil system. The model parameters were optimized to mimic the experimental results. The optimized simulations show good agreement with the experiments, except at intermediate times when the computed recovery was higher than the experimental recovery.

3

Bibliography

[1] A. Saidi, "Simulation of Naturally Fractured Reservoirs," in *Proceedings of SPE Reservoir Simulation Symposium*, vol. v. San Francisco, California, USA: Society of Petroleum Engineers, Nov. 1983.

[2] H. Salimi and J. Bruining, "Upscaling of Fractured Oil Reservoirs Using Homogenization Including Non-Equilibrium Capillary Pressure and Relative Permeability," *Computational Geosciences*, vol. 16, no. 2, pp. 367–389, Dec. 2011.

[3] J. Warren and P. Root, "The Behavior of Naturally Fractured Reservoirs," *Society of Petroleum Engineers Journal*, vol. 3, no. 3, pp. 245–255, Sep. 1963.

[4] N. R. Morrow and G. Mason, "Recovery of Oil by Spontaneous Imbibition," *Current Opinion in Colloid & Interface Science*, vol. 6, no. 4, pp. 321–337, Aug. 2001.

[5] A. Mirzaei-Paiaman, M. Masihi, and D. C. Standnes, "Index for Characterizing Wettability of Reservoir Rocks Based on Spontaneous Imbibition Recovery Data," *Energy and Fuels*, vol. 27, pp. 7360–7368, 2013.

[6] T. Babadagli, "Scaling of Cocurrent and Countercurrent Capillary Imbibition for Surfactant and Polymer Injection in Naturally Fractured Reservoirs," *SPE Journal*, vol. 6, no. 4, pp. 19–23, Dec. 2001.

[7] P. P. M. Keijzer and A. S. D. Vries, "Imbibition of Surfactant Solutions," *SPE Advanced Technology Series*, vol. I, no. 2, pp. 110–113, 1990.

[8] D. Schechter, D. Zhou, and F. Orr, "Capillary Imbibition and Gravity Segregation in Low Ift Systems," in *Proceedings of SPE Annual Technical Conference and Exhibition*, no. 1. Dallas, Texas, USA: Society of Petroleum Engineers, Oct. 1991.

[9] D. Schechter, D. Zhou, and F. Orr, "Low IFT Drainage and Imbibition," *Journal of Petroleum Science and Engineering*, vol. 11, no. 4, pp. 283–300, 1994.

[10] X. Zhou, O. Torsaeter, X. Xie, and N. Morrow, "The Effect of Crude-Oil Aging Time and Temperature on the Rate of Water Imbibition and Long-Term Recovery by Imbibition," *SPE Formation Evaluation*, vol. 10, no. 4, pp. 259–265, Dec. 1995.

[11] A. Mirzaei-Paiaman, M. Masihi, and D. C. Standnes, "An Analytic Solution for the Frontal Flow Period in 1d Counter-Current Spontaneous Imbibition Into Fractured Porous Media Including Gravity and Wettability Effects," *Transport in Porous Media*, vol. 89, no. 1, pp. 49–62, Mar. 2011.

[12] W. Plug and J. Bruining, "Capillary Pressure for the Sand-CO2-Water System under Various Pressure Conditions. Application to CO2 Sequestration," *Advances in Water Resources*, vol. 30, no. 11, pp. 2339–2353, Nov. 2007.

[13] G. Barenblatt, T. Patzek, and D. Silin, "The Mathematical Model of Non-Equilibrium Effects in Water-Oil Displacement," in *Proceedings of SPE/DOE Improved Oil Recovery Symposium*, no. December. Society of Petroleum Engineers, Apr. 2002, pp. 409–416.

[14] C. Mattax and J. Kyte, "Imbibition Oil Recovery from Fractured, Water-Drive Reservoir," *Old SPE Journal*, vol. 2, pp. 177–184, 1962.

[15] O. Torsaeter, "An Experimental Study of Water Imbibition in Chalk from the Ekofisk Field," in *Proceedings of SPE Enhanced Oil Recovery Symposium*. Tulsa, Oklahoma, USA: Society of Petroleum Engineers, Apr. 1984.

[16] S. Ma, N. Morrow, and X. Zhang, "Generalized Scaling of Spontaneous Imbibition Data for Strongly Water-Wet Systems," in *Proceedings of Technical Meeting / Petroleum Conference Of The South Saskatchewan Section*. Society of Petroleum Engineers, Oct. 1995.

[17] A. Mirzaei-Paiaman and M. Masihi, "Scaling Equations for Oil/Gas Recovery from Fractured Porous Media by Counter-Current Spontaneous Imbibition: from Development to Application," *Energy and Fuels*, vol. 27, pp. 4662–4676, 2013.

[18] S. Ghedan and F. Poettmann, "Effect of Polymers on the Imbibition Process: a Laboratory Study," *SPE Reservoir Engineering*, vol. 6, no. 1, pp. 84–90, Feb. 1991.

[19] K. Li, K. Chow, and R. Horne, "Influence of Initial Water Saturation on Recovery by Spontaneous Imbibition in Gas/Water/Rock Systems and the Calculation of Relative Permeability," *SPE Reservoir Evaluation & Engineering*, vol. 9, no. 4, pp. 295–301, Aug. 2006.

[20] L. Kewen, C. Kevin, and R. Horne, "Effect of Initial Water Saturation on Spontaneous Water Imbibition," in *Proceedings of SPE Western Regional/AAPG Pacific Section Joint Meeting*. Anchorage, Alaska, USA: Society of Petroleum Engineers, May 2002.

[21] X. Zhou, N. Morrow, and S. Ma, "Interrelationship of Wettability, Initial Water Saturation, Aging Time, and Oil Recovery by Spontaneous Imbibition and Waterflooding," *SPE Journal*, vol. 5, no. 2, pp. 21–24, Jun. 2000.

[22] H. Kazemi, J. Gilman, and A. Elsharkawy, "Analytical and Numerical Solution of Oil Recovery from Fractured Reservoirs With Empirical Transfer Functions (Includes Associated Papers 25528 and 25818)," *SPE Reservoir Engineering*, vol. 7, no. 2, May 1992.

[23] B. Bourbiaux and F. Kalaydjian, "Experimental Study of Cocurrent and Countercurrent Flows in Natural Porous Media," *SPE Reservoir Engineering*, vol. 5, no. 3, pp. 361–368, Aug. 1990.

[24] M. Chahardowli, A. Zholdybayeva, R. Farajzadeh, and H. Bruining, "Solvent-Enhanced Spontaneous Imbibition in Fractured Reservoirs," in *Proceedings of 75th EAGE Conference & Exhibition incorporating SPE EUROPEC 2013*. Society of Petroleum Engineers, Jul. 2013.

[25] M. Chahardowli, R. Farajzadeh, and H. Bruining, "Numerical Simulation of Mutually Soluble Solvent-Aided Spontaneous Imbibition in Fractured Reservoirs," in *14th European Conference on the Mathematics of Oil Recovery*, Catania, Sep. 2014.

[26] A. Chernetsky, S. Masalmeh, D. Eikmans, P. D. Boerrigter, C. Parsons, A. Parker, D. Boersma, J. Cui, B. Dindoruk, P. te Riele, A. Kindi, and N. Azri, "Experimental Results and Modelling Workflow of the DME Enhanced Waterflood Technology," in *The Abu Dhabi International Petroleum Exhibition and Conference, ADIPEC*. Society of Petroleum Engineers, 2015.

[27] M. Chahardowli, R. Farajzadeh, and H. Bruining, "Experimental Investigation of the Use of the Dimethyl Ether/Polymer Hybrid as a Novel Enhanced Oil Recovery Method," *accepted for publication in Journal of Industrial and Engineering Chemistry*, DOI:10.1016/j.jiec.2016.04.008.

[28] J. Groot, A. Chernetsky, P. Te Riele, B. Dindoruk, J. Cui, L. Wilson, and R. Ratnakar, "Representation of Phase Behavior and PVT Workflow for DME Enhanced Water-Flooding," in *SPE EOR Conference at Oil and Gas West Asia*. Society of Petroleum Engineers, 2016.

[29] P. t. Riele, C. Parsons, P. Boerrigter, J. Plantenberg, B. Suijkerbuijk, J. Burggraaf, A. Chernetsky, D. Boersma, and R. Broos, "Implementing a Water Soluble Solvent Based Enhanced Oil Recovery Technology-Aspects of Field Development Planning," in *SPE EOR Conference at Oil and Gas West Asia*. Society of Petroleum Engineers, 2016.

[30] A. Alkindi, N. Al-Azri, D. Said, K. AlShuaili, and P. Te Riele, "Persistence in EOR-Design of a Field Trial in a Carbonate Reservoir Using Solvent-Based Water-Flood Process," in *SPE EOR Conference at Oil and Gas West Asia*. Society of Petroleum Engineers, 2016.

[31] M. Chahardowli, R. Farajzadeh, and H. Bruining, "Experimental Investigation of the Use of Dimethyl Ether/Polymer Hybrid as an Enhanced Oil Recovery Method," in *SPE EOR Conference at Oil and Gas West Asia*, 2016.

[32] S. Shenawi and C. Wu, "Compositional Simulation of Carbonated Waterfloods in Naturally Fractured Reservoirs," in *Proceedings of SPE/DOE Improved Oil Recovery Symposium*. Tulsa, Oklahoma: Society of Petroleum Engineers, Apr. 1994.

[33] A. Leo, C. Hansch, and D. Elkins, "Partition Coefficients and Their Uses," *Chem. Rev.*, vol. 71, no. 6, 1971.

[34] M. Riazi, M. Jamiolahmady, and M. Sohrabi, "Theoretical Investigation of Pore-Scale Mechanisms of Carbonated Water Injection," *Journal of Petroleum Science and Engineering*, vol. 75, no. 3-4, pp. 312–326, Jan. 2011.

[35] R. Simon and D. Graue, "Generalized Correlations for Predicting Solubility, Swelling and Viscosity Behavior of CO2 -Crude Oil Systems," *Journal of Petroleum Technology*, vol. 17, no. 1, Jan. 1965.

[36] S. Farouq Ali and S. Thomas, "Enhanced Oil Recovery - What We Have Learned," *Journal of Canadian Petroleum Technology*, vol. 39, no. 2, Feb. 2000.

[37] M. Klins, *Carbon Dioxide Flooding: Basic Mechanisms and Project Design*, ist editio ed. Springer, 1984.

[38] L. Holm and A. Csaszar, "Oil Recovery by Solvents Mutually Soluble in Oil and Water," *Society of Petroleum Engineers Journal*, vol. 2, no. 2, Jun. 1962.

[39] J. N. Israelachvili, *Intermolecular and Surface Forces: Revised Third Edition*. Academic press, 2011.

[40] Y. Dong, B. Dindoruk, C. Ishizawa, E. Lewis, and T. Kubicek, "An Experimental Investigation of Carbonated Water Flooding," in *Proceedings of SPE Annual*

Technical Conference and Exhibition. Denver, Colorado, USA: Society of Petroleum Engineers, Oct. 2011.

[41] L. Lake, *Enhanced Oil Recovery*, 1st ed. Prentice Hall, Jan. 1989, vol. 12, no. 1.

[42] A. E. Peksa, K.-H. A. Wolf, and P. L. Zitha, "Bentheimer sandstone revisited for experimental purposes," *Marine and Petroleum Geology*, vol. 67, pp. 701 – 719, 2015.

[43] S. N. V. B.V., *Shell Smeermiddelen Voor Industrie En Scheepvaart*. Shell Nederland Verkoopmaatschappij B.V, 1992.

[44] S. Budavari, M. O'Neil, A. Smith, and P. Heckelman, "The merck index-encyclopedia of chemicals, drugs and biologicals. rahway, nj: Merck and co," *Inc*, vol. 512, p. 754, 1989.

[45] X. Meng, P. Zheng, J. Wu, and Z. Liu, "Density and viscosity measurements of diethyl ether from 243 to 373k and up to 20mpa," *Fluid Phase Equilibria*, vol. 271, no. 1, pp. 1–5, 2008.

[46] C. U. Hatiboglu and T. Babadagli, "Oil Recovery by Counter-Current Spontaneous Imbibition: Effects of Matrix Shape Factor, Gravity, Ift, Oil Viscosity, Wettability, and Rock Type," *Journal of Petroleum Science and Engineering*, vol. 59, no. 1-2, pp. 106–122, Oct. 2007.

[47] C. Hatiboglu and T. Babadagli, "Dynamics of spontaneous counter-current imbibition for different matrix shape factors, interfacial tensions, wettabilities and oil types," in *Canadian International Petroleum Conference*. Petroleum Society of Canada, 2004.

[48] H. Fischer, S. Wo, and N. Morrow, "Modeling the Effect of Viscosity Ratio on Spontaneous Imbibition," *SPE Reservoir Evaluation & Engineering*, vol. 11, no. 3, pp. 24–27, Jun. 2008.

[49] H. S. Behbahani, G. Di Donato, and M. J. Blunt, "Simulation of Counter-Current Imbibition in Water-Wet Fractured Reservoirs," *Journal of Petroleum Science and Engineering*, vol. 50, no. 1, pp. 21–39, Jan. 2006.

[50] K. S. Schmid and S. Geiger, "Universal Scaling of Spontaneous Imbibition for Water-Wet Systems," *Water Resources Research*, vol. 48, no. 3, p. W03507, Mar. 2012.

[51] L. W. Lake, R. Johns, B. Rossen, and G. Pope, *Fundamentals of Enhanced Oil Recovery*. Society of Petroleum Engineers, 2014.

[52] C. Wilke and P. Chang, "Correlation of Diffusion Coefficients in Dilute Solutions," *AIChE Journal*, vol. 1, no. 2, pp. 264–270, Jun. 2004.

Chapter

4

Mechanisms of oil recovery by dimethyl ether / brine spontaneous imbibition from water-wet and mixed-wet rocks

4.1 Summary

An experimental and numerical study of the enhancement and the acceleration of spontaneous imbibition using dimethyl ether was carried out, both in water-wet sandstone cores and in mixed-wet limestone cores. The primary recovery with brine from four cylindrical water-wet cores, with the top-end, bottom-end, both-ends and all sides open to brine imbibition, was $38 - 46\%$ of the OIIP. The production curves showed that in the laboratory, the recovery mechanism was mainly by capillary forces and that gravity effects were of minor importance. In addition, the recovery in the modified Amott cell was delayed by the attachment of oil droplets to the rock surface. These droplets moved slowly leading to a delay in the measured oil recovery of several days. By adding DME, the additional oil recovery in the water-wet cores was considerable (11-16% of the OIIP). The primary recovery with brine from the mixed-wet tight limestone cores was $1 - 2\%$ of the OIIP. The additional oil recovery in the mixed-wet cores was 43, 50 and 55% of the OIIP, which was much higher than

the additional recovery from the water-wet cores.
A workflow was considered to model DME-enhanced spontaneous imbibition experiments. The model comprises Darcy's law and the simplified phase behavior of the DME-brine-crude oil system. The model parameters were optimized to mimic the experimental results. Numerical simulation shows that the oil recovery is more sensitive to the molecular diffusion coefficient and to the partition coefficient, than to the relative permeability and capillary pressure. In the presence of a higher oil saturation in the core, a higher partition coefficient and a higher DME concentration in the aqueous phase, DME/brine imbibition leads to a higher oil recovery. It can be expected that the main mechanism for enhancing oil recovery by the DME/brine is determined by molecular diffusion. Capillary diffusion transports the water-wet phase quickly into the core, but, due to the exchange of DME with the oleic phase, will be largely depleted from DME. Consequently, transport of DME largely occurs due to diffusion. In view of the long gravity characteristic time, the effect of gravity forces was of minor importance.
The comparison between the theoretical and the experimental results shows that DME can enhance and accelerate the recovery from both water-wet and mixed-wet cores, albeit that slow diffusion is the rate-determining mechanism. The main oil recovery mechanism is oil swelling; oil viscosity reduction also accelerates the recovery.

4.2 Introduction

Spontaneous imbibition of mutually soluble solvents, e.g. diethyl ether, has shown potential possibilities for enhancing the oil recovery from fractured reservoirs [1, 2]. In some fractured reservoirs, the disconnected matrix blocks with a large storage capacity, are completely or partly surrounded by a highly conductive fracture network [3]. Therefore, both the ultimate oil recovery from fractured reservoirs and the oil production rate depend on the matrix-fracture mass exchange [4]. In the presence of a wetting phase in the fracture, spontaneous imbibition, which is driven by capillary forces, is responsible for the oil production from the matrix [5, 6]. In a spontaneous imbibition process, the aqueous phase imbibes into the pore space and displaces the oleic phase. The pressure difference between the oleic phase and the aqueous phase at the boundary of the core results in production of oil in the form of droplets [7]. In a lab experiment, the exiting oleic phase is surrounded by the aqueous phase. Usually, the droplet is bounded to the rock surface due to an opposite charge between the oil-water and rock-water interfaces [8, 9]; surface charges can be calculated by PHREEQC [10].
Moreover, depending on the relative dominance of the capillary or the gravity forces, spontaneous imbibition occurs in a form of countercurrent or co-current flow [11]. Indeed, the initial conditions influence the ultimate recovery as well as the production

rate [12].
However, for oil-wet conditions, gravity is the main mechanism for the oil production [13]. Low permeability of the matrix blocks or high oil viscosity can reduce the imbibition rates. Consequently, a high remaining oil saturation is obtained in practice [1, 2, 14–20].
The purpose of this chapter is to investigate the enhancement of the oil recovery by adding dimethyl ether (DME) to the imbibing aqueous phase. DME is the simplest ether, which has two methyl units connected to an oxygen atom. DME is available in large quantities and in recent years has received an interest as an alternative fuel [21, 22]. DME is in a gas state at atmospheric conditions; it has little impact on the land/water environment and a low toxicity [23–29]. Therefore, it is considered as a clean fuel and an environmentally acceptable chemical component [30]. Moreover, the Global Warming Potential (GWP) index of DME is one order (two orders) of magnitude lower than GWP of CO_2 (methane), i.e. 0.1 for DME, 1 for CO_2 and 21 for methane [31, 32]. Furthermore, liquefied DME has a very low viscosity, a low density and a high solubility in water [33]. DME is mutually soluble in brine and in oil; therefore, upon imbibition of the aqueous phase into the core, DME partitions into the oleic phase through the oil-water interface. Consequently, the volume of the oleic phase increases and the volume of the aqueous phase decreases. We refer to this dilution phenomenon as the swelling mechanism. In addition, because of the difference between the partial molar volumes of DME in the aqueous phase and in the oleic phase, the amount of transported DME has a larger volume in the oleic phase than in the aqueous phase [34], which leads to further oil recovery. At the same time, a part of the remaining oleic phase in the rock consists of dissolved DME, therefore for a given residual oleic phase saturation, less oil is left behind. Furthermore, with the partitioning of DME in the oleic phase, the oleic phase viscosity decreases, resulting in a more favorable displacement efficiency. Thus, DME/brine spontaneous imbibition leads to a higher recovery than brine imbibition without DME.
The purpose of the study is to experimentally quantify the oil recovery enhancement in solvent enhanced imbibition. The experimental results are interpreted using numerical modeling. The comparison shows which mechanisms are responsible for improved oil recovery.
The chapter is organized as follows: section 4.3 describes the experimental study. Section 4.4 introduces a theory of solvent enhanced imbibition and derives the ensuing model equations. Section 4.5 describes the experimental results both for the water-wet and for the mixed-wet cores and compares the numerical results with the experimental results. Conclusions are drawn at the final section.

4.3 Experimental study

The DME/brine imbibition experiments measure the oil production rate and the cumulative oil production at atmospheric conditions. It can be expected that DME has largely evaporated from the oleic phase. Indeed, the vapor pressure of pure DME at 20^oC is 5.1 bar, whereas the vapor pressure of crude oil is less than the vapor pressure of hexadecane (3×10^{-6} bar), and has much lower viscosity. A relation between the boiling point and the viscosity shows that a higher viscosity corresponds to a higher boiling point (Eq. 1.5-11 on page 31 Transport Phenomena 2001, Bird) [35]. Consequently, the evaporation rate of crude oil is negligible with respect to the evaporation rate of DME.

In addition, the effects of both the initial brine saturation and the boundary conditions on both the ultimate recovery and the imbibition rates were measured. The experiment used an in-house built modified Amott imbibition cell that made it possible to perform high-pressure (maximum 10 bar) spontaneous imbibition experiments (see Fig. 4.1). The reason for performing high-pressure experiments was to liquefy and mix DME with brine. Therefore, it was possible to immerse an oil-saturated core in a mixture of 10 ± 0.2 $mol\%$ DME in brine (DMEB). The rationale behind such a design was to keep DME dissolved in the system (in the liquid state). The imbibing fluid (brine or DMEB) was injected into the cell using a high precision Quizix pump that supplied DME through PEEK pipes. PEEK was chosen because it is compatible with DME [36]. A back-pressure valve adjusted the operating pressure of 9 ± 0.5 bar in the Amott cell. The produced oil from the sample was collected at the top graded part and was measured as a function of time.

4.3.1 Rock and fluid properties

The experiments used two different types of crude oil, two rock types with different permeabilities and different wetting properties, i.e. mixed-wet and water-wet core samples. A cylindrical plug of 38 ± 0.1 cm in length and 3 ± 0.1 cm in diameter was drilled from a cubic meter block of Berea and then cut in seven pieces. Limestone cores were prepared from core plugs obtained from a reservoir during the drilling operation. Afterwards, the cores were sawn to the desired length of 5.00 ± 0.1 cm using a water-cooled diamond saw. The diameter of all core samples was 3.00 ± 0.1 cm. The cores were dried in an oven at 55°C for about 24 $hours$. The used Berea sandstone was layered; hence all Berea cores were drilled perpendicular to the lamination ($\varphi \cong 20 \pm 1\%$, $k = 150 - 250$ mD). The Berea core samples were fully saturated with crude oil C, i.e. the initial brine saturation was zero ($S_{wi} = 0$). Epoxy resin $RentCast^*CW2215$ was combined with Ren^* HY 5160 hardener in a proportion of 100 : 20 to seal the core boundaries. The epoxy was suitable for elevated temperatures

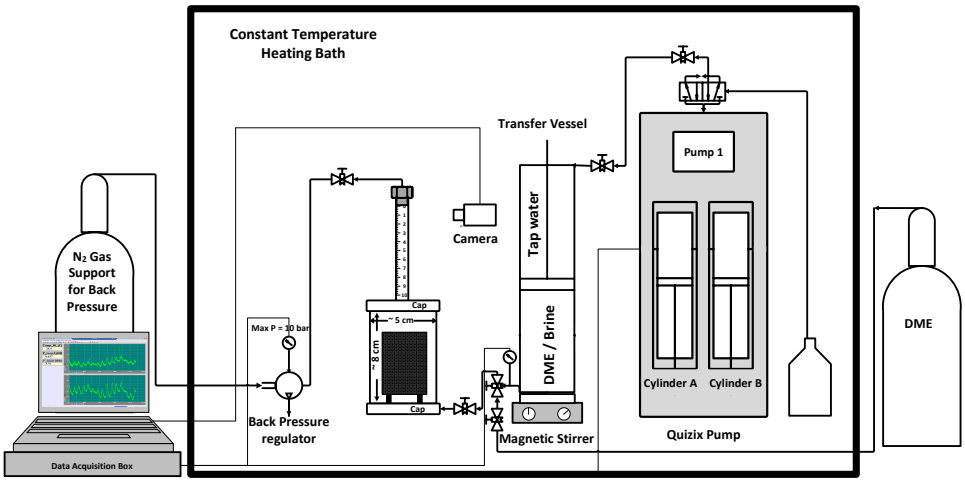

Figure 4.1: Schematic drawing of a high-pressure Amott imbibition cell is shown. A core was placed in the Amott cell and caps at the top and at the bottom of the cell were closed. The cell was connected to the back-pressure to keep a constant operating pressure. Then, the cell was filled with N_2. The pressure was monitored to verify that the system was leak-free. Afterwards, an aqueous mixture was injected from a transfer vessel into the cell until the liquid-Nitrogen interface reached to the zero level at the top of the graded cylinder. The graded indication had a value of zero at the top and of 10 at the bottom. The set-up was placed in a controlled temperature box (T=25 ± 1°C). The production was monitored versus time. A data acquisition system was used to record operating pressure and temperature. A camera was also implemented to take snapshot photos.

up to $50-55°C$. Afterwards, we used the epoxy to make various boundary conditions for different water-wet cores, e.g. all boundaries open to imbibition (ABO), top-end open to imbibition (TEO), bottom-end open to imbibition (BEO) and two-ends open to imbibition (TEsO). Fig. 4.2 shows the boundary conditions of the water-wet core samples. The epoxy resin penetrated into the core; therefore the effective pore volume was reduced. To determine the Oil Initially In-Place (OIIP), we measured both the weight of the dry epoxy coated samples and of the saturated epoxy coated samples, so that we calculated the weight of oil in the core. Finally, we divided the weight of oil in the core by the oil density at the operating temperature and obtained the volume of the OIIP.

Mixed-wet limestone cores ($\varphi = 27.9 - 30.2 \pm 0.5\%, k = 3.37 - 4.95 \pm 0.05\ mD$) were brine-saturated by injection of brine or oil-saturated by injection of oil using a fluid displacement set-up. A number of mixed-wet cores were completely saturated with crude oil D, i.e. $S_{wi} = 0$. However, other mixed-wet cores contained an initial brine (1 $w/w\%$ NaCl in demi-water) at a saturation varying between 0.169 ± 0.001

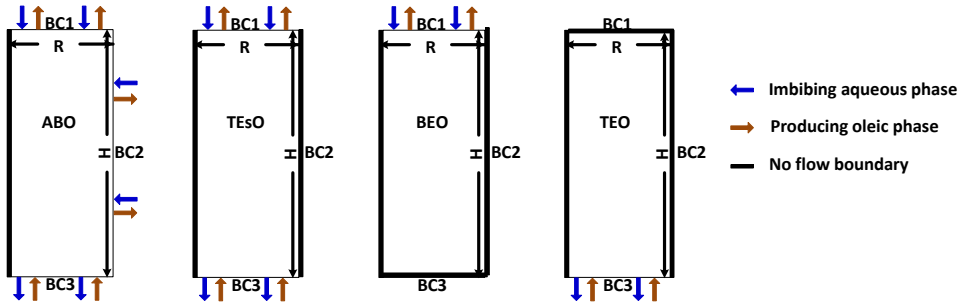

Figure 4.2: Water-wet cores had different boundary conditions. (a) ABO: A vertical core with all boundaries open to imbibition. (b) TEsO: A vertical core with both ends (top and bottom) open to imbibition. (c) BEO: A vertical core with the bottom-end open to imbibition. (d) TEO: A vertical core with the top-end open to imbibition.

and 0.173 ± 0.001. The properties of the crude oils are summarized in Table 4.1.

For imbibition experiments, the aqueous phase consists of 0.5 M sodium chloride

Table 4.1: Physical properties of crude oils at temperature $20°C$.

Name	Density (kg/m^3)	Viscosity $(Pa.s)$
Crude oil C	844	4.1×10^{-2}
Crude oil D	836	6.5×10^{-3}

(NaCl, Merck) in demineralized water ($pH = 6.8 \pm 1$). The DME/brine mixture was prepared by adding 10 ± 0.2 $mol\%$ of dimethyl ether ($(CH3)_2O$, Linde Gas, purity$>$ 99.9%) to 0.5 M brine and stirring it for about $3 - 4$ $hours$ in a pressurized transfer vessel (P$\geq$ 9 bar). The physical properties of dimethyl ether are shown in Table 5.1.

Table 4.2: Physical properties of dimethyl ether at $20°C$ [37].

Property	Value
Liquid viscosity, $(Pa.s)$	1.29×10^{-4}
Molecular weight, $(kg/kmol)$	46.068
Boiling point at, atmospheric pressure, $(°C)$	-24.81
Specific gravity	735.2
Vapor pressure, (bar)	5.1

4.3.2 Experimental set-up

Figure 4.1 shows a schematic of the modified high-pressure imbibition set-up. The high-pressure cell consists of four parts, i.e. a cylindrical non-transparent body ($D = 5 \pm 0.1$ cm and $L = 8.0 \pm 0.1$ cm), a bottom cap and a top cap, all made of Poly-Ethylene-Ether-Ketone (PEEK). A graded glass cylinder (with a diameter of 1 ± 0.1 cm and a length of 14 ± 0.1 cm) was attached to the top cap with Araldite 2020 epoxy, so that oil was collected at the top of the graded glass cylinder, and the production was measured versus time. In order to prepare a condition to expose the core from the bottom as well as all other sides of the core, some spacers, made by Teflon, were put at the bottom of the Amott cell. Moreover, the bottom cap was connected to a transfer vessel through a PEEK pipe, a valve and a Unik 5000 pressure transmitter (calibrated with a precision of 0.01 bar). In addition, the modified Amott cell was connected to a Mity Mite back-pressure regulator using a PEEK tube and a valve. The top of the vessel was connected to a nitrogen cylinder. Therefore, it was possible to provide an initial pressure by injecting N_2 at the top prior to the injection of the pressurized DME/brine mixture. Nitrogen (N_2) was chosen because it has a very low solubility in brine and in hydrocarbons at pressures below 10 $bars$ [38]. Furthermore, the transfer vessel utilizes a Hastelloy stainless steel tube with a floating piston that embraces the two Hastelloy stainless steel caps. The caps are connected with 8 external rods, so that they can be tightened. Besides, we implemented a Viton A 90-shor O-ring type for sealing the different parts of the transfer vessel and the PEEK-PEEK connections of the Amott cell. Viton A 90-shor was chosen, because it is compatible with DME. With the purpose of mixing DME with brine, we put a magnet in the mixing side of the transfer vessel and placed the vessel on a magnetic stirrer. We also used a Quizix QX-500 pump to inject brine in the vessel and a booster pump to inject the pressurized DME into the vessel. We utilized a calibrated $RTX7517$ pressure transmitter (with a precision of 0.01 bar) to measure the pressure at the mixing side of the vessel. It was important to perform the experiments at a constant temperature. Therefore, the whole set-up was placed in a Jardin growth box, and a heating element was implemented to keep an operating temperature of $25 \pm 1°C$ (see Fig. 4.1). Furthermore, we used multiple webcams to take snapshot photos and movies during the spontaneous imbibition experiments.

4.3.3 Experimental procedure

4.3.3.1 Mixing DME and brine

First, brine was injected into the mixing side of the transfer vessel using a Quizix QX-500 pump. Secondly, salt-free water was injected into the other side of the transfer vessel to reach the supporting pressure, both for the mixing of DME and brine and for injection into the Amott cell. Thirdly, DME was pressurized up to

9 ± 0.5 *bars* using a booster pump, so that DME was in the liquid state. In this series of experiments, the mixture of 10 ± 0.2 *mol*% DME in brine was injected into the Amott cell. At pressures above 5.1 *bars*, DME is in the liquid state at the ambient temperature, and the mixture of 10 *mol*% DME in brine corresponds to a mixture of approximately 30 *v/v*% DME in brine at room temperature. During DME injection, the transfer vessel was maintained at a constant pressure (9 ± 0.5 *bars*) and the mixture was stirred. During the stirring period, the pump was programmed for a constant pressure injection mode, while the injected volume was measured. When both the pressure and the volume of the injected supporting liquid reached a steady-state condition, DME and brine were considered to be fully mixed.

4.3.3.2 Imbibition experiments

In both primary and secondary imbibition stages, we put the oil-filled core in a vertical position on Teflon spacers inside the modified Amott imbibition cell. Then, we assembled the Amott cell and filled it with N_2 to pressurize the cell up to 9 ± 0.5 *bars* using the back-pressure regulator. Afterwards, all connections were controlled with Snoopy fluid to find and fix possible leakage sources. Similarly, the pressure of the cell was monitored using the pressure transmitter and the data-acquisition system for a few hours to validate that the system was leak-free.
In the next stage, we injected brine or the DMEB mixture into the cell and displaced N_2 until the level of the liquid reached the top of the graded glass cylinder. Therefore, N_2 occupied the space between the top of the graded level of glass cylinder and the tube connecting to the back-pressure valve. The production was measured and recorded both visually and using a motion detection camera, until the production effectively stopped. At the end of the primary and the secondary imbibition stages in water-wet cores, a large volume of oil in the form of oil droplets was attached to the external surface of the rock. Therefore, we injected brine or DMEB in a low flow rate to detach the drops from the rock surface and displace the produced crude out of the Amott cell. Subsequently, we collected the effluent in graded test tubes at atmospheric conditions. Since we assumed that DME was immediately evaporated from the oleic phase, the amount of dissolved DME in oil was considered negligible at atmospheric pressure. During both brine imbibition and DMEB imbibition in water-wet cores, the adsorption of the oil drops to the rock surface strongly affected the shape of the production curves. Therefore, after releasing the oil drops at the end of the imbibition process, the production curve jumped to a final value (see e.g. Fig. 4.9). Moreover, in DMEB imbibition in the mixed-wet cores, the oil production immediately started with a high production rate. However, after 10 *mL* oleic phase production, the volume of the produced oleic phase exceeded the volume of the transparent glass cylinder and could not be measured. Therefore, we injected DMEB into the cell with a low flow rate to displace the produced oleic phase out of the cell.

Subsequently, we collected oil in graded test tubes and measured the volume of pure oil at atmospheric pressure. In the mixed-wet cores, the volume of the attached oil drops on the rock interface was not significant at the end of the experiment.

4.4 Theory

4.4.1 Numerical model

A 2-D axially-symmetric, two-phase and three-components incompressible fluid flow model was used to interpret the spontaneous DME/brine imbibition into an oil-filled matrix block. Our numerical model describes the fluid transport and the mixing with the spontaneously imbibed DMEB mixture into a vertical cylindrical oil-filled core. We considered brine as a component. The mass conservation of all components in the DMEB spontaneous imbibition reads:

$$\varphi\frac{\partial}{\partial t}(S_o V_{oh}) + \nabla.\big(V_{oh}u_o\big) - \nabla.\big(\varphi D_{os} S_o \nabla.V_{oh}\big) = \quad 0, \tag{4.1}$$

$$\varphi\frac{\partial}{\partial t}(S_a V_{aw}) + \nabla.\big(V_{aw}u_a\big) - \nabla.\big(\varphi D_{as} S_a \nabla.V_{aw}\big) = \quad 0, \tag{4.2}$$

$$\nabla.\big(u_a + u_o\big) = \quad 0, \tag{4.3}$$

where S_α denotes the saturation of phase α, i.e. for the aqueous phase ($\alpha = a$) and for the oleic phase ($\alpha = o$), $V_{\alpha c}$ is the volume fraction of component c, i.e. brine ($c = w$), hydrocarbon ($c = h$) or DME ($c = d$) in phase α, $D_{\alpha s}$ is the molecular diffusion coefficient of DME in phase α (see Eq. (4.17)), φ is the porosity, and u_α is the Darcy velocity of phase α, which is defined by Darcy's equation:

$$u_\alpha(P_\alpha, V_{aw}, S_a) = -\frac{k k_{r\alpha}(S_a)}{\mu_\alpha(V_{aw})}(\nabla P_\alpha + \rho_\alpha(V_{aw}) g \mathbf{e_z}), \tag{4.4}$$

where k is the absolute permeability, μ_α is the viscosity of phase α, ρ_α is the density of phase α, g is the acceleration due to gravity, z is the upward vertical distance with $z = 0$ at the bottom of the core, P_α is the pressure of phase α and $k_{r\alpha}$ is the relative permeability of phase α. The pressure of the aqueous phase (P_a), the volume fraction of brine in the aqueous phase (V_{aw}) and the saturation of the aqueous phase (S_a) are the independent variables. The relative permeability of the aqueous phase and of the oleic phase are defined from Brooks-Corey:

$$k_{ra}(S_a) = k^e_{ra}\, S_e(S_a)^{(3+2/\lambda)}, \tag{4.5}$$

$$k_{ro}(S_a) = k^e_{ro}(1 - S_e(S_a))^2(1 - S_e(S_a)^{(1+2/\lambda)}), \tag{4.6}$$

where k^e_{ra} and k^e_{ro} are the end-point relative permeabilities of the aqueous phase and the oleic phase respectively, λ is the sorting factor ($0.5 \leq \lambda \leq 7$) and S_e is the effective saturation of the aqueous phase and is defined by:

$$S_e(S_a) = \frac{S_a - S_{wc}}{1 - S_{wc} - S_{or}}, \tag{4.7}$$

where S_{wc} and S_{or} are the connate water saturation and the residual oil saturation. We use four additional auxiliary equations to complete the model, viz.,

$$\sum V_{ac} = 1, \qquad c = w, d, \tag{4.8}$$

$$\sum V_{oc} = 1, \qquad c = h, d, \tag{4.9}$$

$$\sum S_{\alpha} = 1, \qquad \alpha = o, a, \tag{4.10}$$

$$P_c(S_{\alpha}) = P_a - P_o, \tag{4.11}$$

$$V_{ad} = K_{oa} V_{od}, \tag{4.12}$$

where V_{od} and V_{ad} are the volume fraction of DME in the oleic phase and in the aqueous phase, K_{oa} is the partition coefficient of DME between the oleic and the aqueous phases. The partition coefficient is defined as the volume fraction of DME in the oleic phase divided by the volume fraction of DME in the aqueous phase (Eq. (4.12)). In addition, the capillary pressure function (P_c) is defined by the Brooks-Corey expression:

$$P_c(S_a) = P_{cb} S_e(S_a)^{(-1/\lambda)}, \tag{4.13}$$

where S_e is the effective saturation, and P_{cb} is the capillary entry pressure, which is defined by:

$$P_{cb} = \gamma\sigma\sqrt{\frac{\varphi}{K}} S_e(0.5)^{(1/\lambda)}, \tag{4.14}$$

where σ is the interfacial tension between the oleic phase and the aqueous phase, and γ is a matching parameter. The capillary pressure function was extended below the connate water saturation ($S_a < S_{wc}$) to avoid instabilities due to infinite capillary pressures near S_{wc}. We disregarded the negative capillary pressure in mixed-wet cores.

We assumed that the viscosity and the density of the DMEB were equal to the viscosity and the density of brine. In addition, the viscosity and the density of the

oleic phase were obtained from equations 4.15 and 4.16 respectively:

$$\mu_o(V_{aw}) = \left(\frac{V_{oh}}{\mu_H^{1/4}} + \frac{V_{od}}{\mu_{DME}^{1/4}} \right)^{-4}, \tag{4.15}$$

$$\rho_o(V_{aw}) = \frac{1}{V_{od}(V_{aw})/\rho_{DME} + V_{oh}(V_{aw})/\rho_H}, \tag{4.16}$$

where μ_W, μ_H and $\mu_{_{DME}}$ are the viscosity of pure brine, of pure oil and of pure DME respectively. Moreover, ρ_H and $\rho_{_{DME}}$ are the density of pure oil and of pure DME.
Furthermore, the molecular diffusion coefficients of DME in oil (D_{od}) or in brine (D_{ad}) are calculated from the Wilke-Chang correlation [39]:

$$D_{sc} = 7.4 \times 10^{-8} \Big(\frac{T(\phi_c\, M_c)^{1/2}}{\mu_c \hat{V}_{DME}^{0.6}} \Big), \tag{4.17}$$

where ϕ_c is the association parameter, which is equal to one, both for crude oil and for brine, M_c is the molecular weight of brine or of oil, $\mu_c[mPa.s]$ is the viscosity of brine or of oil, $\hat{V}_{DME}[cm^3/mol]$ is the molar volume of DME, defined as the volume of a mole of DME at its normal boiling point, and $T[K]$ is the temperature.
We solved the system of equations for the pressure of the aqueous phase (P_a), the saturation of the aqueous phase (S_a) and the concentration of brine in the aqueous phase (V_{aw}) using a commercial finite element package (COMSOL Multiphysics). The geometry of the core was an axially-symmetric cylinder, so that we solved the equations in the radial coordinate (R, Z directions) system, i.e. $r = 1.5\ cm$ and $H = 5\ cm$. The geometry of the model for different boundary conditions is shown in Fig. 4.2.

4.5 Results and discussion

4.5.1 Effects of DME on the oil recovery in spontaneous imbibition

Our hypothesis in this work is that the DME transport mechanism involves convection and diffusion. We assume that there is instantaneous local thermodynamic equilibrium between the components in the oleic and in the aqueous phases. Capillary forces displace the aqueous phase into the core, gravity forces displace the bulk fluid, and molecular diffusion displaces components comprising the oleic and the aqueous phases. Locally, DME partitions instantaneously between the oleic and the aqueous phases. As the volume of the aqueous phase is less affected by the presence of DME than by the volume of the oleic phase, the total volume of the fluids increases.

Furthermore, with the DME dissolution in oil, the production rate is increased due to the oil viscosity reduction.
For reasons of comparison, the effects of DME-enhanced imbibition on the oil recovery are theoretically investigated here by comparing the oil recoveries as a function of the system variables, i.e. the DME partition coefficient, the initial oil saturation, the oil viscosity reduction, the DME concentration in the aqueous phase, the end-point relative permeabilities, the capillary pressure and the DME molecular diffusion. In the numerical modeling studies, we assumed constant initial and boundary conditions for the saturation of the aqueous phase (S_a) and for the volume fraction of brine (V_{aw}) in the aqueous phase. Moreover, for the pressure of the aqueous phase (P_a), the initial condition is constant density ($P = \rho gz$) of both the oleic and the aqueous phase inside the core, and a constant aqueous phase density at the boundary. From the constant density it is possible to determine the pressure as a function of position and we used the pressure continuity in the pressure calculations. The model parameters for the base case simulation are given in Table 4.3. We considered that the end-point relative permeabilities of the aqueous phase and of the oleic phase were representative of mixed-wet cores.

Figure 4.3a shows in the numerical model, the effect of the partition coefficient

Table 4.3: Parameters used in the numerical model - base case simulation.

Parameter	Unit	Value
φ	[1]	0.2
K	m^2	2×10^{-13}
S_{wc}	[1]	0.1
ρ_w	kg/m^3	1000
ρ_o	kg/m^3	850
μ_w	$Pa.s$	0.001
μ_o	$Pa.s$	0.040
σ	N/m	0.030
γ	[1]	1
λ	[1]	2
k^e_{ro}	[1]	1
k^e_{ra}	[1]	1
S_{or}	[1]	0.5
K_{oa}	[1]	2
P_{cb}	Pa	21869
D_o	m^2/s	3×10^{-11}
D_a	m^2/s	8×10^{-10}
V_{awb}	[1]	0.67

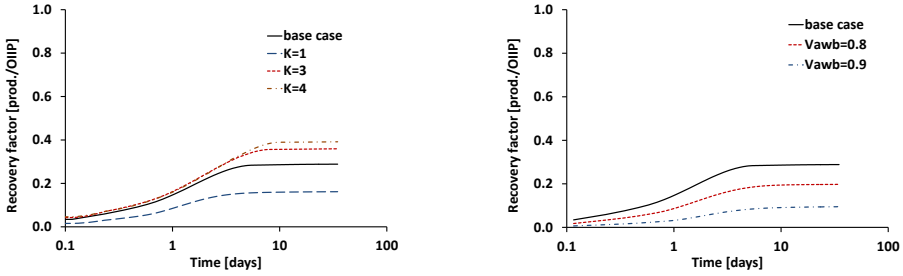

(a) $S_{oi} = 0.5$ (b) $S_{oi} = 0.5$

Figure 4.3: (a) The effect of the partition coefficient on the oil recovery, a higher oil recovery is obtained with a higher partition coefficient. (b) The effect of the DME concentration on the oil recovery is shown. A higher DME concentration leads to a higher oil recovery.

4

($K = 1,\ 2,\ 3$ and 4) on the oil recovery , where we kept the values for all other quantities the same. The results show that a higher partition coefficient leads to a higher oil recovery. The relation between the increase in the partition coefficient and the increase of the oil recovery is not linear as can be observed in Fig. 4.3a.
Figure 4.3b shows the effect of the DME concentration in the aqueous phase on the oil recovery. Similar to an earlier study, we assumed similar model parameters in all simulations and performed simulations for different DME concentrations, i.e. 0.33, 0.2 and 0.1, which corresponds to $V_{aw} =$ 0.67, 0.8 and 0.9 respectively. The numerical results show that a higher DME concentration accelerates and enhances the oil recovery.
Figure 4.4a depicts the effect of the initial (remaining) oil saturation on the incremental oil recovery (the oil production divided by the initial oil). We performed simulations for DMEB imbibition in cores with different initial (remaining) oil saturations, i.e. $S_{oi} = 0.5,\ 0.6,\ 0.7$ and 0.8, and the model parameters presented in Table 4.3. The results show that DMEB imbibition in a core with a higher initial oil saturation leads to a higher incremental oil recovery.
Figure 4.4b shows the effect of the viscosity reduction mechanism on the recovery of light ($\mu_o = 0.004\ Pa.s$), medium ($\mu_o = 0.042\ Pa.s$) and viscous oil ($\mu_o = 0.420\ Pa.s$). In addition to the oil viscosity reduction in the process, it was assumed that the oil swelling contributed to the oil recovery. The other model parameters (in Table 4.3) were similar for all studies. The results show, after a simulation time of 30 *days*, that the DMEB imbibition process leads to more or less similar recoveries of light, medium and viscous oil. Moreover, the viscosity reduction mechanism increases the production rate; the viscosity reduction is more important in the recovery of oil

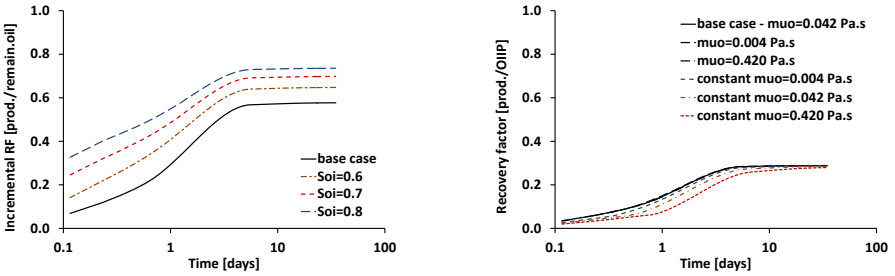

(a) (b)

4

Figure 4.4: (a) The effect of the initial oil saturation on the incremental oil recovery is shown, a higher remaining oil saturation leads to a higher incremental oil recovery due to DME/brine imbibition. (b) The effect of the oil viscosity together with the effect of viscosity reduction on the oil recovery is depicted. The viscosity reduction, accelerated viscous oil recovery; the effect of the viscosity reduction on the recovery acceleration of light and medium oil is small.

with higher viscosity than in the recovery of oil with lower viscosity. For instance, the viscosity reduction of light oil slightly increases the production rate. However, the viscosity reduction of viscous oil ($\mu_o = 0.420\ Pa.s$) considerably increases the imbibition rate.

Figure 4.5 compares the effect of oil viscosity reduction on the recovery of light ($\mu_o = 0.004\ Pa.s$), medium ($\mu_o = 0.042\ Pa.s$) and viscous ($\mu_o = 0.420\ Pa.s$) oils in cores with initial oil saturations of $S_{oi} = 0.5$ and $S_{oi} = 0.8$. We assumed that both the viscosity reduction and the oil swelling contributed to the oil recovery. In cores with an initial oil saturation close to the assumed residual oil after imbibition, i.e. $S_{oi} = 0.5$, the viscosity reduction mechanism (together with oil swelling) results in a similar recovery curve of light, medium and viscous oils (see Fig. 4.5a). In addition, in cores with an initial oil saturation of $S_{oi} = 0.8$, the numerical model predicts a more or less similar additional oil recovery for all simulation scenarios. However, the numerical simulation predicts that in a core with an initial oil saturation of $S_{oi} = 0.8$, the recovery rate decreases with an increase of the oil viscosity (see Fig. 4.5b).

Fig. 4.6a shows the situation initially at residual oil saturation ($S_{oi} = S_{or} = 0.5$) and therefore at zero initial capillary diffusion. During the simulation, the oil saturation increases somewhat above the residual value but still capillary diffusion remains small. In Fig. 4.6b, the oil saturation ($S_{oi} = 0.8$) is well above the residual oil saturation ($S_{or} = 0.5$) and therefore, the capillary diffusion is larger than for case Fig. 4.6a. In fact, capillary diffusion is so effective that is almost complete at time 0.1 *day* (in Fig. 4.6b). Due to transfer of DME dissolved in the imbibed water to the

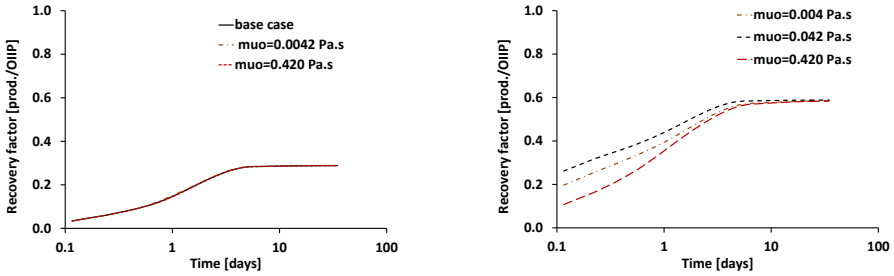

(a) $S_{oi} = 0.5$ (b) $S_{oi} = 0.8$

Figure 4.5: (a) The viscosity reduction mechanism has no impact on the recovery of light, medium and viscous oil when initial oil saturation is similar to residual oil saturation. (b) When initial oil saturation is larger than the residual oil, the numerical model shows that the effect of the viscosity reduction on the acceleration of viscous oil recovery is more important than of light and of medium oil.

oleic phase, the transport of DME due to capillary diffusion is small. In this case, the main transport mechanism is still molecular diffusion. Moreover, both Figs. 4.6a and 4.6b show that the decrease of the DME diffusion coefficient significantly reduced the oil recovery and production rate during a simulation time of 30 *days*. Moreover, we performed numerical modeling only with an assumed zero molecular diffusion coefficient (non- zero capillary pressure). The simulation model shows a very slow and small oil recovery after 30 *days*. As a result, we concluded that the molecular diffusion has a very important impact on the oil recovery by DMEB imbibition; the impact of the DME molecular diffusion on the oil recovery is independent of the initial oil saturation in the core.

Figure 4.7 compares the effect of capillary pressure on the oil recovery in cores with initial oil saturations of $S_{oi} = S_{or} = 0.5$ (4.6a) and of $S_{oi} = 0.8$ (4.6b). We disregarded the hysteresis in the capillary pressure, which we considered to be outside the scope of this research. We performed simulations for the different capillary entry pressures $P_{cb} = 2.2 \times 10^4,\ 2.2 \times 10^3,\ 2.2 \times 10^2$ and $2.2 \times 10^1\ Pa$ for both initial conditions, i.e. $S_{oi} = 0.5$ and of $S_{oi} = 0.8$. Fig. 4.7a shows that the four simulated oil recoveries with an initial saturation of $S_{oi} = 0.5$ approach the same value after 30 *days*; with an increase in capillary pressure, the production rate slightly increases. Fig. 4.7b also shows that, for all capillary entry pressures in the core with an initial oil saturation of $S_{oi} = 0.8$, the same ultimate oil recovery is obtained after 30 *days*. However, an increase of the capillary entry pressure significantly increases the production rate. We observed that the simulated production rates with an initial saturation of $S_{oi} = 0.8$ are more sensitive to the capillary pressure than the

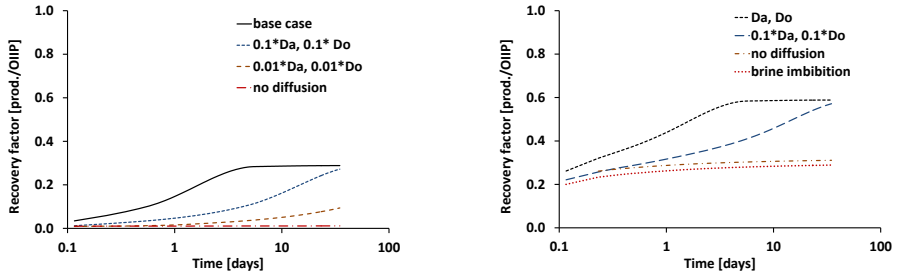

(a) $S_{oi} = 0.5$ (b) $S_{oi} = 0.8$

Figure 4.6: The effect of the DME diffusion coefficient on the oil recovery is compared for both initial oil saturation of $S_{oi} = 0.5$ (a) and of $S_{oi} = 0.8$ (b). Fig. 4.6a shows the situation initially at residual oil saturation and therefore at zero initial capillary diffusion. In Fig. 4.6b, the oil saturation is well above the residual oil saturation and therefore, the capillary diffusion is larger than for case Fig. 4.6a. The remaining oil saturation after imbibition is also equal to 0.5. The decrease of the molecular diffusion coefficient significantly decreases both the production rate and the additional recovery during 30 *days*. With the assumption of a zero molecular diffusion coefficient for both conditions (a) and (b), numerical model shows a very small and slow oil recovery after 30 *days*.

production rates with an initial oil saturation of $S_{oi} = 0.5$.

Figure 4.8 shows the effect of the end-point relative permeabilities on the oil recovery from cores with initial saturations of $S_{oi} = S_{or} = 0.5$ (Fig. 4.8a) and of $S_{oi} = 0.8$ (Fig. 4.8b). We assumed that both oil and brine had the same end-point relative permeabilities. We considered that the end-point relative permeabilities of the aqueous phase and of the oleic phase were representative of mixed-wet cores. We performed simulations with the same model parameters, and only changed the end-point relative permeabilities, i.e. $k^e_{ra} = k^e_{ro} = 0.1,\ 0.5$ and 1. The numerical model shows that in a core with $S_{oi} = 0.5$, the additional cumulative oil recovery from models with different end-points is the same, but that with smaller end-point relative permeabilities we obtain a reduced production rate. Fig. 4.8b also shows that different end-point relative permeabilities results in a more or less similar additional oil recovery from a core with $S_{oi} = 0.8$ after 30 *days*. However, the increase of the end-point relative permeabilities considerably increases the production rate. In conclusion, the numerical model predicts that the effect of the end-point relative permeabilities on the oil recovery rate is significantly larger in a core with $S_{oi} = 0.8$ than in a core with $S_{oi} = 0.5$. The reason is that, a core with $S_{oi} = 0.5$ is mainly dominated by swelling as $S_{oi} = S_{or}$, while for a core with $S_{oi} = 0.8$ the process is affected by both capillary forces and swelling.

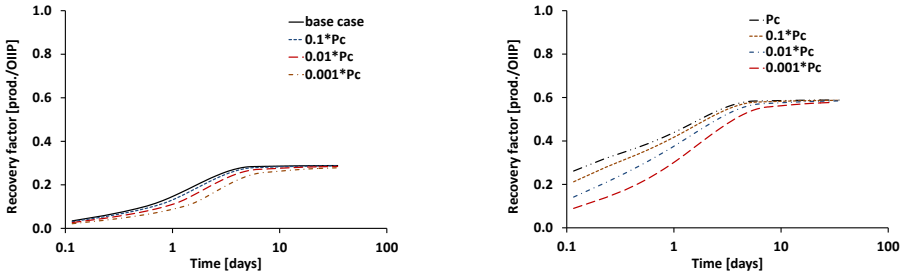

(a) $S_{oi} = 0.5$ (b) $S_{oi} = 0.8$

Figure 4.7: The effect of capillary pressure on the oil recovery is compared both in cores with initial oil saturation of $S_{oi} = 0.5$ (a) and of $S_{oi} = 0.8$ (b). (a) In core with $S_{oi} = 0.5$ the decrease of the capillary entry pressure slightly reduces the production rate, but the oil recovery approaches a same value after 30 *days*. (b) In core with $S_{oi} = 0.8$, the additional recovery is also more or less similar, but the increase of capillary entry pressure significantly increases the production rate.

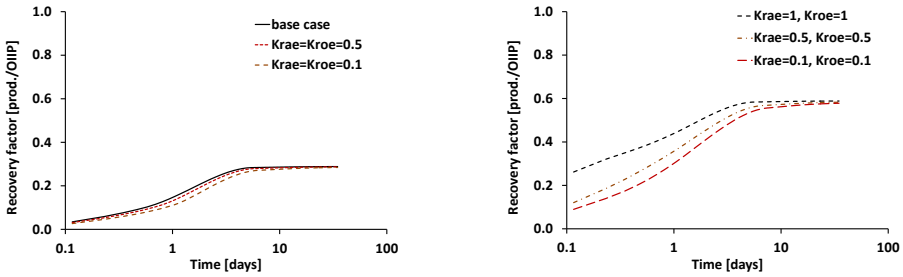

(a) $S_{oi} = 0.5$ (b) $S_{oi} = 0.8$

Figure 4.8: The effect of the end-point relative permeabilities in oil and in brine is compared in cores with $S_{oi} = 0.5$ (a) and $S_{oi} = 0.8$ (b). Lower end-points lead to slower production rates. The effect is more significant in a core with higher oil saturation, $S_{oi} = 0.8$ (b). However, the additional oil recovery after 30 *days* is similar.

4.5.2 Oil recovery from water-wet cores

In this subsection, we present the results for brine (3 w/w% NaCl in demi-water) imbibition and the results for imbibition of a mixture of 10 ± 0.2 mol% DME in brine into water-wet cores. The latter solution will be denoted by DMEB. The purpose of adding DME is to improve the imbibition rate and, thus, the oil recovery

in water-wet cores.

Fig. 4.9 shows the oil recovery versus time in two-stage spontaneous imbibition experiments in cores with different boundary conditions, i.e. top-end open to imbibition (TEO), bottom-end open to imbibition (BEO), two-ends open to imbibition (TEsO) and all boundaries open to imbibition (ABO). In the first stage, brine was imbibed into the core for a period of about 49 *days*, after which the ultimate primary recovery was obtained. The recovery factor was defined as the ratio between the volume of the recovered oil divided by the Oil Initially In-Place (OIIP). In the second stage, the core was exposed to DMEB for a period of about 40 *days* and an additional oil recovery was obtained. The additional oil recovery is the additional volume of the produced oil by DMEB imbibition divided by the volume of the OIIP. The incremental oil recovery is also defined by the incremental volume of the produced oil by DMEB imbibition divided by the volume of remaining oil.

Figures 4.9a and 4.9b show the oil recovery from the cores with top-end open (TEO) and bottom-end open (BEO) to imbibition. With brine imbibition, we obtained the same primary recovery from both cores, i.e. $41 \pm 3\%$ of the OIIP. Nevertheless, the recovery with DMEB differed, i.e. $14 \pm 3\%$ ($11 \pm 3\%$)of the OIIP was recovered from the BEO (TEO) core. Next, Fig. 4.9c shows that with brine imbibition, an oil recovery of $46 \pm 4\%$ of the OIIP was attained from the core with two-ends open to imbibition (TEsO), which was the maximum primary recovery from water-wet cores. Moreover, the oil recovery with DMEB imbibition from the TEsO core was $11 \pm 3\%$ of the OIIP. Finally, the ultimate primary recovery in the core with all boundaries open to imbibition (ABO) was the smallest ultimate primary recovery, i.e. $38 \pm 3\%$ of the OIIP; a secondary recovery of $16 \pm 3\%$ of the OIIP was obtained with DMEB imbibition.

The brine imbibition experiments with top-end (TEO) or bottom-end (BEO) open to imbibition looked very similar. The initial production rate for the experiments with both surfaces exposed to the imbibition (TEsO) showed the fastest rate. Moreover, it appeared that the core with all boundaries open to imbibition (ABO) had the slowest production rate. However, the production curves were strongly affected by the attachment of the drops on the rock surface, which were indeed the largest for the experiment with all sides exposed to the imbibition fluid. When at the end of the primary stage and the secondary stage, the attached droplets were released, it showed the largest jump in oil recovery.

In view of the attachment of the oil droplets at the interface, the difference between the incremental recovery curves of the four water-wet cores was not conspicuous. For instance, extra recovery efficiencies between $11 - 16 \pm 3\%$ of the OIIP were obtained, which corresponded to incremental oil recoveries between $19 - 25 \pm 4\%$ of the remaining oil. The largest extra (incremental) oil recovery, e.g. $16 \pm 3\%$ of the OIIP ($25 \pm 4\%$ of the remaining oil), was obtained for the core with all boundaries open to imbibition, which had the largest surface area exposed to DMEB.

Moreover, adding DME led to little additional oil recovery due to swelling effects. As stated before, with the DME transfer into the oleic phase, the same volume of the oleic phase was expelled out of the core. We refer to this phenomenon as the swelling mechanism. However, the DME molecule has a different effect on the volume of the oleic phase than on the volume of the aqueous phase [34], which can be quantified by the difference of the partial molar volume of DME in the aqueous and in the oleic phases. For reasons of easy reference, we used the measured density data reported in [40] for butane/DME mixtures and in [41] for diesel/DME mixtures to calculate the partial molar volumes of DME in butane and in diesel. The calculated partial molar volume of DME in diesel (butane) was 68.28 cc/mol (69.4 cc/mol). In addition, we estimated the partial molar volume of DME in water as 61.4 cc/mol using Aspen Plus (process simulation and optimization software). The difference of partial molar volumes of DME in the aqueous and in the oleic phases corresponds to an excess molar volume, which adds an extra total volume upon DME transfer from the aqueous phase into the oleic phase.

We observed a large scatter in the production curves both in brine imbibition and in DMEB imbibition (see Fig. 4.9). For instance, in brine imbibition into the TEsO core, the production started after approximately one day; but the oil production started after ten days in the BEO, the TEO and the ABO cores. The reasons for this scatter in the data could be attributed to (1) the presence of asphaltene in the crude oil and wettability effects due to rock-crude interactions and (2) heterogeneity in the Berea cores and (3) attachments of the oil drops to the rock surface, which reduced the imbibition surface. Moreover, the oil production in the form of drops attached to the open face of the core associated a pressure to the oil drop, i.e. capillary back-pressure, which partly opposed the oil production. Following Morrow and Li [42] we refer to the pressure, which is needed to detach the oil droplet as capillary back-pressure. The capillary back-pressure could be significant, e.g. 1/9 to 1/4 of the capillary pressure [42]. In addition, we estimated the time that a detached drop needed to move along the rock surface. Adding the double layer repulsion forces to the attractive Van der Waals forces reach to an interaction potential, and strongly near wall repulsion leads to two minima. Following Redman et al. [43], it appears to be plausible that the detached oil droplet is trapped in a secondary minimum. The driving force for the upward movement of the detached oil drop is gravity. At steady-state, the viscous drag force is equal to the gravity force for a detached drop; therefore, we can obtain an order of magnitude for the average velocity of the oil droplet by [44–46]:

$$V = \frac{2}{3}\frac{\Delta\rho g R}{\mu_o}\delta_{eff}, \tag{4.18}$$

where $V[m/s]$ is the upward velocity of the oil drop, $\Delta\rho[kg/m^3]$ is the density gradient between brine and oil, $\mu_o[Pa.s]$ and $R[m]$ are the viscosity and the radius

of the oil droplet and $\delta_{eff}[m]$ is the effective distance between the oil and the rock surface. We estimated an effective distance of $\delta_{eff} = 1.1\ nm$ for a ionic strength of 0.5 (NaCl 0.5 molar in demi-water) by extrapolating the data presented in reference [43]. Therefore, with the assumption of a radius of 0.001 m for an oil drop, an average velocity of $4.4 \times 10^{-8}\ m/s$ was estimated, which corresponds to a travel time of 13.3 *days* along a height of 0.05 m of the core. This may describe one of the reasons, which delays the oil production. We emphasize that this is a crude estimate, which can only be used to estimate the order of magnitude of the velocity of the droplet along the interface.

Dimensional analysis of the spontaneous imbibition process shows that there are

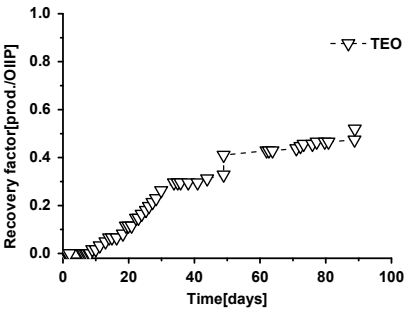

(a) Top end open to imbibition

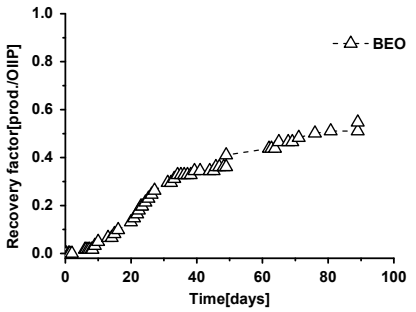

(b) Bottom end open to imbibition

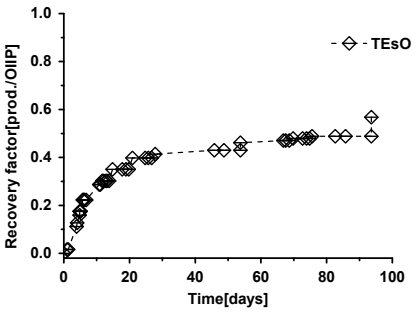

(c) Two ends open to imbibition

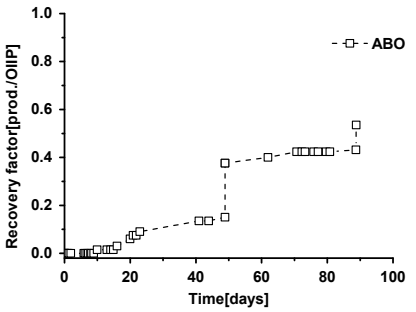

(d) All boundaries open to imbibition

Figure 4.9: This figure shows the results of two-stage spontaneous imbibition experiments in water-wet cores under different boundary conditions. Primary recovery stopped after 49 *days*, when a jump occurred due to releasing drops attached to the rock surface, while the maximum jump happened in the core that was exposed to brine from all sides. The DMEB imbibition started after 49 *days* and continued until 90 *days*, when the second jump appeared in the production curves and the additional and ultimate recoveries were obtained.

three characteristic times, viz. the capillary characteristic time (t_c), the gravity characteristic time (t_g) and the molecular diffusion characteristic time (t_d), which show the relative importance of capillary effects, of gravity effects and of diffusion effects in the imbibition process. They are defined by [47–50]:

$$t_c = \frac{L_c^2\sqrt{\mu_a\mu_o}}{\sigma\sqrt{\frac{k}{\varphi}}}, \tag{4.19}$$

$$t_g = \frac{L_H\sqrt{\mu_a\mu_o}}{\Delta\rho g\frac{k}{\varphi}}, \tag{4.20}$$

$$t_d = \frac{r^2}{D_{DME}}, \tag{4.21}$$

where r is the radius of the core, e.g. 0.015 m in this study, the molecular diffusion of DME in brine ($8\times10^{-10}\ m^2/s$) or in oil ($1.6\times10^{-11}\ m^2/s$), which was estimated from the Wilke-Chang correlation (see Eq. (4.17)). The molecular diffusion characteristic time is only applicable for the DMEB imbibition process. Moreover, L_H denotes the height of the block and L_c is the characteristics length, which is defined by [51]:

$$L_c = \left(\frac{V_b}{\sum\frac{A_i}{l_i}}\right)^{0.5}. \tag{4.22}$$

In Eq. (4.22), A_i is the area open to imbibition, V_b is the bulk volume of the core, and L_i is the distance from the surface open to imbibition to the center of the core. The characteristics length for a core with all boundaries open to imbibition fluid is calculated in Appendix A.4. Table 4.4 gives the characteristic length for water-wet cores with different boundary conditions, the capillary characteristic times and the gravity characteristic times for brine imbibition in water-wet cores.

The capillary characteristic time in brine imbibition varied between 2.5×10^{-4} –

Table 4.4: Dimensionless analysis of brine imbibition in water-wet cores.

Process	L_c [m]	t_g [*days*]	t_c [*days*]
TEO (brine)	3.54×10^{-2}	2.39	3.2×10^{-3}
BEO (brine)	3.54×10^{-2}	2.39	3.2×10^{-3}
TEsO(brine)	2.50×10^{-2}	2.39	1.6×10^{-3}
ABO (brine)	9.8×10^{-3}	2.39	2.5×10^{-4}

3.2×10^{-3} *days* depending on the surface open to imbibition; a larger surface area open to imbibition led to a faster imbibition rate. Moreover, the gravity characteristic time was approximately 2.39 *days*. Therefore, depending on the boundary conditions, the capillary characteristic time in the brine imbibition stage was $3-4$ orders of magnitude faster than the gravity characteristic time. This indicated that during

brine imbibition, capillary diffusion was the main mechanism for brine imbibition into water-wet cores.

Prior to numerical modeling of brine imbibition in water-wet cores, we simulated a countercurrent imbibition study as presented by Bourbiaux and Kalaydjian [52], and compared our numerical results with their simulation results. They performed a water-oil countercurrent imbibition experiment in the "GVB-3" sandstone core, which was a strongly water-wet core. They simulated the experimental results and they found a good agreement between simulated and experimental results. The rock and fluid properties that they used in their studies are presented in Table 4.5. We compared our numerical results with the numerical results presented by Bourbiaux and Kalaydjian as shown in Fig. 4.10. There was a good agreement between our results and the results of Bourbiaux and Kalaydjian.

Subsequently, we performed numerical simulations of brine imbibition experiments

Table 4.5: Properties used in the experimental and the numerical studies after Bourbiaux and Kalaydjian [52].

Property	Value	Unit
K	1.224×10^{-13}	$[m^2]$
ϕ	0.233	[1]
S_{wi}	0.40	[1]
K_{ro}	0.46	[1]
K_{rw}	0.044	[1]
S_{or}	0.422	[1]
σ	0.035	$[N/m]$

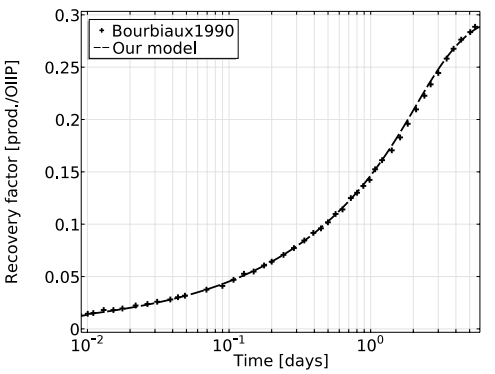

Figure 4.10: Comparison between the numerical results obtained by our model to the numerical results presented by Bourbiaux and Kalaydjian in the reference [52].

in water-wet cores. As shown in Fig. 4.11, our production curves showed a lot of scatter. The reasons for the delay in the production curve are listed on page

85. Therefore, we only were able to match the ultimate primary recovery. The results are shown in Fig. 4.11. Numerical results are shown by solid lines and the experimental data are shown by circles (∘). In addition, we assumed that the jump, which appeared in the production curve, occurred continuously and we adapted the production curve with a linear correction. Thus, instead of the jump we used the correction over the entire duration of the experiment. We showed the data points by square symbols (□) in Fig. 4.11. The matching parameters used for the modeling of brine imbibition experiments are given in Table 4.6.

We estimated the concentration dependence of all characteristic times by our

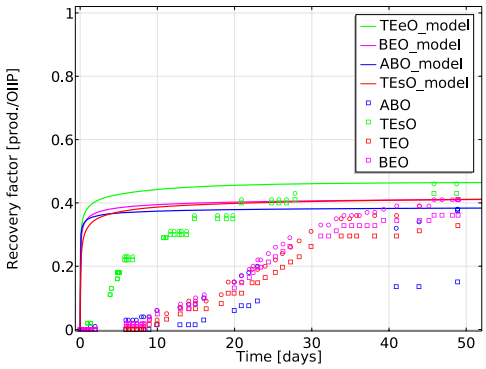

Figure 4.11: This figure shows the experimental and the numerical results for brine imbibition experiments in water-wet cores with different boundary conditions. Primary recovery stopped after 49 *days*, where a jump occurred due to releasing drops attached to the rock surface. The maximum jump happened in the core that was exposed to brine from all sides. The primary recovery for all cores was $38-46\%$ of the OIIP. Numerical model matched the recovery efficiencies.

Table 4.6: Model parameters used in the numerical simulations of brine imbibition in water-wet rocks.

Parameter	ABO	TEsO	BEO	TEO
P_{cb}, Pa	4593	9501	9330	8923
K^e_{ra}	1	1	1	1
K^e_{ro}	1	1	1	1
λ	2	2	2	2
ROS	0.62	0.54	0.59	0.59

numerical model. We disregarded the effect of concentration on the interfacial tension and we assumed that the density and the viscosity of the aqueous phase were equal to the density and the viscosity of pure brine. Figure 4.12 compares the concentration dependence of the capillary characteristic time and the gravity

characteristic time during DMEB imbibition in water-wet cores. Figure 4.12 also compares the molecular diffusion characteristic time both in the oleic phase and in the aqueous phase. The comparison between the capillary characteristic time, the gravity characteristic time and the molecular diffusion characteristic time shows that the capillary characteristic time is approximately 3 orders of magnitude shorter than the gravity characteristic time, and approximately $2-3$ orders of magnitude shorter than the molecular diffusion time in both the oleic and the aqueous phase. After imbibition of the aqueous phase due to capillary diffusion, the distance between the oleic and the aqueous blobs is sufficiently small such that the molecular diffusion time on this scale is relatively fast. Consequently, at the small scale the molecular diffusion time is faster than the capillary diffusion time over the entire length ($5\ cm$) or radius ($1.5cm$) of core scale depending on the open surface to imbibition.

We also carried out simulations to match the incremental oil recoveries for DMEB

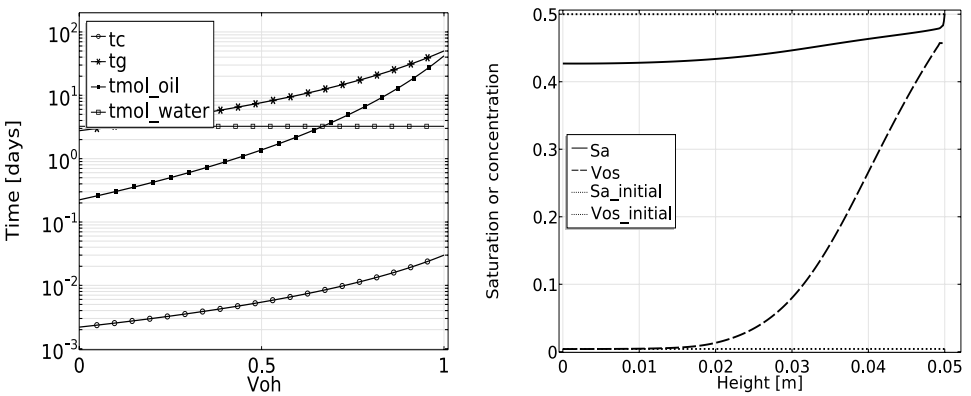

(a) (b)

Figure 4.12: (a) The capillary characteristic time, the gravity characteristic time and the molecular diffusion characteristic time for DME/brine imbibition in the water-wet cores are shown as a function of concentration. The capillary characteristic time was approximately 3 $(3-4)$ orders of magnitude shorter than the gravity time (molecular diffusion time both in oil and in brine), which indicated that the imbibition process was dominated by capillary forces; the gravity forces were of minor importance. (b) The saturation of the aqueous phase and the DME concentration in the oleic phase are shown for time $2.5 \times 10^5\ s$. The transport of DME is retarded imbibition due to the fact that DME in the imbibing phase is transferred to the oleic phase. Penetration of DME in the core is controlled by molecular diffusion.

imbibition. We took both oil swelling and viscosity reduction mechanisms into account in numerical studies of DMEB imbibition in water-wet cores. We assumed that the density and the viscosity of the aqueous phase were equal to the density and the viscosity of brine (without DME) and we disregarded the concentration

dependence of interfacial tension. Similar to the brine imbibition curves, the DMEB production curves were delayed for reasons explained on page 85. For the modeling of DMEB imbibition, we used the same model parameters as for brine imbibition (Table 4.6). The partition coefficient and the capillary entry pressure are parameters to be optimized to get the best correspondence between experimental and numerical results. As shown in Fig. 4.13, the highest imbibition rate was predicted for the core with all boundaries open to imbibition.

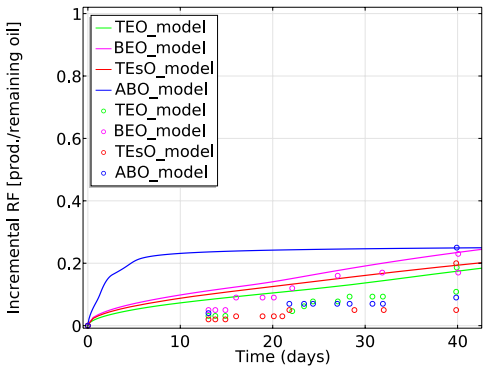

Figure 4.13: The incremental recovery with DMEB imbibition is shown. Incremental recoveries varied between $19-25\%$ of the remaining oil ($11-16\%$ of the OIIP). The numerical simulation results are compared for BEO, TEsO, TEO and ABO cores (see symbol list). The DMEB production curves were delayed for reasons explained on page 85. We matched the final recoveries.

4.5.3 Oil recovery from mixed-wet cores

In the mixed-wet cores, we performed primary imbibition tests with brine ($3\ w/w.\%$) and secondary imbibition tests using a solution of $10 \pm 0.2\ mol\%$ DME in brine (DMEB) with the same salinity. We carried out these primary and secondary imbibition tests in three cores, viz. $Lim1$ ($\varphi = 27.9\%$, $K = 3.44\ mD$) with an initial water saturation $S_{wi} = 0.173$, $Lim4$ ($\varphi = 29.7\%$, $K = 4.52\ mD$) with an initial water saturation of $S_{wi} = 0.169$ and $Lim7$ ($\varphi = 30.0\%$, $K = 4.67\ mD$) with an initial water saturation of $S_{wi} = 0$. These three cores were open from all sides to imbibition, and the primary imbibition results (time $t = 0 - 36\ days$) and the secondary imbibition results (time $t = 36 - 90\ days$) are shown in Fig. 4.14a. The primary recovery with brine imbibition was very slow and small, i.e. $1-2\%$ of the OIIP after 36 *days* (See Fig. 4.14a). This is a consequence of the mixed-wet conditions, which led to a weak capillary imbibition process. During brine imbibition in mixed-wet cores, the initial water saturation did not influence the oil recovery or imbibition rate.

In the absence of DME and in view of the long gravity characteristic time ($t_g \approx 56$ *days*), capillary diffusion is apparently responsible for the small oil recovery from mixed-wet cores.

Figure 4.14a also shows DMEB imbibition into mixed-wet limestone cores (time $t = 36 - 90$ *days*). For reasons of comparison, the incremental oil recoveries from mixed-wet cores are compared in Fig. 4.14b; the time $t = 0$ started upon DMEB imbibition. Fig. 4.14b uses a logarithmic scale to highlight the recovery rate at the early stages of DMEB imbibition. Both Figs. 4.14a and 4.14b show that with DMEB imbibition, the oil recovery started almost instantaneously after exposure of the core to DMEB. This can be attributed to DMEB imbibition. The production rate was fast, for instance 90% of the recovered oil was produced within one day, after which it reached a more or less steady state condition after 1.5 *days*. No extra oil recovery was observed between 1.5 *days* and 54 *days* (see Fig. 4.14b). A similar pattern was obtained for all mixed-wet cores, but the incremental recovery showed large variations. The oil recovery from *Lim*1 was $55 \pm 5\%$ of the OIIP, which was the maximum incremental oil in mixed-wet cores; *Lim*1 had the maximum initial water saturation, i.e. 17.3%. The minimum oil recovery was obtained from *Lim*7 ($43 \pm 5\%$ of the OIIP was produced). The *Lim*7 core had a zero initial water saturation. The incremental oil recovery from *Lim*4 ($S_{wi} = 0.169$) was $50 \pm 5\%$ of the OIIP. The fast oil recovery from the mixed-wet rocks can be attributed to the oil viscosity reduction, which led to a higher DME molecular diffusion coefficient in oil and also to a higher capillary diffusion coefficient, which both improve the DME transport to the oleic phase. In addition, DME may change the wettability of the rock surface by removal of wetting modifiers or the dilution of the oil film that covers the rock surface. However, the wettability alteration is out of the scope of this study.

Figure 4.15 shows the gravity, the capillary and the molecular diffusion characteristic times versus the oil concentration in the oleic phase during DMEB imbibition in mixed-wet rocks. The capillary diffusion characteristic time shown in Fig. 4.15 was estimated for a contact angle of 89.5. Similar to DMEB imbibition in water-wet cores, the long gravity time indicates that the gravity does not play an important role in the oil recovery process. It appears that the molecular diffusion time is the fastest characteristics time. With the partitioning of DME into oil, a DME-rich oil zone is formed; therefore, molecular diffusion transports DME from the DME-rich oil zone into the DME-free oil zone. With the dissolution of DME in the oleic phase, the DME molecular diffusion in the diluted-oil increases, which further improves the transport of DME into oil-free zone.

For zero initial water saturation, the overall diffusion process is governed by diffusion in the oleic phase, which is relatively slow due to a higher oleic phase viscosity than the aqueous phase viscosity. A higher diffusion coefficient in the aqueous phase indeed enhances the overall diffusion process as can be inferred from Fig. 4.12b. Moreover, DME-oil mixtures have a higher diffusion coefficient than pure oil. In

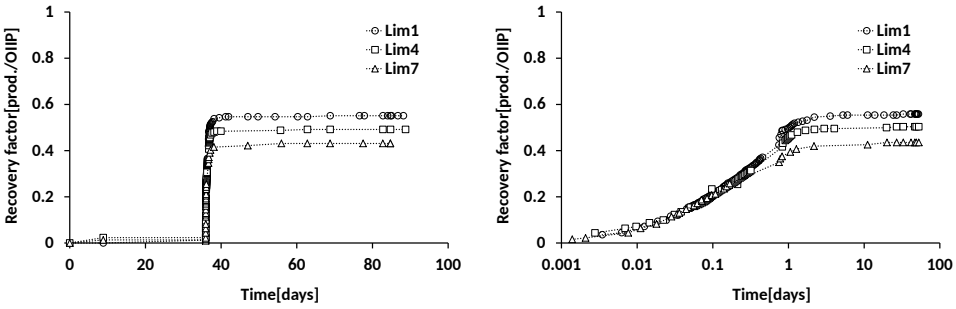

(a) (b)

Figure 4.14: Two-stage imbibition recovery from mixed-wet cores. The left figure shows the two-stage imbibition process, i.e. primary recovery without DME (before 36 days) and secondary recovery (after 36 days). The initial water saturation, $S_{wc} = 0.173$ for $Lim1$, $S_{wc} = 0.169$ for $Lim4$ and $S_{wc} = 0$ for $Lim7$ was different in the cores. The right figure shows the incremental oil recovery after 36 days; the time $t = 0$ started upon DMEB injection, which is plotted logarithmically to highlight the recovery rate at the early stages of DMEB imbibition. A similar pattern was obtained in all mixed-wet cores. The maximum oil recovery was obtained from $Lim1$ and the minimum oil recovery was obtained from $Lim7$.

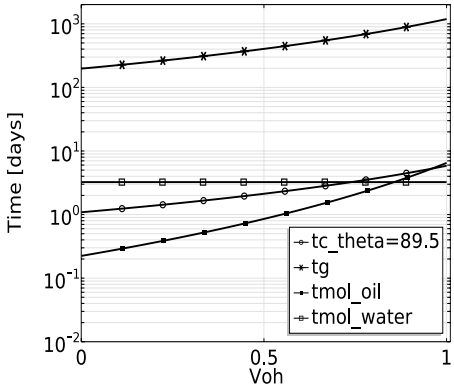

Figure 4.15: The molecular diffusion characteristic time depends on the oil viscosity. Once oil is diluted by the partitioning of DME, the molecular diffusion increases and, thus, the molecular diffusion characteristic time decreases. The molecular diffusion time is estimated from Eq. (4.21) based on the time that is needed for a DME molecule to diffuse in oil over an area of $r^2 = 2.25 \times 10^{-4}\ m^2$.

other words, the diffusion in the aqueous phase may be conducive to a faster transfer to the oleic phase, which again enhances the diffusion transport.

The history matched experimental results for DMEB imbibition in mixed-wet cores

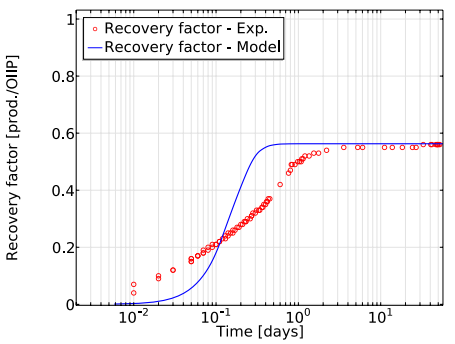

(a) *Lim*1

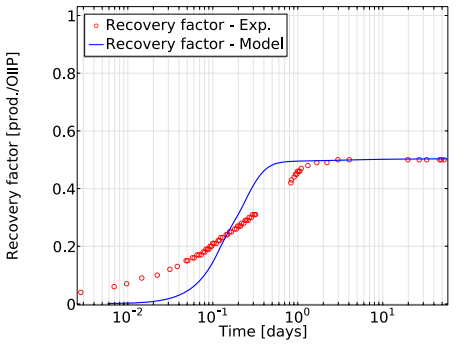

(b) *Lim*4

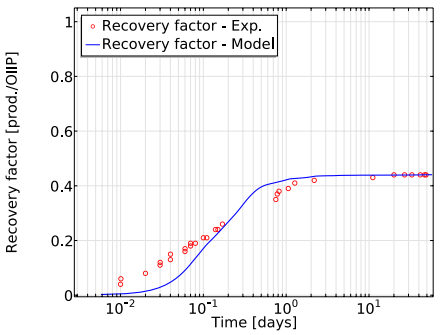

(c) *Lim*7

Figure 4.16: Numerical simulation for DMEB imbibition in mixed-wet *Lim*1 (a), *Lim*4 (b) and *Lim*7 (c) cores is shown.

have been given in Fig. 4.16. By "history matching", we mean simulation with optimized parameters for optimal agreement between experimental and numerical results. We implemented both oil swelling and viscosity reduction in the model; wettability modification was disregarded. Indeed, in this study, the difference between the experimental and the theoretical production curves was minimized by varying the capillary entry pressure and the partition coefficient. Such an optimization is not unique and therefore, it is possible that negative capillary pressures can occur and that the relatively fast recovery is due to other mechanisms, such as swelling and viscosity reduction. The model parameters are shown in Table 4.7. Despite of optimization there is a large discrepancy between theoretical and numerical results. We also performed a sensitivity analysis on the model parameters to discern the most important parameters on oil recovery in mixed-wet rocks. The sensitivity analysis results for *Lim*4 core, as a representative for mixed-wet cores, is given in Figure 4.17. First, the model shows that both the oil recovery and the production rate

were largely determined by the partition coefficient (see Fig.4.17a). Secondly, Fig. 4.17b shows that with a decrease of the DME molecular diffusion, the recovery rate decreased. Moreover, with the assumption of zero DME molecular diffusion in oil and in brine, the oil recovery in the simulation time scale was unrealistically small and slow. Thirdly, Fig. 4.17c shows the effect of the viscosity reduction on the oil recovery. The figure shows that the oil viscosity reduction improved the production rate, and that slightly higher oil recovery was obtained due to viscosity reduction. Lastly, Fig. 4.17d shows that the effect of capillary pressure was not significant on the oil recovery from mixed-wet cores.
As none of the typical reservoir and fluid parameters can explain the discrepancy observed in Fig. 4.16, we assert the delayed production is primarily responsible for the impossibility to get a better match between experimental and numerical results.

Table 4.7: Model parameters used in the numerical simulations of DME imbibition in mixed-wet rocks.

Parameter	$Lim1$	$Lim4$	$Lim7$
$P_{cb},\ Pa$	15.4	13.7	11.4
K^e_{ra}	1	1	1
K^e_{ro}	1	1	1
λ	2	2	2
ROS	0.81	0.81	0.97
K_{oa}	2	1.8	2

4.6 Concluding remarks

We studied the acceleration and the enhancement of oil recovery from water-wet and mixed-wet cores by the addition of dimethyl ether to brine. Brine spontaneous imbibition experiments in four cylindrical water-wet sandstone cores with the top-end and bottom-end, both-ends and all sides open to imbibition fluid led to a primary oil recovery of $38-46\%$ of the OIIP. By adding DME, an additional oil recovery of 11-16% of the OIIP was obtained from the water-wet cores. Brine spontaneous imbibition in three mixed-wet tight limestone cores led to a small primary oil recovery ($1-2\%$ of the OIIP). With DMEB imbibition, the oil recovery started almost instantaneously after exposure of mixed-wet cores to DMEB. The production rate was fast and an additional oil recovery of $43-55\%$ of the OIIP was produced within 1.5 days. Numerical modeling of DMEB imbibition experimental results in water-wet cores showed that capillary diffusion transports the water-wet phase quickly into the core, but, due to the exchange of DME with the oleic phase, will be largely depleted from DME. Consequently, transport of DME largely occurs due to

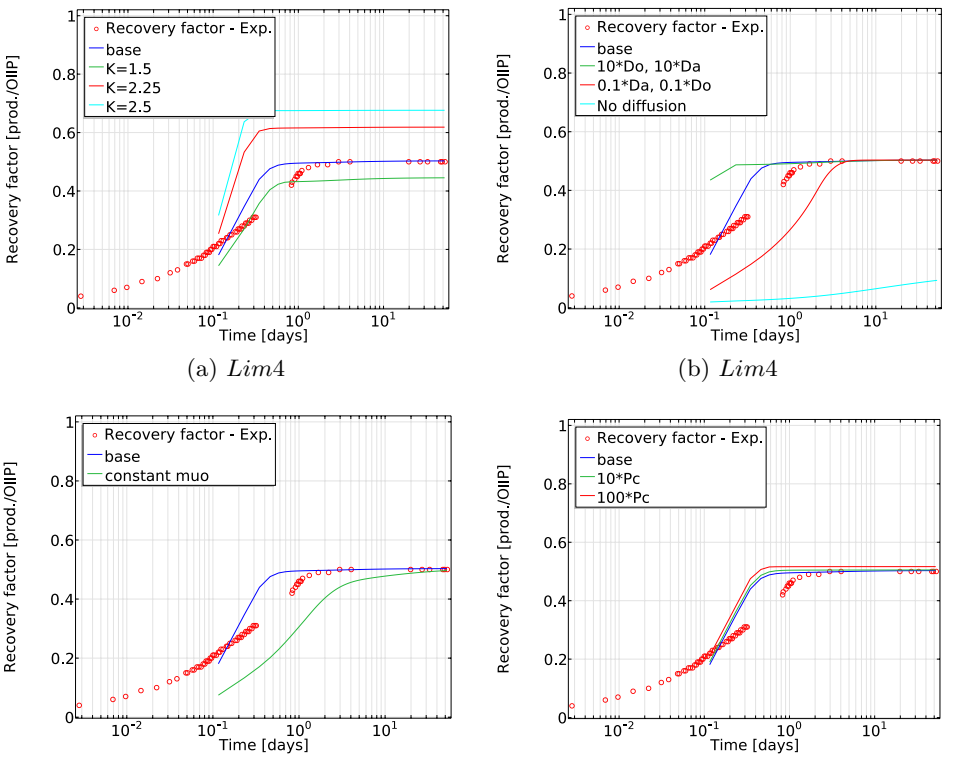

(a) *Lim4* (b) *Lim4*

(c) *Lim4* (d) *Lim4*

Figure 4.17: Sensitivity of the numerical simulation results of *Lim4* to model parameters, i.e. (a) the partition coefficient (b) the DME molecular diffusion (c) the viscosity reduction (d) capillary pressure.

diffusion. In view of the long gravity characteristic time, the effect of gravity forces was of minor importance. In mixed-wet cores, the slightly water-wet behavior partly contributed to the initial imbibition of brine without DME into the mixed-wet cores. The presence of DME reduces the viscosity of the oleic phase, and therefore, increases the imbibition rate. The mechanisms of the transfer of DME from the aqueous into the oleic phase, assuming instantaneous thermodynamic equilibrium, depend on the molecular diffusion in both the aqueous and oleic phases. The diffusion coefficient in the DME-free oleic phase is slow, but increases upon dilution by a factor of 50 in pure DME. Diffusion in the aqueous phase is faster and thus the presence of an initial water saturation accelerates the diffusion process. DME occupies a larger volume in the oleic phase than in the aqueous phase and the ensuing volume increase pushes some oil out of the core. This recovery is an addition to the recovery due to oil swelling, which is mainly a dilution effect and causes the oil that is left behind to

be diluted with DME.

Bibliography

[1] M. Chahardowli, A. Zholdybayeva, R. Farajzadeh, and H. Bruining, "Solvent-Enhanced Spontaneous Imbibition in Fractured Reservoirs," in *Proceedings of 75th EAGE Conference & Exhibition incorporating SPE EUROPEC 2013*. Society of Petroleum Engineers, Jul. 2013.

[2] M. Chahardowli, R. Farajzadeh, and H. Bruining, "Numerical Simulation of Mutually Soluble Solvent-Aided Spontaneous Imbibition in Fractured Reservoirs," in *14th European Conference on the Mathematics of Oil Recovery*, Catania, Sep. 2014.

[3] J. Warren, and P. J. Root, "The behavior of naturally fractured reservoirs," *Society of Petroleum Engineers Journal*, vol. 3, no. 03, pp. 245–255, 1963.

[4] H. S. Behbahani, G. Di Donato, and M. J. Blunt, "Simulation of Counter-Current Imbibition in Water-Wet Fractured Reservoirs," *Journal of Petroleum Science and Engineering*, vol. 50, no. 1, pp. 21–39, Jan. 2006.

[5] N. R. Morrow and G. Mason, "Recovery of Oil by Spontaneous Imbibition," *Current Opinion in Colloid & Interface Science*, vol. 6, no. 4, pp. 321–337, Aug. 2001.

[6] A. Haugen, M. a. Ferno, G. Mason, and N. R. Morrow, "Capillary Pressure and Relative Permeability Estimated from a Single Spontaneous Imbibition Test," pp. 66–77, 2014.

[7] G. Mason and N. R. Morrow, "Developments in Spontaneous Imbibition and Possibilities for Future Work," *Journal of Petroleum Science and Engineering*, vol. 110, pp. 268–293, 2013.

[8] G. Hirasaki, "Wettability: Fundamentals and surface forces," *SPE Formation Evaluation*, vol. 6, no. 02, pp. 217–226, 1991.

[9] P. V. Brady and J. L. Krumhansl, "A surface complexation model of oil-brine-sandstone interfaces at 100 C: Low salinity waterflooding," *Journal of Petroleum Science and Engineering*, vol. 81, pp. 171 – 176, 2012.

[10] D. L. Parkhurst and C. Appelo, "User's guide to phreeqc (version 2): a computer program for speciation, batch-reaction, one-dimensional transport, and inverse geochemical calculations," 1999.

[11] B. Bourbiaux, "Understanding the Oil Recovery Challenge of Water Drive Fractured Reservoirs," *Proceedings of International Petroleum Technology Conference*, 2009.

[12] M. Pooladi-Darvish and A. Firoozabadi, "Cocurrent and Countercurrent Imbibition in a Water-Wet Matrix Block," *SPE Journal*, no. March, pp. 3–11, 2000.

[13] Z. Tavassoli, R. W. Zimmerman, and M. J. Blunt, "Analysis of Counter-Current Imbibition With Gravity in Weakly Water-Wet Systems," *Journal of Petroleum Science and Engineering*, vol. 48, no. 1-2, pp. 94–104, jul 2005.

[14] A. Chernetsky, S. Masalmeh, D. Eikmans, P. D. Boerrigter, C. Parsons, A. Parker, D. Boersma, J. Cui, B. Dindoruk, P. te Riele, A. Kindi, and N. Azri, "Experimental Results and Modelling Workflow of the DME Enhanced Waterflood Technology," in *The Abu Dhabi International Petroleum Exhibition and Conference, ADIPEC*. Society of Petroleum Engineers, 2015.

[15] M. Chahardowli, R. Farajzadeh, and H. Bruining, "Experimental Investigation of the Use of the Dimethyl Ether/Polymer Hybrid as a Novel Enhanced Oil Recovery Method," *accepted for publication in Journal of Industrial and Engineering Chemistry*, DOI:10.1016/j.jiec.2016.04.008.

[16] J. Groot, A. Chernetsky, P. Te Riele, B. Dindoruk, J. Cui, L. Wilson, and R. Ratnakar, "Representation of Phase Behavior and PVT Workflow for DME Enhanced Water-Flooding," in *SPE EOR Conference at Oil and Gas West Asia*. Society of Petroleum Engineers, 2016.

[17] P. t. Riele, C. Parsons, P. Boerrigter, J. Plantenberg, B. Suijkerbuijk, J. Burggraaf, A. Chernetsky, D. Boersma, and R. Broos, "Implementing a Water Soluble Solvent Based Enhanced Oil Recovery Technology-Aspects of Field Development Planning," in *SPE EOR Conference at Oil and Gas West Asia*. Society of Petroleum Engineers, 2016.

[18] A. Alkindi, N. Al-Azri, D. Said, K. AlShuaili, and P. Te Riele, "Persistence in EOR-Design of a Field Trial in a Carbonate Reservoir Using Solvent-Based Water-Flood Process," in *SPE EOR Conference at Oil and Gas West Asia*. Society of Petroleum Engineers, 2016.

[19] M. Chahardowli, R. Farajzadeh, and H. Bruining, "Experimental Investigation of the Use of Dimethyl Ether/Polymer Hybrid as an Enhanced Oil Recovery Method," in *SPE EOR Conference at Oil and Gas West Asia*, 2016.

[20] S. Shenawi and C. Wu, "Compositional Simulation of Carbonated Waterfloods in Naturally Fractured Reservoirs," in *Proceedings of SPE/DOE Improved Oil*

Recovery Symposium. Tulsa, Oklahoma: Society of Petroleum Engineers, Apr. 1994.

[21] H. Erdener, A. Arinan, and S. Orman, "Future fossil fuel alternative; dme (a review)," *International Journal of Renewable Energy Research (IJRER)*, vol. 1, no. 4, pp. 252–258, 2012.

[22] I. M. Sivebaek and J. r. Jakobsen, "The Effect of Gasses on the Viscosity of Dimethyl Ether," *Tribology International*, vol. 41, pp. 839–843, 2008.

[23] A. Basu, M. Gradassi, R. Sills, T. Fleisch, and R. Puri, "Use of dme as a gas turbine fuel," in *ASME Turbo Expo 2001: Power for Land, Sea, and Air*. American Society of Mechanical Engineers, 2001, pp. V002T01A003–V002T01A003.

[24] H. J. Curran, S. L. Fischer, and F. L. Dryer, "Reaction Kinetics of Dimethyl Ether. II: Low-Temperature Oxidation in Flow Reactors," *International Journal of Chemical Kinetics*, vol. 32, no. 12, pp. 741–759, 2000.

[25] H. J. Curran, W. J. Pitz, C. K. Westbrook, P. Dagaut, J.-C. Boettner, and M. Cathonnet, "A Wide Range Modeling Study of Dimethyl Ether Oxidation," *International Journal of Chemical Kinetics*, vol. 30, pp. 229–241, 1998.

[26] H. Erdener, A. Arinan, and S. Orman, "Future Fossil Fuel Alternative; Di-Methyl Ether (DME) a Review," *Int. J. Ren. Ener. Res*, vol. 1, no. 4, pp. 252–258, 2011.

[27] T. H. Fleisch, a. Basu, and R. a. Sills, "Introduction and Advancement of a New Clean Global Fuel: the Status of DME Developments in China and Beyond," *Journal of Natural Gas Science and Engineering*, vol. 9, pp. 94–107, 2012.

[28] T. Fleisch, A. Basu, M. Gradassi, and J. Masin, "Dimethyl ether: a fuel for the 21st century," *studies in surface science and catalysis*, vol. 107, pp. 117–125, 1997.

[29] T. A. Semelsberger and R. L. Borup, "Thermodynamic Equilibrium Calculations of Dimethyl Ether Steam Reforming and Dimethyl Ether Hydrolysis ?" vol. 152, pp. 87–96, 2005.

[30] S. L. Fischer, F. L. Dryer, and H. J. Curran, "Reaction Kinetics of Dimethyl Ether. I: High-Temperature Pyrolysis and Oxidation in Flow Reactors," *International Journal of Chemical Kinetics*, vol. 32, pp. 713–740, 2000.

[31] D. A. Lashof and D. R. Ahuja, "Relative contributions of greenhouse gas emissions to global warming," 1990.

[32] T. a. Semelsberger, R. L. Borup, and H. L. Greene, "Dimethyl Ether (DME) as an Alternative Fuel," *Journal of Power Sources*, vol. 156, pp. 497–511, 2006.

[33] A. Laesecke and D. S. Cousins, "Sealed Gravitational Capillary Viscometry of Dimethyl Ether and Two Next-Generation Alternative Refrigerants," p. 231, 2012.

[34] J. N. Israelachvili, *Intermolecular and Surface Forces: Revised Third Edition*. Academic press, 2011.

[35] R. Bird, W. Stewart, and E. Lightfoot, "Transport Phenomena," 2002.

[36] R. Bouclier, M. Capeáns, C. Garabatos, G. Manzin, G. Million, L. Ropelewski, F. Sauli, and K. Silander, "Study of materials outgassing and their effect on gaseous detector lifetime," *CMS TN96/38, march*, 1996.

[37] K. S. Wain, J. M. Perez, E. Chapman, and A. L. Boehman, "Alternative and Low Sulfur Fuel Options: Boundary Lubrication Performance and Potential Problems," *Tribology International*, vol. 38, pp. 313–319, 2005.

[38] R. Battino, T. R. Rettich, and T. Tominaga, "The solubility of nitrogen and air in liquids," *Journal of Physical and Chemical Reference Data*, vol. 13, no. 2, 1984.

[39] C. Wilke and P. Chang, "Correlation of diffusion coefficients in dilute solutions," *AIChE Journal*, vol. 1, no. 2, pp. 264–270, 1955.

[40] K. Fujimoto and Y. Ohno, "Dme handbook," in *Japan DME Forum, Ohmsha, Tokyo*, 2007.

[41] W. Ying, Z. Longbao, and W. Hewu, "Diesel emission improvements by the use of oxygenated dme/diesel blend fuels," *Atmospheric Environment*, vol. 40, no. 13, pp. 2313–2320, 2006.

[42] K. Li, K. Chow, and R. Horne, "Influence of Initial Water Saturation on Recovery by Spontaneous Imbibition in Gas/Water/Rock Systems and the Calculation of Relative Permeability," *SPE Reservoir Evaluation & Engineering*, vol. 9, no. 4, pp. 295–301, Aug. 2006.

[43] J. a. Redman, S. L. Walker, and M. Elimelech, "Bacterial Adhesion and Transport in Porous Media: Role of the Secondary Energy Minimum," *Environmental Science and Technology*, vol. 38, no. 6, pp. 1777–1785, 2004.

[44] F. Brochard, "Motion of Droplets on Solid Surfaces Induced by Chemical Or Thermal Gradients," *Langmuir*, vol. 5, no. 3, pp. 432–438, 1989.

[45] S. Daniel, S. Sircar, J. Gliem, and M. K. Chaudhury, "Ratcheting Motion of Liquid Drops on Gradient Surfaces," *Langmuir*, vol. 20, no. 10, pp. 4085–4092, 2004.

[46] V. G. Levich, and S. Technica, *Physicochemical Hydrodynamics*. Prentice-hall Englewood Cliffs, NJ, 1962, vol. 689.

[47] A. Ameri, R. Farajzadeh, D. V. S. Suicmez, M. Verlaan, and J. Bruining, "Dynamic interactions between matrix and fracture during miscible gravity drainage in naturally fractured reservoirs," *Industrial & Engineering Chemistry Research*, 2015.

[48] G. Di Donato, Z. Tavassoli, and M. J. Blunt, "Analytical and Numerical Analysis of Oil Recovery by Gravity Drainage," *Journal of Petroleum Science and Engineering*, vol. 54, no. 1-2, pp. 55–69, 2006.

[49] D. Schechter, D. Zhou, and F. Orr, "Low ift drainage and imbibition," *Journal of Petroleum Science and Engineering*, vol. 11, no. 4, pp. 283–300, 1994.

[50] X. Xie and N. R. N. Morrow, "Oil Recovery by Spontaneous Imbibition from Weakly Water-Wet Rocks," *PETROPHYSICS-HOUSTON-*, vol. 42, no. 1, pp. 313–322, 2001.

[51] S. Ma, X. Zhang, N. Morrow, and X. Zhou, "Characterization of Wettability from Spontaneous Imbibition Measurements," *Journal of Canadian Petroleum Technology*, vol. 38, no. 13, 1999.

[52] B. Bourbiaux and F. Kalaydjian, "Experimental Study of Cocurrent and Countercurrent Flows in Natural Porous Media," *SPE Reservoir Engineering*, vol. 5, no. 3, pp. 361–368, Aug. 1990.

Chapter

5

Experimental investigation of the use of the dimethyl ether / polymer hybrid for enhanced oil recovery

5.1 Summary

Injection of dimethyl ether (DME) dissolved in water can enhance the recovery efficiency with respect to water flooding. In this enhanced oil recovery method, DME partitions from water into the oil; decreases oil viscosity and increases its volume, and mobilizes the trapped oil again. In this work, DME-enhanced water flooding is combined with polymer and considered for cases in which a favorable mobility control between water and oil does not exist.
In order to reduce the remaining oil, slugs of the mixed solution of DME and polymer was injected into the cores containing oil and then followed by injection of a chase fluid. This recovery method benefits both (a) from the presence of polymer, and

This chapter is adapted from Chahardowli et al. "Experimental Investigation of the Use of the Dimethyl Ether/Polymer Hybrid as a Novel Enhanced Oil Recovery Method", accepted for publication in Journal of Industrial and Engineering Chemistry, doi:10.1016/j.jiec.2016.04.008.

the oil viscosity reduction caused by DME dissolution and (b) from oil swelling due to DME dissolution. It appears from experimental data that the injectivity of a DME/polymer (DMEP) solution is higher than the injectivity of a polymer solution without DME; this indicate the presence of DME can reduce the viscosifying effect of the polymer. The main experimental observations are: (1) a higher oil recovery is obtained from continuous DMEP flooding than from continuous DME-brine Flooding, (2) the presence of polymer in the DME slug and in the chase phase reduced the remaining oil after a finite slug injection, (3) a larger DME slug and mobility control of the chase phase can improve the oil recovery after a finite slug injection.
In summary, the experiments show that combining polymer and DME improves the ultimate recovery significantly and shortens the duration of oil production.

5.2 Introduction

Pioneering studies on the application of mutually soluble solvents, i.e. carbonated water and alcohols, to enhance oil recovery are reported in 1950 and 1960's [1–4]. The most successful mutually soluble solvent to date is carbonated water flooding (CWF), which was applied in the field in 1960's [5–7]. The effect of Diethyl ether (DEE), as a mutually soluble solvent, on oil recovery from a core immersed in DEE/brine to mimic the process in a fractured reservoir is also studied [8]. Moreover, in recent years, DME has been considered as an oil recovery agent. To the best of our knowledge, there is very little published work on dimethyl ether (DME) for enhanced oil recovery [9–14].
DME is a solvent that is available in large quantities. It is considered as an alternative to diesel fuel. Unintentional release of DME to the atmosphere has less global warming potential compared to other hydrocarbons. DME is less environmentally hazardous and has a low toxicity [15]. DME has a low viscosity, a low density in the liquid state (see Table 5.1), and is highly soluble in water, i.e. 17.6 $mol\%$ at 5.1 bar and 20^oC [16]. Furthermore, DME is soluble both in brine and in oil. It has been experimentally observed that DME effectively reduces the residual oil subjected to water flooding [14]. In DME-enhanced water (DEW) flooding, DME partitions between the aqueous phase and the oleic phase. Consequently, the residual oleic phase consists partly of DME and less oil is left behind [8, 14, 17]. This is referred to as the swelling mechanism. Moreover, with the DME dissolved in oil, the viscosity of the oleic phase is reduced, which improves the mobility and, thus, improves the displacement efficiency of the process. In the displacement process, there is a region (between the DME-rich and DME-free zones) in which the DME concentration increases from zero to the injected value (see Fig. 5.1). Inside this region, the oil viscosity decreases from its original viscosity to the DME-oil mixture viscosity. Therefore, this reduces the viscosity of the displaced phase and improves the displacement efficiency and the sweep efficiency [18, 19]. However, at the same time, it gives rise to instabilities

depending on the exact oil and brine viscosities. The stability of the displacement can be controlled by adding a mobility-control agent such as polymer molecules to the aqueous phase. A mobility control agent lowers the mobility ratio between the displacing fluid and the oil, which increases the displacement efficiency and enhances the vertical and areal sweep efficiency [20, 21].

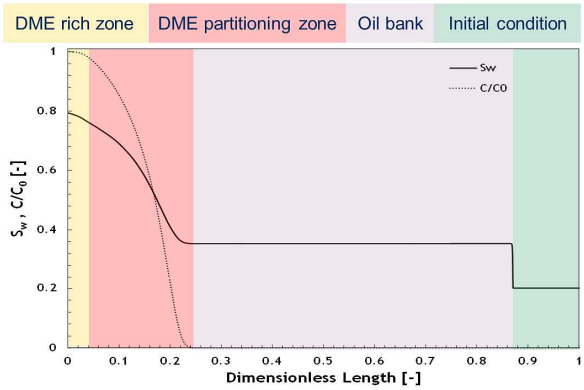

Figure 5.1: In a DME displacement process, there are four regions, i.e. the DME-rich zone, the DME-partitioning zone, the oil bank (DME-free) and the initial condition.

Previous studies on DME-enhanced water flooding have focused mainly on light oils, in which the main recovery mechanism is oil swelling [14]. In this study, the application range of DME-based EOR is extended to more viscous oils. Hence, the oil-viscosity reduction becomes an important contribution to the ultimate oil recovery. To reduce the mobility of the displacing fluid [22–25], hydrolyzed polyacrylamide (HPAM) molecules are added to the brine containing DME. Therefore, it was necessary to investigate the compatibility of polymer and DME. Several experiments were conducted in which a slug of DME-brine solution (with and without polymer) was injected into a porous medium containing oil. The slug injection was followed in each experiment with a DME-free chase fluid (with and without polymer). Unexpectedly, while carrying out the experiments, it was found that the crude oil contains large amounts of asphaltenes and, therefore, its effect on the DME-enhanced oil recovery was also investigated. The chapter is organized as follows: section 5.3 describes the experimental study in detail. In section 5.4 the experimental results are discussed and interpreted. We also include the effects of the presence of asphaltenes and its effects on the recovery. Conclusions are drawn at the final section.

5.3 Experimental study

The purpose of the experiments is to investigate the oil recovery improvements with the injection of a slug of DME/polymer or DME/brine followed by a chase fluid with and without polymer. A sandstone core was subjected to $4-15$ PV of water flooding to bring the oil saturation down to the remaining oil saturation; afterwards, a slug of DME/polymer or DME/brine was injected and was displaced by a chase fluid (polymer flooding or water flooding).

5.3.1 Materials

For brine we used 3 $w/w\%$ (0.5 mol/L) sodium chloride (NaCl, Merck) in demi-water ($pH = 6.8\pm0.1$). Polymer Flopaam 3630S (from SNF) in powder form was mixed with brine to obtain a viscous polymer solution. Flopaam 3630S is a synthesized partially hydrolyzed polyacrylamide (HPAM) polymer, which is composed of acrylamide monomers with a degree of $25-30$ $mol\%$ hydrolysis. The approximate average molecular weight of Flopaam 3630S is 18.5 million Dalton (18.5×10^6 g/mol). The Flopaam 3630S molecule is a poly-electrolyte, which forms a random coil (flexible chain) that interacts with the ions in the mixture. Figs. 5.2a and 5.2b show the chemical formula of the acrylamide monomer and a 3D view of a part of the HPAM polymer chain respectively [26]. The polymer powder was used without any treatment, i.e. as received from the company. Polymer solutions were prepared at a concentration of 1500 ppm using brine (0.5 molar NaCl in demi-water) for all experiments. The shear rate dependence of the viscosity of a mixture of 1500 ppm HPAM in brine is shown in Fig. 5.3a. We used a synthetic crude oil E (a blend of 20% C_{16} and 80% of crude oil F) to saturate the core samples for all flow experiments. The viscosity of crude oil E is shown in Fig. 5.3b. DME (Purity$>$ 99%) was supplied from Linde gas in a gas cylinder containing 10 kg DME under a pressure of 5 bar. DME (CH_3-O-CH_3) liquefies at pressures above 5.1 bars at ambient temperature and it is commercially available. DME is a colorless, highly flammable gas, which is soluble both in water and in oil. DME is a strong solvent, which only allows to use a few materials that are compatible with DME [27]. The physical properties of DME are given in Table 5.1.

5.3.2 Experimental set-up

The experimental flow set-up is shown in Fig. 5.4, and consists of a Hassler type core holder that keeps the core in a vertical position inside a rubber sleeve. A booster pump was used to inject hydraulic oil to provide a confining pressure over the sleeve. Fluids were injected into the core or produced via two Hastelloy stainless steel caps that were in direct contact with the core. The core holder was placed in

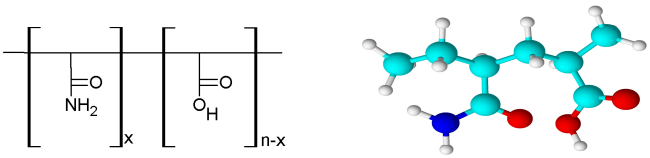

(a) (b)

Figure 5.2: (a) The structure of HPAM polymer (b) A 3D view of the HPAM monomer.

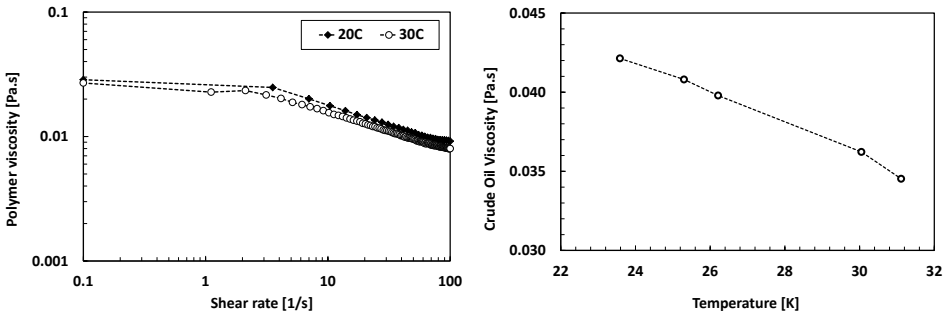

(a) (b)

Figure 5.3: (a) Viscosity of a polymer solution (1500 ppm Flopaam 3630S in brine) versus the shear rate at different temperatures. (b) Temperature dependence of the viscosity of crude oil E.

Table 5.1: Physical properties of dimethyl ether at 20°C [16].

Property	Value
Liquid Viscosity*, $(Pa.s)$	1.29×10^{-4}
Liquid density*, (kg/m^3)	670
Surface tension*, (N/m)	1.25×10^{-2}
Boiling Point**, $(°C)$	-24.81
Molecular Weight, $(kg/kmol)$	46.07
Vapor pressure, (bar)	5.1

* at pressures above 5.1 *bar*

** at atmospheric pressure

a thermometric water bath to perform the experiments at a constant temperature of $30 \pm 1°C$ in all experiments. The temperature of both the water bath and the injected fluid at the inlet face of the core were measured using thermometers. Quizix QX-500 pumps were used to inject brine or polymer solution and oil. The transfer vessel shown in Fig. 5.4 was used to prepare and inject DME/brine (DMEB) or

DME/polymer (DMEP). The transfer vessel consists of a Hastelloy stainless steel tube with a floating piston that embraces two Hastelloy stainless steel caps. The caps of the transfer vessel were connected with eight external rods, so that they could be tightened. We used a Viton A 90-shor O-ring, compatible with DME, both in the transfer vessel and in the core holder to seal the various connections. We put a magnet in the mixing side of the transfer vessel, and we put it over an IKA magnetic stirrer; therefore, we could stir and mix DME with brine or with polymer. A booster compressor pump was utilized to pressurize, liquefy and inject DME into the mixing side of the transfer vessel. In addition, tap water was pumped to the supporting side of the piston in the transfer vessel to keep a supporting pressure of 20 ± 0.5 *bars* during both the mixing and injection periods. The pressure in the injection line, the production line and the transfer vessel were measured with RTX7517 pressure transmitters. The differential pressure between the inlet and outlet of the core was measured using a differential pressure transmitter (Bronchorst between -40 and 40 ± 0.01 *bar*). A Miti Mite back-pressure regulator was implemented to keep a constant operating pressure of 20 ± 0.5 *bars* during all experiments. The produced liquid samples were collected in graded tubes in a Frac920AKTA fraction collector. The pressure transducers and thermometers were connected to a data acquisition box and their responses were digitized using an in-house program installed on a desktop.

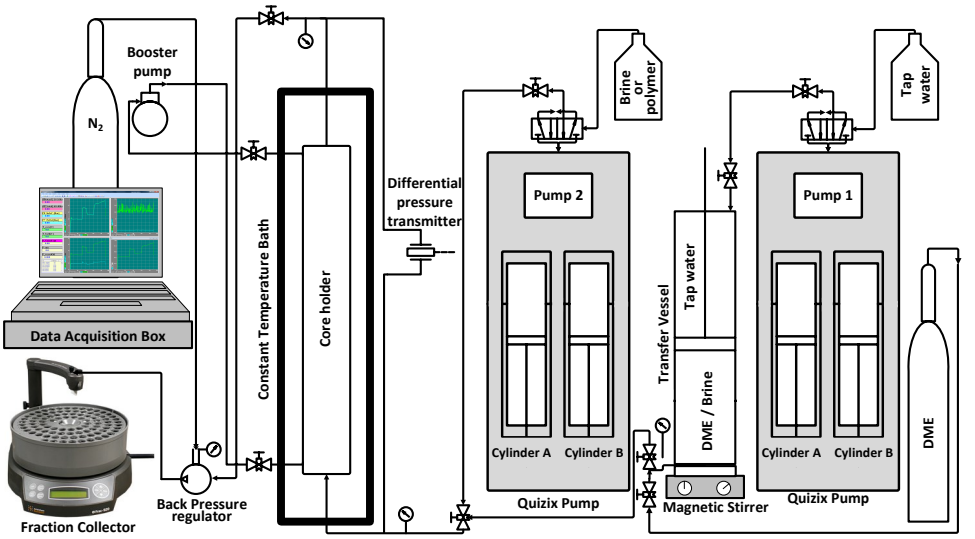

Figure 5.4: Schematic drawing of the core set-up used in coreflood experiments.

5.3.3 Core samples

Bentheimer sandstone cores with a diameter of 5.1 ± 0.1 *cm* were drilled from a cubic meter plug. Bentheimer is a consolidated nearly homogeneous sandstone consisting of 91.7 $w/w\%$ quartz, 2.7 $w/w\%$ clay (kaolinite and montmorillonite) and 4.9 $w/w\%$ feldspar, 0.4 $w/w\%$ carbonate minerals and 0.3 $w/w\%$ oxide minerals [28]. Then, all cores were sawn to a length of 15.0 ± 0.1 *cm* using a water-cooled diamond saw. Next, we put the cores in an oven, at a temperature of 60°C for a period of 48 hours, to dry the core samples.

5.3.4 Experimental methods

Preventing DME leakage from the setup. One of the challenging steps of the DME flooding experiments was to prevent DME leakage in the core holder. To solve this problem, a fit for purpose of core wrapping methodology was implemented. Afterwards, a rubber sleeve was used to support the core and caps. In the next stage, we assembled the core holder and we maintained a confining pressure of approximately 40 *bars* larger than the operating pressure over the sleeve by injection of hydraulic oil using a booster pump.

Preparation of the polymer solution. Prior to the preparation of the polymer solution, the make-up brine (0.5 *molar* or 3 $w/w\%$ NaCl in demi-water) was degassed by evacuation, using a vacuum pump for a few hours. Then, we added 50 ppm sodium bisulphite to scavenge the remaining oxygen in the make-up brine. Afterwards, 0.4 $w/w\%$ ITW mixture was added to the mixture; ITW is a mixture of 15 $w/w\%$ isopropyl alcohol, 7.5 $w/w\%$ thiourea and 77.5 $w/w\%$ of demi-water. The ITW package protects the polymer solution from degradation due to the presence of oxygen. Next, a magnet was placed in the vessel, and we put the vessel above the magnetic stirrer to establish a vortex. At the same time, nitrogen gas (N_2) was blown into the vessel to prevent contact of the liquid with oxygen. Then, the polymer powder Flopaam 3630S was slowly added to the make-up brine. Afterwards, the mixture was stirred and it was kept in contact with N_2 until the polymer powder was largely dissolved in the make-up brine. Subsequently, we reduced the stirring speed to 200 rpm and continued the stirring for a period of 24 hours at room temperature. Next, the polymer solution was filtered using paper filters (grade: $5H/N$ Sartorius, 40 μm) to remove any solid or micro-gel that was left in the solution. The viscosity of the polymer solution was measured over a wide range of shear rates using a MCR302 Anton Paar rotational rheo-meter. The shear rate dependent viscosity of an HPAM solution of 1500 ppm at temperatures 20^oC and 30^oC are shown in Fig. 5.3a.

Preparation of DME/polymer or DME/brine mixtures. To prepare DMEP or DMEB mixtures, first, the polymer solution or brine was injected into the transfer vessel. Secondly, tap water was injected at the supporting side of the vessel to maintain the pressure at 20 *bars*. Subsequently, DME was pressurized and

liquefied using an air compressor pump, before injecting it into the transfer vessel. Simultaneous with the DME injection, the mixture was stirred to mix polymer or brine with DME under pressure. In all experiments, DME was mixed with brine or polymer in a proportion of 10.0 ± 0.2 *mol*%. Mixing was continued until both the pressure in the vessel and the volume of the injected tap water into the supporting side of the vessel reached a steady state.

Polymer and DME compatibility. First of all, the compatibility between DME and polymer needs to be experimentally confirmed. Therefore, we used a high-pressure transparent cell made of Plexiglas (polymethyl methacrylate, PMMA) (see Figs. 5.5a and 5.5b). We mixed DME and polymer in the cell using a magnetic stirrer. After a few hours, we observed that black spots appeared in the mixture (see Fig. 5.5c and 5.5d). Upon inspection of the transfer vessel, we figured out that DME is not compatible with normal O-rings used in the vessel, because O-rings were deformed. In another experiment, after mixing of DME and polymer, the color of the bronze disk of the transfer vessel was changed, possibly due to the incompatibility of contaminants of the bronze disc with DME (see Fig. 5.5e). In addition, we observed that PMMA had swollen after about two weeks of keeping the DMEP mixture in the PMMA cell. Consequently, it appears that PMMA is not suitable for a long-term contact with DME mixtures. Therefore, as an alternative, we implemented a simple, but manageable, compatibility test using a chemical-resistance-transparent pipe connected to the transfer vessel (see Fig. 5.5f). Then, we replaced the incompatible materials by DME-compatible materials, i.e. the bronze piston was replaced by a Hastelloy stainless steel piston and the normal O-rings were replaced by the Viton A 90-shor O-rings. Subsequently, the compatibility test was performed visually in the sampling pipe, and it was observed that the samples remained transparent without showing any sign of solid precipitation.

Mixing crude oil with brine and DMEB. Fig. 5.6a shows the mixed crude oil E with brine; there is no visual evidence of the formation of a separate emulsion phase between the oil and brine phase. This does not exclude the formation of emulsion when salt concentration changes. In addition, we mixed DMEB and DMEP with crude oil E in a high-pressure transparent cell to investigate the effect of DME on crude oil E. After mixing, we collected the samples at atmospheric conditions. We observed that three phases were formed, i.e. an aqueous phase, a stable middle phase with a brownish color, which has been called emulsion and an oleic phase with a black color (see Fig. 5.6b).

A tentative explanation of the part of the experimental results depends on the following concepts. Crude oil contains many compounds that stabilize emulsions albeit through different mechanisms. Emulsions are defined as a single phase that consists of a stabilizing compound, oil and water. Emulsions can be stabilized by the presence of asphaltenes [29, 30]. The size of emulsion drops can be in the same order of magnitude of the pore throats. Consequently, at low injection flow rates,

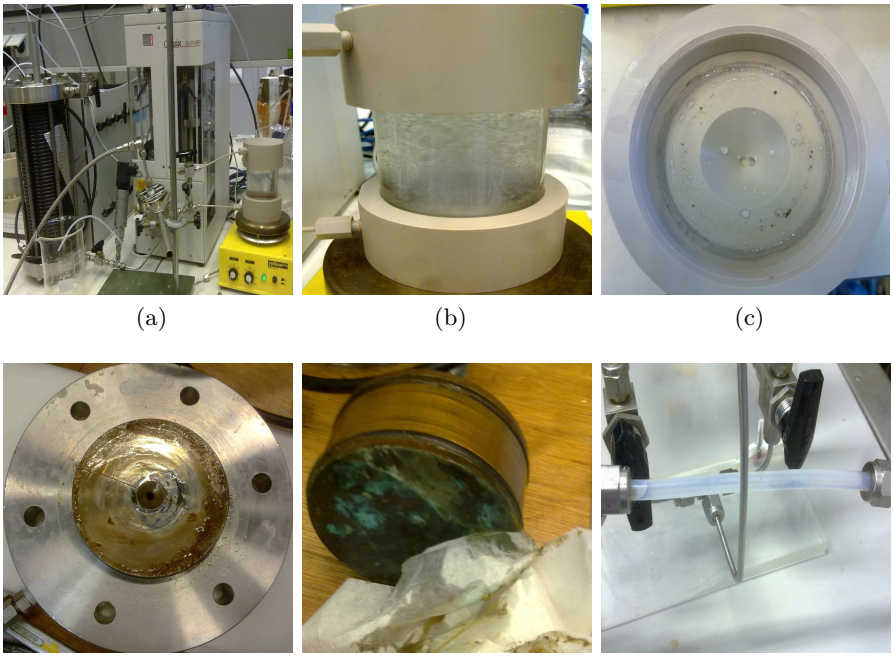

(a) (b) (c)

(d) (e) (f)

Figure 5.5: Compatibility test of Polymer and DME. (a) Primary compatibility test set-up (b) Compatibility PMMA cell, black spots are visible after mixing DME with polymer. The reason is incompatibility of DME with the materials used in the transfer vessel. (c) Black spots at the bottom cap of the transparent cell, after displacing the DME/polymer mixture out of the cell. (d) The precipitated black spots were also observed on the bottom cap of the transfer vessel. The reason was perhaps the dissolution of the normal O-ring in DME. (e) The incompatibility of DME and contaminant of bronze piston used in the transfer vessel is shown. (f) The compatibility was tested using a chemical-resistance-transparent pipe connected to the transfer vessel.

the smallest pores can be partially blocked by large drops leading to permeability damage. However, it appears that this phenomenon is partly reversible. Because with the increase of the flow rate, the pressure gradient will become large enough to move the drops through the pore throats [31]. The composition of the aqueous phase can be influenced by the geochemical properties of the Bentheimer sandstone rock. The mineral interactions occurs through rate dependent processes, i.e. see example 6 on page 310 of user's guide of PHREEQC [32]. This mechanism could be the cause of erratic production and pressure gradient behavior. The viscosity of the brownish phase was measured to be $7.95 \pm 0.05 \times 10^{-1}$ $Pa.s$ in bulk. The viscosity of the black oleic phase was $3.4 \pm 0.1 \times 10^{-2}$ $Pa.s$ at $30^{o}C$, which was close to the

viscosity of the original crude oil E, i.e. $3.6 \pm 0.1 \times 10^{-2}$ $Pa.s$ at 30^oC. The small difference can be attributed to the asphaltene drop out from crude oil E. Moreover, Fig. 5.6c shows that after water flooding a very small amount of the brownish phase was collected at the bottom of the tubes.

Dilution of oil with a volatile component like DME can lead to asphaltene precipitation [33], which can lead to a decreased mobility in the formation and an increased pressure drop. In summary, asphaltene can increase the pressure drop by two mechanisms, i.e. by the stimulating emulsions formation and by asphaltene precipitation. The interpretation of the experiments, which is based on these proposed mechanisms, is plausible but not proven; however, it helps to put the experiments in a conceptual framework.

The increased pressure drop due to the formation of emulsions was observed in the water flooding stage of most flow experiments. It appears that the addition of DME increased the asphaltene precipitation effects, which further improved the formation of emulsions. We also observed that during continuous DME/polymer flooding in the cores, the brownish emulsion phase collected in test tubes appeared in larger quantities. Fig. 5.6d shows the collected samples from the effluent after centrifuging. We heated the samples up to $80°C$ to investigate the thermal stability of the brownish phase; it was visually observed that no changes occurred to the brownish phase and that it remained as a separate phase (see Fig. 5.6e).

Injectivity experiments. The injectivity is defined as the injection flow rate divided by the pressure drop. We saturated the core with brine. Then, we injected the brine with a Darcy velocity of 3.5×10^{-5} m/s, which corresponds to an injection flow rate of 1 mL/min and recorded the pressure drop. Subsequently, an injectivity test was conducted by injection of polymer or DME/polymer solutions at the same Darcy velocity into the core, and again the pressure drop was recorded.

Coreflood tests. The oil displacement experiments were performed to determine the oil recovery for different injection scenarios. The sequence of the performed core flooding experiments was as follows: (1) a helium leakage test to verify that the system was leak-free, (2) evacuation of the core for a period of about 24 hours to remove the trapped air from the core, (3) CO_2 injection to pre-flush the core, (4) brine injection to saturate the core and to obtain the absolute permeability and an estimate of the pore volume, (5) oil flooding (OF) to establish the initial oil and water saturations, (6) water flooding (WF), while monitoring the pressure drop and collecting the effluent liquids, by water flooding we mean the injection of brine (3 $w/w\%$ NaCl in demi-water), (7) slug or continuous injection of DMEB or DMEP, (8) chase phase flooding to displace the oil bank and the slug in the core, (9) repeating step (7) with a DMEP slug, (10) repeating step (8) with a chase polymer. The recovery curve was obtained from a fraction collector with samples of $7 - 10$ mL. The production curve was corrected for both the dead volume (11 mL) of the tube, between the pump and the injection side of the core, and the dead volume (10.6 mL)

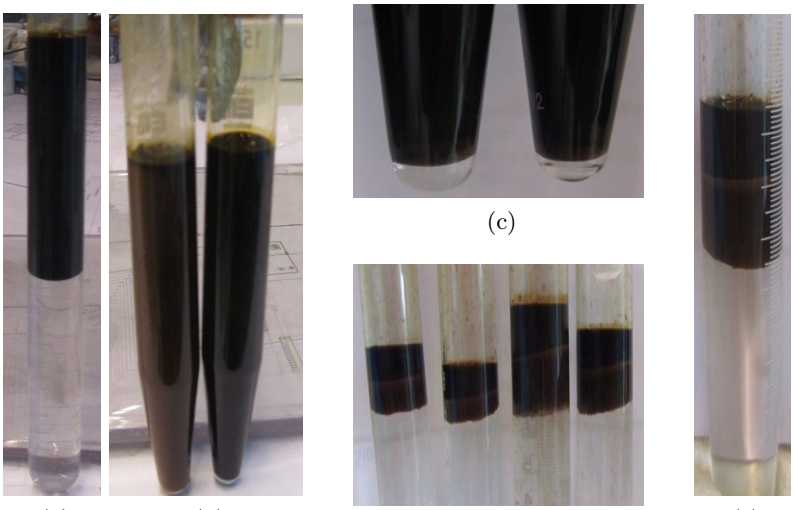

(a) (b) (c) (d) (e)

Figure 5.6: (a) Mixing of crude oil E with brine, there is no sign of emulsion between the phases. (b) Mixing of the crude oil E with DMEB; we observed three separate phases, an aqueous phase, an intermediate brownish phase (left) and a black oleic phase (right). (c) In water flooding, precipitation of the dark brownish phase was observed; however, the amount of the brownish phase was very small. (d) Formation of three phases after DME/Polymer flooding. (e) We heated up samples up to 80^oC, and we observed that the brownish phase was thermally stable.

of the tube from the production side to the fraction collector. The apparent viscosity was plotted versus the injected pore volumes, from which the dead volume (11 mL) of the tube from the pump to the injection side of the core was subtracted. Only the volume of the black oleic phase was considered as the oil production and the oil contained in the emulsion phase was excluded. The experiments are summarized in Table 5.2.

5.4 Results and discussion

Flow experiments are presented in terms of both the oil production divided by the Oil Initially In-Place (OIIP), and the apparent viscosity versus the injected pore volumes of the displacing fluid. The apparent viscosity is the ratio between the average measured pressure gradient ($\Delta P/L$) and the Darcy velocity (Q/A) multiplied by the measured average absolute permeability (k). The apparent viscosity (μ_{app})

Table 5.2: Summary of the coreflood experiments indicated in steps for each experiment, k_{av} is the average measured permeability.

Exp.	Step						k_{av}
No.	**4**	**5**	**7**	**8**	**9**	**10**	**[D]**
1	Preparation	WF	Polymer inj.	-	-	-	0.66
2		WF	DMEP inj.	-	-	-	0.67
3		OF-WF	cont. DMEB	-	-	-	1.42
4		OF-WF	cont. DMEP	-	-	-	1.56
5		OF-WF	PF	cont. DMEP	-	-	1.33
6		OF-WF	0.3 PV DMEB	WF	0.3 PV DMEP	PF	1.21
7		OF-WF	0.5 PV DMEB	PF	-	-	1.07
8		OF-WF	0.5 PV DMEP	WF	0.5 PV DMEP	PF	1.02
9		OF-WF	0.5 PV DMEP	PF	-	-	1.21

was calculated using Darcy's law:

$$\mu_{app} = -\frac{kA}{Q}\frac{\Delta P}{L}, \tag{5.1}$$

where A is the cross-sectional area of the core and L is the length of the core.

5.4.1 Experiments #1 and #2: Evaluation of injectivity

The purpose of these experiments was to evaluate and compare the apparent viscosity and the injectivity of the polymer flood and the DMEP flood.
In order to estimate the polymer viscosity in the core, we estimated the shear rate from [20]:

$$\dot{\gamma} = \alpha\frac{4u}{(8k/\varphi)^{(1/2)}} \tag{5.2}$$

where $\dot{\gamma}[1/s]$ is the shear rate, α is a shape parameter, which refers to the characteristic of the pore structure, is reported to be in the range 3.0-5.0 [20] and assuming $\alpha = 3.0$, $u[m/s]$ is the Darcy velocity, $k[m^2]$ is the absolute permeability and φ is the porosity. Therefore, a shear rate of $\dot{\gamma} = 64\ 1/s$ was obtained. The bulk viscosity of the polymer solution at this shear rate was $9 \times 10^{-3}\ Pa.s$ (see Fig. 5.3a).
Figure 5.7 compares the apparent viscosity versus the injected pore volume for

polymer injection and for DME/polymer (DMEP) injection. In both experiments, we injected fluids into the core with a Darcy velocity of 3.5×10^{-5} m/s. Prior to the polymer injection test or the (DMEP) injection test, brine-saturated cores were flooded by brine, and an approximately steady state apparent viscosity of 1×10^{-3} $Pa.s$ was obtained in both cores. In the consecutive polymer injectivity test (without DME), the apparent viscosity (black curve in Fig. 5.7) varied after an initial build up from 4×10^{-3} $Pa.s$ to a steady apparent viscosity of about 6×10^{-3} $Pa.s$ after 12 PV polymer injection. The apparent viscosity of polymer took time to reach a steady value, which can be attributed to the internal filtration and mechanical entrapment of polymer molecules in the core [34]. The steady apparent viscosity of 6×10^{-3} $Pa.s$ was lower than the bulk viscosity of polymer, i.e. 9×10^{-3} $Pa.s$. This can be attributed to (1) the capillary bundle model is not accurate enough for the estimation of the shear rate, (2) the assumed shape parameter, α, is not exact, and (3) shear degradation of polymer due to flow through pump, lines and valves. In the DMEP injectivity test (red curve in Fig. 5.7), 16.5 PV DMEP was injected into the brine-saturated core. The apparent viscosity versus the injected pore volume in the DMEP injection was different from the apparent viscosity in the polymer injectivity test. For instance, an apparent viscosity of about 2×10^{-3} $Pa.s$ was obtained, which is much smaller than the apparent viscosity obtained from the polymer injectivity test. The higher apparent viscosity for the pure polymer injectivity test shows that the DMEP solution has a higher injectivity than the polymer solution (without DME). A tentative explanation of the viscosity loss of DME/polymer is that the degree of hydrolysis of HPAM is strongly affected by the decrease of the dielectric coefficient from $\epsilon = 80$ to $\epsilon = 60$ in the presence of 10 $mol\% \approx 30$ $v/v\%$ of DME leading to shrinkage of the HPAM coil; such a shrunk coil has a smaller viscosifying effect [20, 35, 36]. Another possible mechanism for DME to decrease the viscosity of the DME/polymer mixture is that DME affects the Flory-Huggins mixing parameter ($\chi = \frac{z}{\kappa T}(u_{op} - \frac{1}{2}u_{oo} - \frac{1}{2}u_{pp})$), where the subscript o denotes the solvent (DME/brine), and the subscript p denotes the polymer [37, 38]. This interaction affects the skeleton of the polymer chains in the solution. A precise quantification of these mechanisms is considered outside of the scope of this paper. We also did not observe precipitation of polymer after mixing with DME.

5.4.2 Experiment #3 and #4: Continuous injection of DMEB and DMEP

The objective of Experiments #3 and #4 was to compare the oil recovery improvements of the continuous injection of DMEB and DMEP solutions into the cores subjected to water flooding.

Experiment #3 shows the improvements of the oil recovery by adding DME to the injected brine. First, the usual preparation steps 1-5 were carried out. The

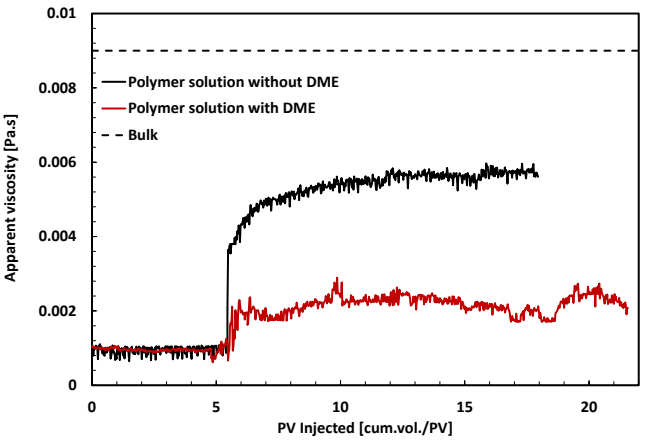

Figure 5.7: Polymer and DMEP injectivity experiments. The apparent viscosity is shown for Experiment #1, polymer injectivity test (black curve) and for Experiment #2, DMEP injectivity test (red curve).

subsequent steps are shown in Fig. 5.8.

The produced oil was collected in graded tubes using a fraction collector and the cumulative oil divided by the OIIP was calculated. Moreover, Fig. 5.8 shows both the recovery and the apparent viscosity curves versus the injected pore volume of the aqueous phase for continuous DMEB flooding.

In the water flooding step of Experiment #3, 45% of the OIIP was recovered during the first 3 PV of brine injection. An unsteady apparent viscosity was observed during $3-5$ PV injection followed by a sudden increase in the apparent viscosity. In this low injection stage, there is no significant increase in the oil recovery. It is possible that the increased apparent viscosity is due to formation of an emulsion phase, which can be stabilized by the presence of asphaltenes (see page 111). At 7.2 PV, the flow rate was increased and the apparent viscosity decreased; a steady state was never attained, but it appears that the apparent viscosity was negatively correlated with the flow rate. Small increase in the oil recovery was also observed. In total, 56% of the OIIP was recovered after 11.6 PV brine injection. It turns out that the initial water flooding step in various experiments led to recoveries that varied between $40-63\%$.

Next, with the continuous injection of a 10.0 ± 0.2 *mol*% DMEB solution into the core, the oil production was delayed and it resumed after half a pore volume. The delay can be attributed to the formation of an oil bank, which needs time to reach the outflow end. The same phenomenon is also observed by Chernetsky et al. [14]. With the continuous DMEB injection, the oil production increased gradually until an extra oil recovery of 24% was obtained after a cumulative injection of 18 PV. At the same time, the apparent viscosity increased. The increase of the apparent viscosity may be attributed to asphaltene precipitation due to DME [33]. The main

mechanisms of improved oil recovery by DME are swelling and oil viscosity reduction. Moreover, DME has a somewhat larger $(10-12\%)$ partial molar volume in the oleic phase than in the aqueous phase, which further contributes to the oil recovery.

Figure 5.9 shows the histories of the oil recovery and the apparent viscosity for

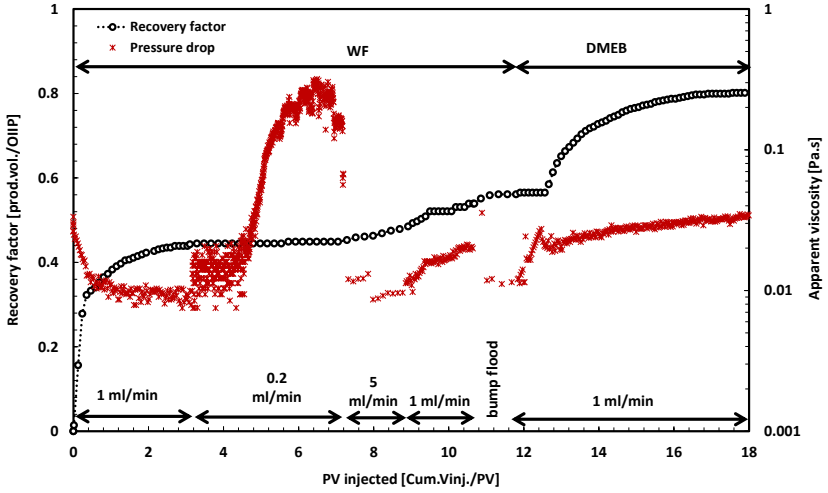

Figure 5.8: Oil recovery and apparent viscosity of Experiment #3. Experimental sequence: water flooding and continuous DME/brine (DMEB) flooding experiment.

the continuous DMEP flooding experiment. The brine-flooding stage consists of a sub-stage of $1.67 \times 10^{-8}\ m^3/s$ from 0 to 5 PV, a sub-stage of $1.67 \times 10^{-9}\ m^3/s$ from 5 to 14 PV, and a bump flood from 14 to 15 PV brine injection; an oil recovery of 64.8% of the OIIP was obtained. By the bump flood, we mean the increase of the injection flow rate by a factor of 2 until achieving an injection flow rate of $1.33 \times 10^{-7}\ m^3/s$ $(8\ mL/min)$. In the sub-stage of the brine injection with a flow rate of $1.67 \times 10^{-9}\ m^3/s$, the apparent viscosity increased and then decreased with the increase of the flow rate. This can be attributed to the appearance and the disappearance of emulsion (see page 111).

In a second stage, DMEP was continuously injected until the produced oil in the effluent was negligible and not measureable. Therefore, an extra oil recovery of 33% of the OIIP was obtained. Similar to the results for continuous DMEB injection, the production was delayed by half a pore volume.

The apparent viscosity of the continuous DMEP flooding also increased sharply, which cannot be only attributed to the viscosity of DMEP solution and needs to be investigated further. No further increase of the apparent viscosity is observed, which indicates that there is no significant polymer plugging or asphaltene precipitation inside the core.

The comparison between the results of continuous DMEB flooding and continuous DMEP flooding tests shows that the oil recovery with DMEP was larger and faster; and the apparent viscosity of the DMEP flood was higher than the apparent viscosity of the DMEB flood, which is due to the higher viscosity of DMEP solution.

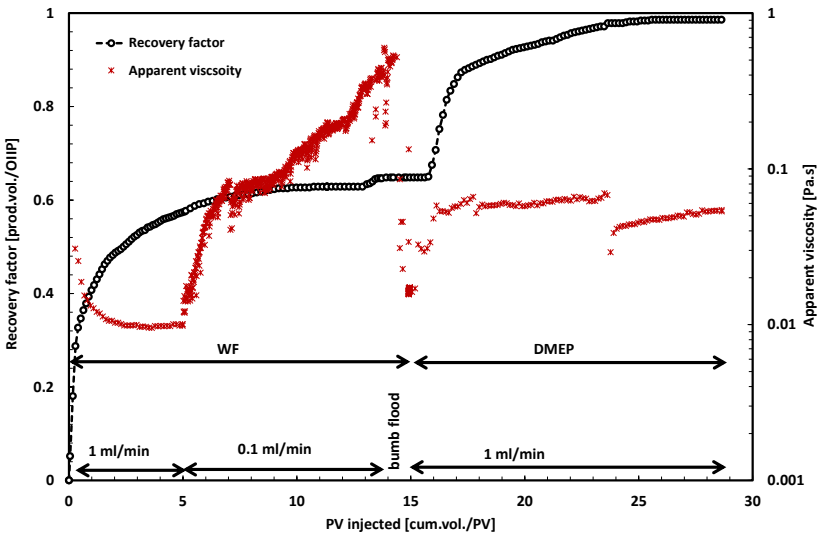

Figure 5.9: Oil recovery and apparent viscosity of Experiment #4. Experimental sequence: water flooding and continuous DME/polymer (DMEP) injection.

5.4.3 Experiment #5: Polymer flood followed by continuous DMEP flood

The idea of this experiment was to achieve a more favorable displacement process with the reduction of mobility ratio by adding polymer to the flooded water. Consecutively, the core was flooded with continuous DMEP to study its effect on the recovery of the residual oil.

The results of this experiment are shown in Fig. 5.10. First, water flooding led to an oil production of 48% of the OIIP and the apparent viscosity reached a steady state value of about 7×10^{-3} $Pa.s$. In a second stage, polymer flooding recovered additional oil of about 7% of the OIIP due to more favorable mobility ratio. Moreover, with polymer flooding, the apparent viscosity increased by a factor of 23, which is possibly due to emulsion formation. However, the decreased polymer injection flow rate decreased the apparent viscosity. In the third stage, with DMEP flooding, 42% additional oil was recovered with again a delay of half a pore volume. The apparent viscosity decreased due to the lower viscosity of DMEP with respect to the polymer viscosity, subsequently increased, and then decreased, which may be attributed to

replacement of oil by DMEP.

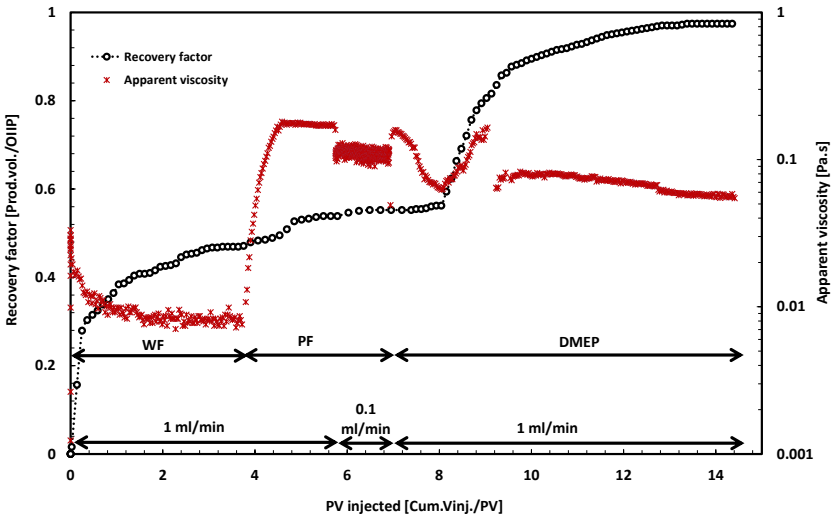

Figure 5.10: Oil recovery and apparent viscosity of Experiment #5. Experimental sequence: water flooding, polymer flooding and continuous DME/polymer (DMEP) injection.

5.4.4 Experiment #6: DMEB slug injection followed by chase brine

The objective of this experiment was to explore the oil recovery improvements by the injection of 0.3 PV DMEB followed by water flooding. In addition, after DMEB flooding, the core was flooded by 0.3 PV DMEP followed by polymer injection to study the effect of the presence of polymer both in the slug and in the chase phase. The results are shown in Fig. 5.11. Again, we observed an increasing apparent viscosity for a decreasing injection flow rate in the water flooding stage (stage 1). Moreover, 50% of the OIIP was produced after 8 PV brine injection.
The consecutive injection of a slug of 0.3 PV DMEB and brine injection led to an extra oil recovery of 15% of the OIIP and increased the apparent viscosity, which is possibly due to asphaltene precipitation (stage 2). The injection of another 0.3 PV DMEB slug and consecutive displacement of the slug with brine injection (stage 3), led to no extra oil recovery but the apparent viscosity increased and reached a value twice as higher as in the previous stage most likely due to asphaltene precipitation. Next, the injection of a slug of 0.3 PV DMEP followed by a slug of polymer led to an extra oil recovery of 15% of the OIIP after a delay of 1 PV (stage 4). It appears that smaller remaining oil led to a somewhat reduced frontal velocity of

the oil bank, which delayed the arrival of the oil bank. With DMEP flooding, a sharp decline in the apparent viscosity was observed which was due to oil production; subsequently, the apparent viscosity increased with the consecutive polymer injection. As concluded from Experiment #6, the second 0.3 PV DMEB slug injection did not contribute to recovery of the remaining oil, while, the consecutive injection of 0.3 PV DMEP and polymer chase slug (stage 4) contributed to the production of oil. The viscosity of the DMEP solution (polymer solution) was twice (six times) as high as the viscosity of brine, therefore, it appeared that the consecutive injection of DMEP and polymer slug reduces the amount of remaining oil after injection of DMEB slug followed by chase water.

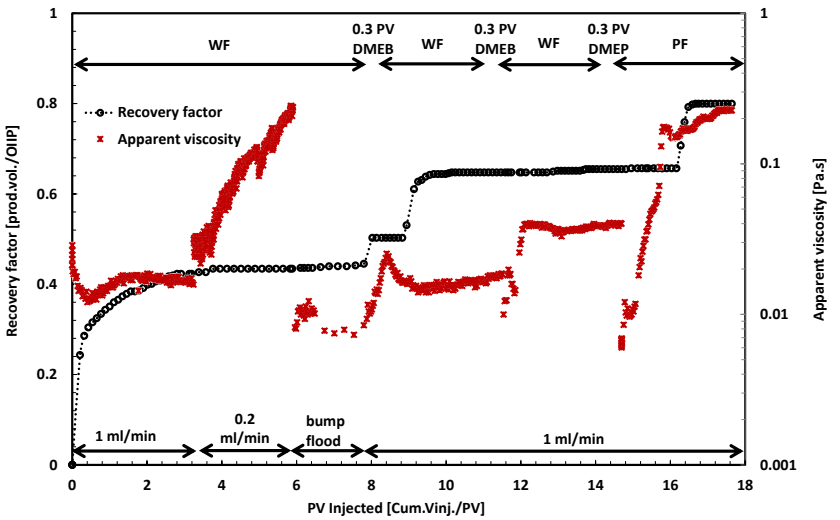

Figure 5.11: Oil recovery and apparent viscosity of Experiment #6. Experimental sequence: Water flooding, 0.3 PV DMEB, water flooding, 0.3 PV DMEB, water flooding, 0.3PV DMEP, polymer flooding, 0.3PV DMEP and polymer flooding.

5.4.5 Experiment #7: DMEB slug injection followed by chase polymer

This experiment was designed to investigate the oil recovery enhancement by the displacement of the injected DMEB slug followed by the polymer solution as a chase phase.

The oil recovery history and the apparent viscosity history of the experiment are shown in Fig. 5.12. First, the flooding of the core with brine led to an oil recovery of 39% of the OIIP and after 1.5 PV, the apparent viscosity reached an approximately steady state value.

Secondly, 0.5 PV DMEB was injected into the core and consecutively displaced with a polymer chase, which led to an extra oil recovery of 45% of the OIIP. It was observed that with DMEB injection, the apparent viscosity increased. The increased trend of the apparent viscosity was also continued with the injection of the polymer chase. The initial increase of the apparent viscosity can be attributed to asphaltene precipitation and the second increase can be attributed to the higher viscosity of the polymer chase.
In stage 2 of Experiment #6, it was observed that, with the consecutive injection of 0.3 PV DMEB and brine, an extra oil recovery of 15% was obtained. However, in this experiment the injection of a larger DMEB slug (0.5 PV DMEB) followed by a viscous chase (polymer) led to an extra oil recovery of 45%. Therefore, the higher extra oil recovery can be due to the presence of a larger amount of DME in the slug and to the displacement of the slug with a viscous chase, which possibly reduces the remaining oil after water flooding. This observation is valid only in a one-dimensional displacement.

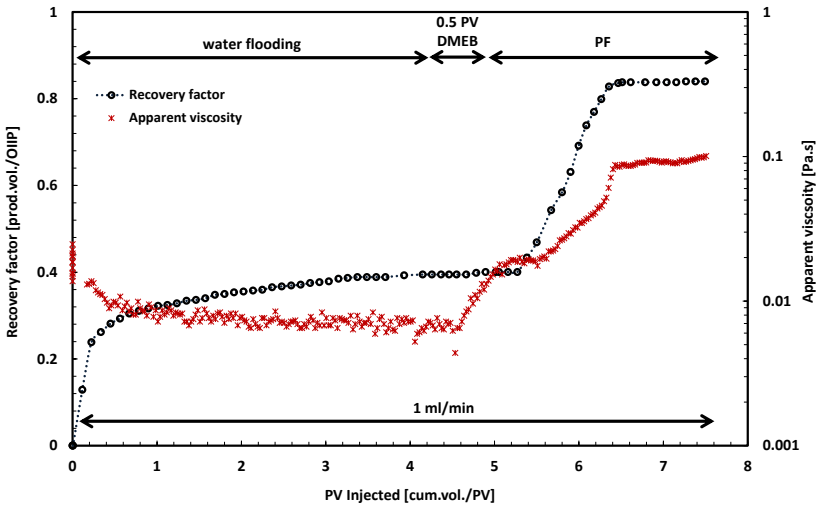

Figure 5.12: Oil recovery and apparent viscosity of Experiment #7. Experimental sequence: water flooding, 0.5 PV DMEP, water flooding, 0.5 PV DMEP and polymer flooding

5.4.6 Experiment #8: DMEP slug injection followed by chase brine

The objective of this experiment was to study and compare the effect of oil recovery enhancement by displacement of the injected DMEP slug by brine injection as a

chase phase.
Figure 5.13 shows the oil recovery and the apparent viscosity curves versus the injected pore volume of the aqueous phase. First, water flooding led to an oil recovery of 51% of the OIIP and to a stabilized apparent viscosity. Then, lowering the injection flow rate led to no significant extra oil recovery, while the apparent viscosity increased by a factor of 10, and subsequently decreased with the increase of the injection flow rate. This can be attributed to the appearance and disappearance of emulsion (see page 111).
In the next stage, the core was flooded by 0.5 PV DMEP and thus the apparent viscosity increased. Consecutively, the 0.5 PV DMEP slug was displaced by a brine slug. As a result, 26% of the OIIP was recovered. After 9 PV injection, the apparent viscosity reached approximately a steady state value.
Subsequently, one more slug of 0.5 PV DMEP followed by a polymer chase slug was injected, which led to an additional oil recovery of 14% of the OIIP and an increase of the apparent viscosity. With the injection of the second DMEP slug, the apparent viscosity reduced and subsequently increased. The increasing trend continued with the consecutive polymer chase injection, until it reached a steady-state value of about 1×10^{-3} $Pa.s$ after 13 PV injection. It appears that the reason for the increased apparent viscosity is again the higher viscosity of the DMEP slug and polymer chase. In addition, the additional oil recovery in stage 3 shows a higher efficiency of the viscous chase phase than of the brine chase phase. The extra oil recovery in stage 3 can be attributed to the reduction of the remaining oil after water flooding.

5.4.7 Experiment #9: DMEP slug injection followed by chase polymer

The objective of Experiment #9 was to study the effect of the increase of viscosity of both the DME slug and the chase phase by adding polymer, on the oil recovery. The production and the apparent viscosity histories are shown in Fig. 5.14. The oil recovery by water flooding was 54%. Here, with a constant injection flow rate of 1.67×10^{-8} m^3/s, the apparent viscosity increased after 2.7 PV injection, before a sudden jump at 3.8 PV. Increase and decrease of the apparent viscosity may be attributed to the appearance and the disappearance of an emulsion (see page 111). Next, 0.5 PV DMEP was injected and was consecutively displaced by a polymer solution slug, which led to an extra oil recovery of 39% of the OIIP and an increased apparent viscosity. Afterwards, the apparent viscosity slightly decreased in comparison to DMEP flooding at 8 PV, possibly due to the production of the oil bank and to the reduction of the remaining oil after water flooding.
In step 2 of Experiment #8, an extra oil recovery of 26% was obtained by consecutive injection of the DMEP slug and a low viscous chase phase. However, in Experiment #9, with the displacement of the DMEP slug with a viscous chase phase, an extra

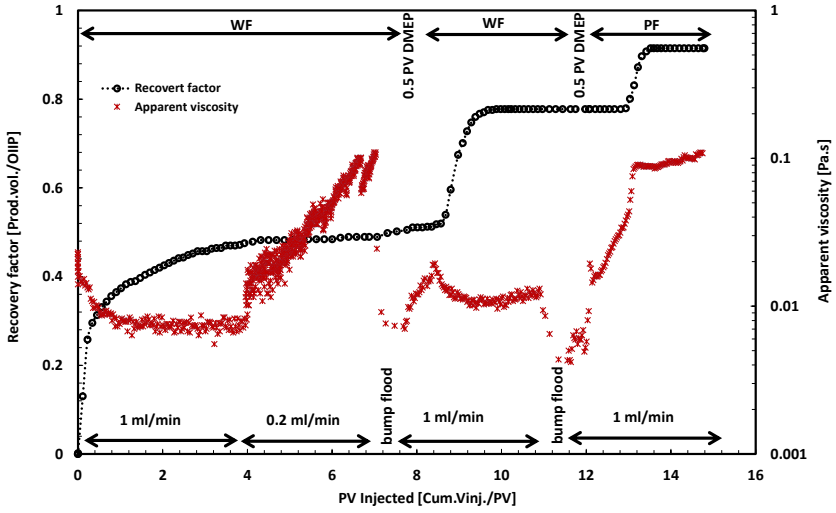

Figure 5.13: Oil recovery and apparent viscosity of Experiment #8. Experimental sequence: Water flooding, 0.5 PV DMEP, water flooding, 0.5 PV DMEP and polymer flooding.

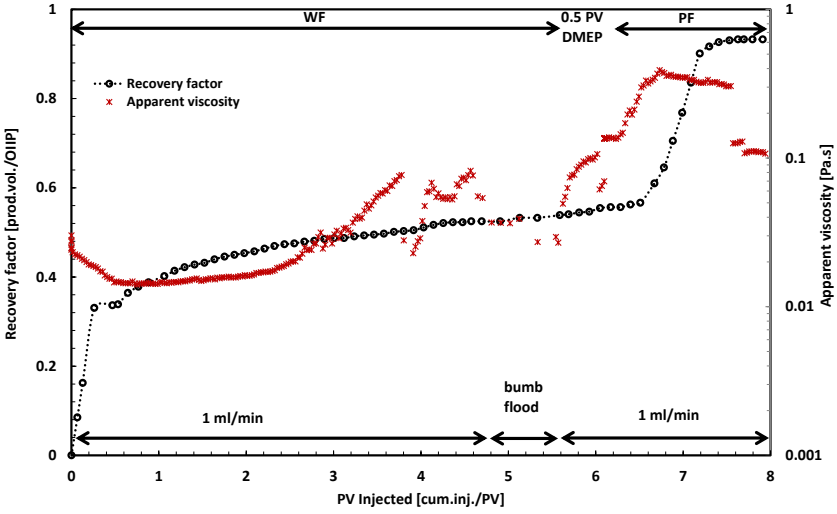

Figure 5.14: Oil recovery and apparent viscosity of Experiment #9. Experimental sequence: Water flooding, 0.5 PV DMEP injection and polymer flooding.

oil recovery of 44% was attained. Therefore, it can be concluded that the presence of the mobility control agent (polymer) in the chase phase improves the oil recovery during a finite slug injection. A possible reason is that, with the assumption of an end-point relative permeability of 0.15 for the aqueous phase in Bentheimer core, an end-point mobility ratio of 5.2 was obtained in water flooding. In the continuous DMEP flooding (Experiment #4), the end-point mobility ratio reduced to 2.6, due to a higher viscosity of the DMEP fluid ($\mu = 2 \times 10^{-3}\ Pa.s$) than the viscosity of brine solution. In Experiment #9, the polymer chase ($\mu = 6 \times 10^{-3}\ Pa.s$) obtained a mobility ratio of less than the unity ($M = 0.88$), which led to a more efficient and stable oil recovery.

5.5 Concluding remarks

We studied the improvements of oil recovery from core flooding experiments by adding DME and a polymer to the displacing aqueous phase. DME/polymer flooding was considered for cases in which a favorable mobility control between water and oil does not exist. Slugs of the mixed solution of DME and polymer were injected into the cores containing oil and then they were displaced by an injection of a chase fluid. Experiments show that the injectivity of a DME/polymer (DMEP) solution was higher than the injectivity of a polymer solution (without DME). The main experimental observations were: (1) a higher oil recovery was obtained from continuous DMEP flooding than from continuous DME-brine Flooding, (2) the presence of polymer in the DME slug and in the chase phase reduced the remaining oil after a finite slug injection, (3) a larger DME slug and mobility control of the chase phase can improve the oil recovery after a finite slug injection. Overall, hybrid DME/polymer method improves the ultimate recovery significantly and shortens the duration of oil production. Therefore, hybrid DME/polymer EOR can be considered as a viable method in the laboratory.

Bibliography

[1] L. Holm, "Carbon Dioxide Solvent Flooding for Increased Oil Recovery," *Trans., AIME*, vol. 216, pp. 225–231, 1959.

[2] C. Gatlin and R. L. Slobod, "The Alcohol Slug Process for Increasing Oil Recovery," vol. 219, 1960.

[3] L. Holm and A. Csaszar, "Oil Recovery by Solvents Mutually Soluble in Oil and Water," *Society of Petroleum Engineers Journal*, vol. 2, no. 2, Jun. 1962.

[4] J. Taber and W. Meyer, "Investigations of Miscible Displacements of Aqueous and Oleic Phases from Porous Media," in *the Annual SPE Fall Meeting*, New Orleans, 1963.

[5] R. J. Christensen, "Carbonated Waterflood Results–Texas and Oklahoma," *Annual Meeting of Rocky Mountain Petroleum Engineers of AIME*, 1961.

[6] C. Hickok and H. R. Jr, "Case Histories of Carbonated Waterfloods in Dewey-Bartlesville Field," *SPE Secondary Recovery Symposium*, 1962.

[7] J. Scott and C. Forrester, "Performance of Domes Unit Carbonated Waterflood-First Stage," *Journal of Petroleum Technology*, 1965.

[8] M. Chahardowli, A. Zholdybayeva, R. Farajzadeh, and H. Bruining, "Solvent-Enhanced Spontaneous Imbibition in Fractured Reservoirs," in *Proceedings of 75th EAGE Conference & Exhibition incorporating SPE EUROPEC 2013*. Society of Petroleum Engineers, Jul. 2013.

[9] M. Chahardowli, R. Farajzadeh, and H. Bruining, "Experimental Investigation of the Use of the Dimethyl Ether/Polymer Hybrid as a Novel Enhanced Oil Recovery Method," *accepted for publication in Journal of Industrial and Engineering Chemistry*, DOI:10.1016/j.jiec.2016.04.008.

[10] J. Groot, A. Chernetsky, P. Te Riele, B. Dindoruk, J. Cui, L. Wilson, and R. Ratnakar, "Representation of Phase Behavior and PVT Workflow for DME Enhanced Water-Flooding," in *SPE EOR Conference at Oil and Gas West Asia*. Society of Petroleum Engineers, 2016.

[11] P. t. Riele, C. Parsons, P. Boerrigter, J. Plantenberg, B. Suijkerbuijk, J. Burggraaf, A. Chernetsky, D. Boersma, and R. Broos, "Implementing a Water Soluble Solvent Based Enhanced Oil Recovery Technology-Aspects of Field Development Planning," in *SPE EOR Conference at Oil and Gas West Asia*. Society of Petroleum Engineers, 2016.

[12] A. Alkindi, N. Al-Azri, D. Said, K. AlShuaili, and P. Te Riele, "Persistence in EOR-Design of a Field Trial in a Carbonate Reservoir Using Solvent-Based Water-Flood Process," in *SPE EOR Conference at Oil and Gas West Asia*. Society of Petroleum Engineers, 2016.

[13] M. Chahardowli, R. Farajzadeh, and H. Bruining, "Experimental Investigation of the Use of Dimethyl Ether/Polymer Hybrid as an Enhanced Oil Recovery Method," in *SPE EOR Conference at Oil and Gas West Asia*, 2016.

[14] A. Chernetsky, S. Masalmeh, D. Eikmans, P. M. Boerrigter, A. Fadili, C. A. Parsons, A. Parker, D. M. Boersma, J. Cui, B. Dindoruk, P. M. te Riele, A. Alkindi,

and N. Azri, "A Novel Enhanced Oil Recovery Technique: Experimental Results and Modelling Workflow of the DME Enhanced Waterflood Technology," in *Abu Dhabi International Petroleum Exhibition and Conference*. Society of Petroleum Engineers, nov 2015.

[15] T. a. Semelsberger, R. L. Borup, and H. L. Greene, "Dimethyl Ether (DME) as an Alternative Fuel," *Journal of Power Sources*, vol. 156, pp. 497–511, 2006.

[16] K. Fujimoto and Y. Ohno, "Dme handbook," in *Japan DME Forum, Ohmsha, Tokyo*, 2007.

[17] M. Chahardowli, R. Farajzadeh, and H. Bruining, "Numerical Simulation of Mutually Soluble Solvent-Aided Spontaneous Imbibition in Fractured Reservoirs," in *14th European Conference on the Mathematics of Oil Recovery*, Catania, Sep. 2014.

[18] J. Hagoort, "Displacement Stability of Water Drives in Water-Wet Connate-Water-Bearing Reservoirs," *Society of Petroleum Engineers Journal*, vol. 14, no. 1, pp. 63–74, 1974.

[19] M. King and V. Dunayevsky, "Why Waterflood Works: a Linearized Stability Analysis," *SPE Annual Technical Conference and Exhibition*, 1989.

[20] K. Sorbie, *Polymer-Improved Oil Recovery*. Blackie, 1991.

[21] L. W. Lake, R. Johns, B. Rossen, and G. Pope, *Fundamentals of Enhanced Oil Recovery*. Society of Petroleum Engineers, 2014.

[22] S. Hosseini-Nasab, C. Padalkar, E. Battistutta, and P. Zitha, "Mechanistic modelling of alkaline/surfactant/polymer flooding process at under-optimum salinity condition for enhanced oil recovery," in *SPE Asia Pacific Enhanced Oil Recovery Conference*. Society of Petroleum Engineers, 2015.

[23] S. Hosseini Nasab and P. Zitha, "Systematic phase behaviour study and foam stability analysis for optimal alkaline/surfactant/foam enhanced oil recovery," in *IOR 2015: 18th European Symposium on Improved Oil Recovery, Dresden, Germany, 14-16 April 2015*. EAGE, 2015.

[24] M. Simjoo, Y. Dong, A. Andrianov, M. Talanana, and P. L. Zitha, "Novel insight into foam mobility control," *SPE Journal*, vol. 18, no. 03, pp. 416–427, 2013.

[25] M. Simjoo, Y. Dong, A. Andrianov, M. Talanana, and P. Zitha, "Ct scan study of immiscible foam flow in porous media for enhancing oil recovery," *Industrial & Engineering Chemistry Research*, vol. 52, no. 18, pp. 6221–6233, 2013.

[26] A. M. Mansour, R. S. Al-Maamari, A. S. Al-Hashmi, A. Zaitoun, and H. Al-Sharji, "In-Situ Rheology and Mechanical Degradation of EOR Polyacrylamide Solutions under Moderate Shear Rates," *Journal of Petroleum Science and Engineering*, vol. 115, pp. 57–65, 2014.

[27] K. S. Wain, J. M. Perez, E. Chapman, and A. L. Boehman, "Alternative and Low Sulfur Fuel Options: Boundary Lubrication Performance and Potential Problems," *Tribology International*, vol. 38, pp. 313–319, 2005.

[28] A. E. Peksa, K.-H. A. Wolf, and P. L. Zitha, "Bentheimer sandstone revisited for experimental purposes," *Marine and Petroleum Geology*, vol. 67, pp. 701 – 719, 2015.

[29] O. V. Gafonova and H. W. Yarranton, "The Stabilization of Water-In-Hydrocarbon Emulsions by Asphaltenes and Resins," *Journal of Colloid and Interface Science*, vol. 241, no. 2, pp. 469–478, 2001.

[30] J. Czarnecki, P. Tchoukov, T. Dabros, and Z. Xu, "Role of Asphaltenes in Stabilisation of Water in Crude Oil Emulsions," *Canadian Journal of Chemical Engineering*, vol. 91, no. 8, pp. 1365–1371, 2013.

[31] M. I. Romero, "Flow of emulsions in porous media," in *SPE Annual Technical Conference and Exhibition*. Society of Petroleum Engineers, 2009.

[32] D. L. Parkhurst, and C. Appelo, *User's Guide to Phreeqc (Version 2): a Computer Program for Speciation, Batch-Reaction, One-Dimensional Transport, and Inverse Geochemical calculations*. US Geological Survey Denver, 1999.

[33] J. S. Buckley, "Asphaltene Deposition," *Energy & Fuels*, vol. 26, no. 7, pp. 4086–4090, 2012.

[34] R. Farajzadeh, M. Lotfollahi, and P. Bedrikovetsky, "Simultaneous sorption and mechanical entrapment during polymer flow through porous media," in *SPE Kuwait Oil and Gas Show and Conference*. Society of Petroleum Engineers, 2015.

[35] C. J. F. Böttcher, O. C. van Belle, P. Bordewijk, and A. Rip, *Theory of Electric Polarization*. Elsevier Science Ltd, 1978, vol. 2.

[36] D. Shah and R. S. Schechter, *Improved Oil Recovery by Surfactant and Polymer Flooding*, 1977.

[37] J. T. G. Overbeek, *Colloid and Surface Chemistry: a Self-Study Course*, Department of Chemical Engineering and Center for Advanced Engineering Study, 1971.

[38] P. J. Flory, *Principles of Polymer Chemistry*, Cornell University Press, 1953.

Chapter

6

Conclusions

6.1 General conclusions

This thesis concerns an extensive study of oil recovery by mutually soluble solvents with low boiling points. We chose diethyl ether (DEE) and dimethyl ether (DME) as representative solvents. The main research questions are by which mechanisms the solvents can improve the oil recovery. We also studied co-injection of DME and a solution of hydrolyzed polyacrylamide (HPAM) in brine into Bentheimer cores, to investigate how much a favorable mobility ratio improves the oil recovery. We reach the following generic conclusions.

- Solvents improve the oil recovery both in linear flow experiments and in fractured reservoirs. This improvement benefits from partial solubility of DEE and DME in brine and complete solubility in oil.

- The main mechanisms are (1) swelling (dilution), (2) excess volume expansion and (3) viscosity reduction.

- On the laboratory scale, molecular diffusion and capillary diffusion play an important role.

- The mechanisms can be studied experimentally using an Amott cell or core flooding set up.
- The results can be largely interpreted by comparison of experimental results with numerical modeling.

The chapters are addressing specific aspects of volatile solvents enhanced oil recovery. Chapter 2 studies the partition coefficient, which is important if models with sophisticated phase behavior were required. Chapter 3 studies the fracture-matrix interaction using DEE/brine solutions, which can be performed at atmospheric pressure and was used to design a modified Amott cell that can operate at high pressures and applied for DME/brine imbibition tests. The high pressure cell is described in chapter 4. Chapter 5 addresses DME/polymer studies. As opposed to chapter 3 and 4, which address solvent enhanced recovery in fractured media, chapter 5 focuses on linear sandstone core studies. The conclusions specific to each chapter are summarized below.

6.2 Measurement of the partition coefficient

The aim of study described in chapter 2 was to obtain the partition coefficient of diethyl ether (DEE) and tetrahydrofuran (THF) in brine/oil and demi-water/oil systems. In particular, each study investigated the effect of the presence of salt, solvent concentration and oil type (hexadecane, Ondina 919 and Ondina 933) on the partition coefficient of THF or DEE between aqueous and oleic phases. The specific conclusions are:

- The partition coefficient can be measured using either a refractometer or a density-meter. The logarithm of the measured partition coefficient of DEE between demi-water (brine) and hexadecane between refractometer and density-meter, $\log_{10} K_{oa}^{DEE}$, differed maximally of 0.1 in demi-water/C_{16} and 0.17 in brine/C_{16}.
- Added salt increases the partition coefficient (due to lower solubility in the aqueous phase) by $10^{(0.215\ I)}$. Our experimental results at ionic strength of 0.5 molar showed an increase in terms of the logarithm of partition coefficient of maximally 0.28 using an Abbe refractometer and of maximally 0.55 using an Anton Paar density-meter. Considering the experimental error, the results for C_{16} agreed with the expected values due to the salting out effect. However, prediction of salting out effects using the Setschenow on the partition coefficient of DEE or THF between aqueous phase and Ondina oils led to standard deviations that exceeded the experimental error.
- Only a few literature data, mainly by Abraham, are available on the DEE partition coefficient in the demi-water/C_{16} system. The data of Abraham

were a factor of 3.5 bigger than the measured data reported in this study. We have no explanation for such a difference, and given the fact that the solutions were shaken for 24 hours and with estimates of the evaporation rates, it is unlikely that these mechanisms can explain the discrepancies.

- Our results for the logarithm of the partition coefficient of DEE in the demi-water/C_{16}, i.e., $\log_{10} K_{oa}^{DEE}$ between 0.25 and 0.48 in molar ratios measured by the refractometer was closer to the prediction using Meyer and Maurer's correlation, i.e., $\log_{10} K_{oa}^{DEE} = 0.24$ than the prediction using Abraham's correlation, i.e., $\log_{10} K_{oa}^{DEE} = 0.86$. As mentioned both in Meyer and Maurer's paper and in Abraham's paper, the proposed models do not predict the $\log_{10} K_{oa}^{THF}$ correctly.
- The partition coefficients of DEE and of THF are weak functions of the initial solvent concentration in the aqueous phase. It was observed that the partition coefficients of DEE or THF were consistently higher in aqueous/Ondina 933 than in aqueous/Ondina 919 systems. The partition coefficient of DEE in all oil types was higher than the partition coefficient of THF for the initial solvent concentration of 1.1 $mol\%$ in brine.
- More laboratory experiments are needed to obtain accurate partition coefficients for DEE/brine/oil and THF/brine/oil systems.

6.3 Spontaneous imbibition of DEE/brine into oil-filled rocks

Mixed-wet and water-wet cores were exposed to brine (3 $w/w\%$ NaCl) imbibition with or without 7 v/v% DEE in Amott imbibition cells. The recovery factor and the recovery rate were monitored by reading a graded cylinder, which was mounted on top of the Amott cell. The specific conclusions are:

- The prevailing mechanisms of DEE/brine enhanced recovery can be investigated using an Amott cell, which allows to read the recovery in the graded cylinder.
- The experiments show that the presence of DEE can enhance primary and secondary recovery efficiencies. For the water-wet Berea sandstone the primary recovery was approximately $46 - 67\%$ of the OIIP and the additional recovery was approximately $1 - 11\%$ of the OIIP. For the mixed-wet Berea (dolomite) the primary and secondary recoveries were approximately $49 - 50(6 - 8)\%$ of the OIIP and $29 - 37(27 - 29)\%$ of the OIIP respectively.
- A model that describes the DEE enhanced imbibition effects could be developed. The input parameters could be partly from the literature, and partly by

minimizing the difference between model and experimental results. The model involves oil swelling (dilution) and oil viscosity reduction as the main oil recovery mechanisms. The optimized simulations shows good agreement with the experiments, except at intermediate times when the computed recovery was higher than the experimental recovery. The discrepancy could be partly attributed to delayed production of oil that remains bounded to the rock surface.

6.4 Spontaneous imbibition of DME/brine into oil-filled rocks

We studied the acceleration and the enhancement of oil recovery due to spontaneous imbibition of DME/brine (DMEB) solutions. Natural imbibition experiments in four cylindrical water-wet sandstone cores with the top-end and bottom-end, both-ends and all sides open to imbibition fluid were carried out. In addition, imbibition tests were carried out in three mixed-wet (aged) tight limestone cores. First, the primary recovery efficiency without DME was obtained and subsequently the additional recovery after exposing the core to a mixture of DME/brine was measured. The numerical model for DEE/brine imbibition was adapted to interpret DME/brine imbibition in water-wet and in mixed-wet rocks. The model parameters were optimized to minimize the difference between experimental and numerical results. The specific conclusions are:

- The primary recovery with brine from the four cylindrical water-wet cores was $38-46\%$ of the OIIP. The production curves show that in the laboratory, the recovery mechanism is by capillary forces and that gravity effects are of minor importance. In addition, the recovery in the modified Amott cell was delayed by attachment of oil droplets to the rock surface. These droplets slowly moved, leading to a delay in the measured oil recovery of several days. By adding DME, the additional oil recovery in the water-wet core was considerable (11-16% of the OIIP). The primary recovery in the mixed-wet limestone cores was $1-2\%$ of the OIIP. The additional oil recovery in the mixed-wet cores was 43, 50 and 55% of the OIIP, which was much higher than the additional recovery from the water-wet cores.

- Numerical simulation shows that DMEB imbibition with a higher initial oil saturation in the core leads to a higher incremental oil recovery. Numerical simulation predicts that with the increase of the partition coefficient, a higher oil recovery is obtained. However, a linear relation between the increase of the partition coefficient and the increase of the oil recovery is not observed. Numerical simulation shows that a higher DME concentration in the aqueous

recovers more oil.

- It can be expected that the main mechanism for enhancing oil recovery by the DME/brine imbibition is determined by molecular diffusion. Capillary diffusion transports the water-wet phase quickly into the core, but due to the exchange of DME with the oleic phase will be largely depleted from DME. Consequently, transport of DME occurs due to diffusion. In view of the long gravity characteristic time, the effect of gravity forces is of minor importance.
- Numerical simulation shows that the oil recovery is more sensitive to the molecular diffusion coefficient and to the partition coefficient than to the relative permeability and to the capillary pressure. With DMEB, numerical simulation shows that the end-point relative permeabilities and the capillary entry pressure only affect the production rate but not the additional recovery during the simulation time. The oil viscosity reduction only increased the production rate.
- The comparison between the theoretical and the experimental results shows that the main oil recovery mechanism is oil swelling; oil viscosity reduction also accelerated the recovery.

6.5 Hybrid DME/polymer EOR

The purpose of this study was to investigate the improvements of oil recovery from core flooding experiments by adding DME and polymer to the displacing aqueous phase. It was found that hybrid DME/polymer EOR method is a viable method in the laboratory. The specific conclusions (technical and experimental) are:
Technical conclusions

- One of the main experimental problems in a DME flooding experiment is leakage prevention from the core holder. A fit for purpose of core wrapping methodology was implemented to prevent leakage during DME experiments
- It was observed that a mixture of 1500 ppm Flopaam 3630S in brine (0.5 molar NaCl in demi-water) was compatible with DME (10.0 ± 0.2 $mol\%$). However, the presence of incompatible materials like impurities in bronze, normal O-rings or Plexiglas (PMMA) in the set-up causes chemical degrading of the DME/polymer solution.
- The apparent viscosity for a pure polymer injectivity test was higher than the apparent viscosity of the DME/polymer injectivity test. This indicates that the injectivity of the polymer/DME mixture was higher than the injectivity of the polymer solution.

Conclusions from experimental observations

- Experiments can be tentatively interpreted in a conceptual framework, which includes oil swelling and viscosity reduction by DME, partial molar volume increase, mobility ratio improvement, asphaltene stabilized emulsion formation and asphaltene precipitation.
- The coreflood experiments showed that the initial oil recovery by water flooding in different core samples, varied between $40 - 63\%$ of the oil initially in-place, which was possibly due to the heterogeneity of cores and the presence of an emulsion.
- A higher oil recovery was obtained from continuous DMEP flooding compared to continuous DMEB Flooding. The extra oil production after injection of a DMEP slug followed by a polymer slug after DMEB injection, showed that the presence of polymer in the DME slug and in the chase phase reduced the remaining oil.
- The experimental results showed that a larger DME slug followed by a viscous chase slug (polymer) improved the oil recovery after a finite slug injection with respect to a smaller DME slug followed by low viscous chase phase (brine). In addition, the displacement of a DME/polymer slug by a viscous chase (polymer) led to a higher oil recovery with respect to the displacement of the DME/polymer slug by a low viscous chase (brine).
- The laboratory experiments suggest that the hybrid DME/polymer method can be a viable enhanced method for the recovery of medium oil viscosity from sandstone cores.

Appendix

A

Appendix

A.1 Derivation of DEE concentration in the aqueous phase

The derivation is obtained as follows:

$$n^o_{DEE} = \frac{c^o_{DEE} n^i_h}{1 - c^o_{DEE}},$$

where n^o_{DEE} and n^i_h are the number of moles of DEE and the number of moles of oil in the oleic phase respectively. Afterwards, using total DEE mass conservation, the number of the mole of DEE in the aqueous phase was determined and then the mole fraction of DEE in the aqueous phase was determined by:

$$c^a_{DEE} = \frac{n^i_{DEE} - n^o_{DEE}}{n^i_w + n^i_{DEE} - n^o_{DEE}},$$

where c^a_{DEE} is the mole fraction of DEE in the aqueous phase, n^i_{DEE} is the initial number of moles of DEE in the aqueous phase, which was measured precisely at the lab temperature, and n^i_w is the number of mole of make-up water.

A

A.2 Calibration curves

A.3 Derivation of the salting out coefficient

The partition coefficient can be derived by comparing the Henry coefficient of DEE or THF between oleic phase and an imaginary gas phase to the Henry coefficient of DEE or THF between the aqueous phase and the (imaginary) gas phase. The Henry constant at equilibrium condition is formulated as:

$$K_{ag}^{H} = \frac{a_{a,s}}{a_{g,s}} = \frac{m_{a,s}\gamma_{a,s}}{f_{g,s}}, \tag{A.1}$$

$$K_{og}^{H} = \frac{a_{o,s}}{a_{g,s}} = \frac{m_{o,s}\gamma_{o,s}}{f_{g,s}}, \tag{A.2}$$

Therefore, we define the equilibrium constant by

$$K_{oa} = \frac{K_{og}^{H}}{K_{ag}^{H}} = \frac{m_{o,s}\gamma_{o,s}}{m_{a,s}\gamma_{a,s}}, \tag{A.3}$$

where γ and m are activity coefficient and molality of DEE or THF in the aqueous or oleic phase, and K_{oa} is the partition coefficient. The activity of pure water is close to one, however, the activity of brine can be determined from Setchenow correlation:

$$\log_{10}\gamma_{s,a} = K_s\mu = \frac{1}{2}K_s\Sigma_{j=1}^{N}c_j z_j^2, \tag{A.4}$$

where, μ is the ionic strength of the solution, z_i is valency of ion, and K_s is the salting out coefficient (Setchenow coefficient).
In addition, the Setchenow (salting out) coefficient can be estimated by dividing the partition coefficient of MSS between oil and pure water by the partition coefficient of MSS between oil and brine:

$$\log_{10}\frac{K_{wo}}{K_{bo}} = K_s\ c_b, \tag{A.5}$$

where K_{wo} and K_{bo} are the partition coefficient of DEE or THF in the demi-water/oil system and in the brine/oil system that are calculated in mole fraction, K_s is the Setchenow coefficient and c_b is the salt concentration in molarity.

A.4 Calculation of the characteristics length

Assume a core with all boundaries open to imbibition with a diameter of $D = 3\ cm$ and a length of $L = 5\ cm$. The bulk volume of the core is $V_b = 35.3\ cm^3$. The area of the sides and the length from the sides to the center of the core are $A_s = 47.12\ cm^2$

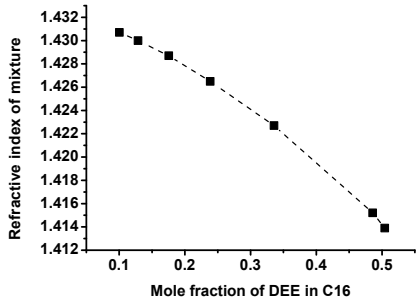

(a) Refractive index of the mixture of DEE and C_{16}

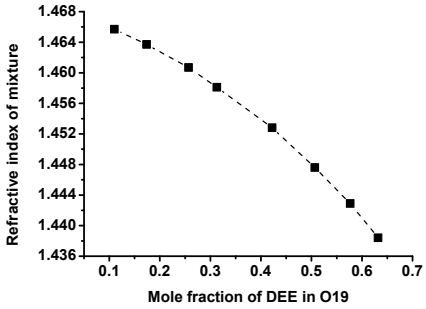

(b) Refractive index of the mixture of DEE and $O19$

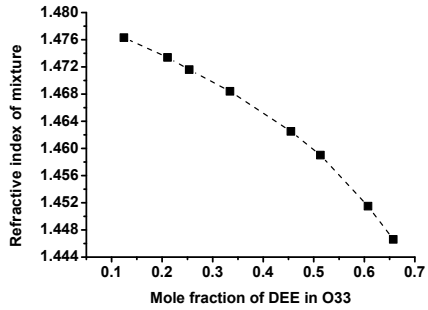

(c) Refractive index of the mixture of DEE and $O33$

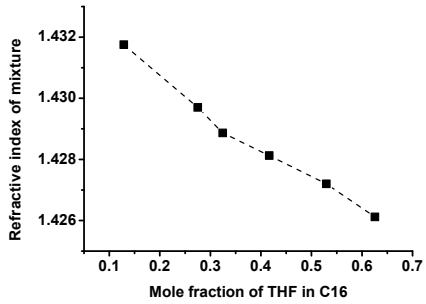

(d) Refractive index of the mixture of THF and C_{16}

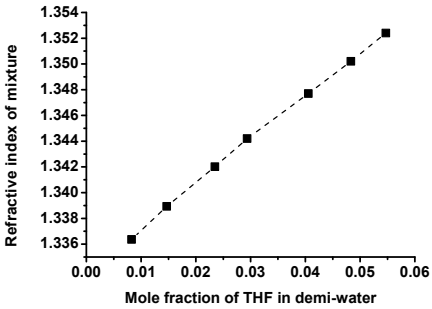

(e) Refractive index of the mixture of THF and demi-water

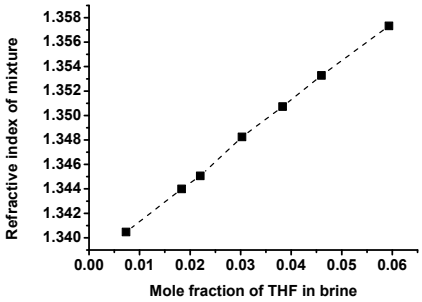

(f) Refractive index of the mixture of THF and brine

Figure A.1: Reference curves

A

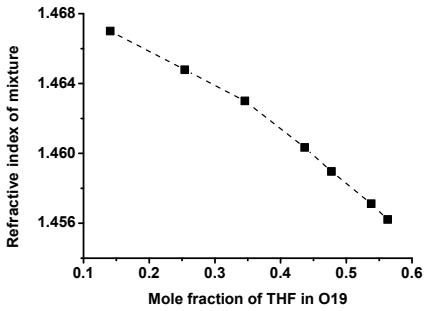

(a) Refractive index of the mixture of THF and O19

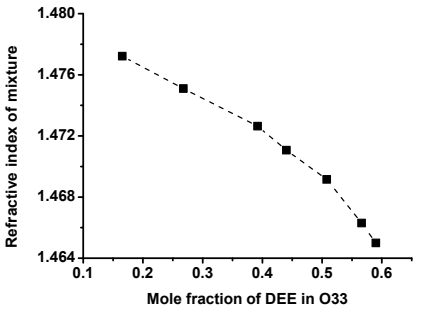

(b) Refractive index of the mixture of THF and O33

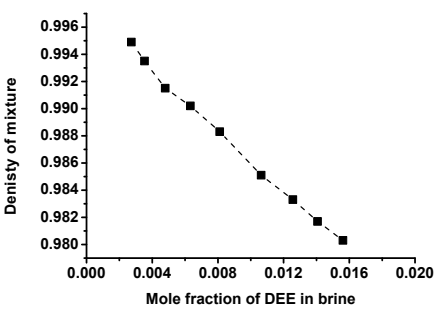

(c) Density of the mixture of DEE and demi-water

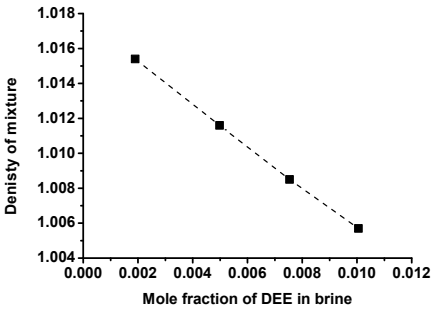

(d) Density of the mixture of DEE and brine

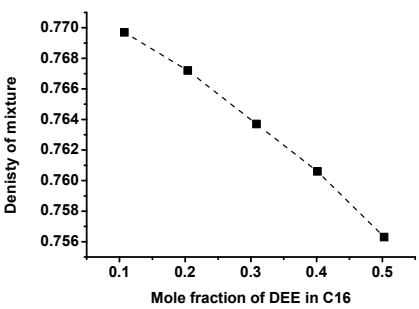

(e) Density of the mixture of DEE and C_{16}

Figure A.2: Reference curves

and $l_s = 1.5\ cm$, respectively. Moreover, the area of each end and the length from each end to the center of the core are $A_e = 7.07\ cm^2$ and $l_s = 2.5\ cm$, respectively.

Therefore, the characteristics length can be calculated by Equation (3.2):

$$L_c = \sqrt{35.347.12/1.5 + 2 \times 7.07/2.5} = 0.98\ cm. \tag{A.6}$$

Summary

Enhanced oil recovery seeks to reduce the oil left behind after conventional recovery, i.e. primary recovery (natural reservoir drive) and secondary recovery (e.g. water injection), as $50-70\%$ of the oil remains in the reservoir. This residual or remaining oil has been captured by capillary forces or is left behind in the reservoir, due to poor displacement and poor sweep efficiency (bypassing).
Water-soluble solvents, e.g. diethyl ether (DEE) and dimethyl ether (DME) can enhance oil recovery from both conventional and fractured reservoirs. With the injection of the aqueous phase, e.g. DME(DEE)-brine or DME-polymer, DME(DEE) partitions between the aqueous phase and the oleic phase, which dilutes (swells) the oleic phase and lowers the oil viscosity.
The principal objective of this thesis is to obtain more insight in oil recovery by mutually soluble solvents, especially dimethyl ether (DME). The main research question is by which mechanisms the solvents (DME or DEE) can improve the oil recovery from conventional and fractured reservoirs. In order to answer the research question, we have performed systematic bulk and porous media laboratory studies. The objectives of this thesis are as follows:

- to perform an extensive study of oil recovery enhancement by the mutually soluble solvents diethyl ether (DEE) and dimethyl ether (DME).

- to obtain experimental values for the partition coefficient of several mutually soluble solvents (DEE and tetrahydrofuran) between the aqueous and oleic phase in the presence of salt; additional objectives are to quantify the effect of the initial solvent concentration, of the presence of salt, and of the oil type (hexadecane, Ondina 919 and Ondina 933) on the partition coefficient.

- to demonstrate the potential of DME and DEE to improve oil recovery from sandstone and carbonate rocks; to find experimental evidence whether DME and DEE can enhance the spontaneous imbibition process.

- to describe and to understand the oil recovery enhancement mechanisms in spontaneous imbibition of DME/brine (DEE/brine) into a single oil-filled matrix by a comparison between experimental results and numerical modeling.

- to perform mobility control experiments with a solution of hydrolyzed polyacrylamide (HPAM) in Bentheimer cores for DME-enhanced water flooding in the laboratory and to investigate how much a favorable mobility ratio improves the oil recovery.

The general introduction seeks to define the importance of DME and DEE enhanced oil recovery in the framework of the enhanced oil recovery activities. Each chapter addresses different aspects of oil recovery by the mutually soluble solvents, which can aid the quantification of the recovery enhancement. Chapter 2 studies the partition coefficient of diethyl ether (DEE) in brine/oil and in water/oil systems. For reason of comparison, we have also measured the partition coefficient of tetrahydrofuran (THF) in brine/oil and in water/oil systems. The measurements include the effect of the presence of salt, the solvent concentration and the model oil type (hexadecane, Ondina 919 and Ondina 933) on the partition coefficient of THF and DEE between the oleic and the aqueous phases. The results of these measurements were used for the estimation of the order of magnitude of the partition coefficient used in the simulations in chapter 3 to interpret DEE/brine spontaneous imbibition experiments. The experimental part of chapter 3 is relevant for the fracture-matrix interaction using DEE/brine solutions, which can be performed at atmospheric pressure. The experiments were conducted in Amott cells, where both oil saturated mixed-wet (aged) and water-wet Berea cores and oil saturated mixed-wet dolomite cores were exposed to brine with or without DEE. Moreover, we combined mass conservation of the components and Darcy's law with a simplified (constant partition coefficient) phase behavior of the DEE-brine-crude oil system to develop a numerical model for DEE/brine spontaneous imbibition. Comparison between the experimental results and the numerical results shows which mechanisms are responsible for the oil recovery. Based on the results of this chapter, we designed the experimental and the numerical studies for chapter 4, where the DEE was replaced by DME. We have designed a modified Amott cell that can operate at high pressures and can be applied for DME/brine imbibition tests. We have carried out two-stage spontaneous imbibition experiments with brine and with DME/brine mixtures in water-wet and in mixed-wet cores. We have adapted our numerical model for DEE/brine spontaneous imbibition to interpret DME/brine spontaneous imbibition experiments. In addition to the spontaneous imbibition experiments relevant for fractured media, we have also carried out flooding experiments that are relevant for non-fractured sandstone media, as described in chapter 5. In the flooding experiments, the purpose is to quantify the enhancement effect of DME-water flooding of medium oil viscosity and the improvement due to mobility control, using a solution of hydrolyzed polyacrylamide

(HPAM). For these experiments, we used a sequence of the injection conditions. We started with co-injection of a mixture of DME/brine or DME/polymer. Subsequently, we displaced the DME slug by a polymer slug chase or brine slug chase, and measured the oil recovery enhancements. The improvements comprise not only the mobility control effects, but also enhanced-dissolution effects. The thesis ends with the summary of the main conclusions in chapter 6.

Overall, it is shown that mutually soluble solvents improve the oil recovery both in linear displacement flow experiments in Bentheimer sandstone and in fractured reservoirs. The improvement profits from partial solubility of DEE and DME in brine and complete solubility in oil. The results can be largely interpreted by comparison of experimental results with numerical modeling. The main mechanisms are (1) swelling (dilution), (2) excess volume expansion, (3) viscosity reduction and (4) mobility enhancement by.

Samenvatting

Verbeterde oliewinning streeft ernaar om de achtergebleven olie na conventionele winning, d.w.z. primaire winning (vloeistof expansie, porie compressibiliteit, gas desaturatie, gaskap expansie) en secundaire winning (water injectie) te verminderen. Zonder deze verbetering blijft 50-70% van de olie achter in het reservoir. De residuele of achterblijvende olie kan zijn ingevangen door capillaire krachten of achtergelaten door het slechte veeg-rendement (er langs schieten).
Water oplosbare oplosmiddelen, bijv. diëthylether (DEE) en dimethylether (DME) kunnen de oliewinning verbeteren zowel in conventionele als in gebroken reservoirs. Met injectie van een waterige fase met DME(DEE)/pekel of DME/polymeer, verdeelt DME(DEE) zich tussen de waterige en olieachtige fase, zodat de olieachtige fase verdunt (zwelt) en de viscositeit verlaagt.
De hoofddoelstelling van dit proefschrift is om meer inzicht te krijgen in oliewinning met behulp van wederzijds oplosbare oplosmiddelen, in het bijzonder dimethylether (DME). De belangrijkste onderzoeksvraag is door welke mechanismen de oplosmiddelen (DME of DEE) de oliewinning uit conventionele en gebroken reservoirs kan verbeteren. Om de onderzoeksvraag te beantwoorden, hebben wij systematische bulk- en poreuze media-laboratorium experimenten uitgevoerd. De doelstellingen van dit proefschrift zijn alsvolgt:

- het uitvoeren van een uitgebreide studie naar de verbetering van oliewinning met behulp van de wederzijds oplosbare oplosmiddelen diëthylether (DEE) en dimethylether (DME).

- het verkrijgen van experimentele waarden voor de verdelingscoëfficiënt van een aantal wederzijds oplosbare oplosmiddelen (DEE en tetrahydrofuraan) tussen de waterige en olieachtige fase in de aanwezigheid van zout; aanvullende doelstellingen zijn het kwantificeren van het effect van de concentratie van het oplosmiddel, de aanwezigheid van zout, en het olietype (hexadekaan, Ondina 919, en Ondina 933) op de verdelingscoëfficiënt.

- het aantonen van het potentieel van DME en DEE om de oliewinning in zandsteen en carbonaatgesteente (gebroken reservoir) te verbeteren; om experimentele bewijskracht te vinden of DME en DEE het spontane imbibitie proces kunnen stimuleren.
- het beschrijven en begrijpen van de oliewinningsverbeteringsmechanismen bij spontane imbibitie van DME/pekel (DEE/pekel) in een enkel met olie gevuld matrixblok door een vergelijking tussen experimentele resultaten en numerieke modellering.
- uitvoering van mobiliteitsbeheersingsexperimenten met een oplossing van gehydrolyzeerd polyacrylamide (HPAM) in kernen van Bentheimer gesteente ten behoeve van met DME gestimuleerde waterverdringing in het laboratorium en te onderzoeken in hoeverre een gunstige mobiliteitsverhouding de oliewinning verbetert.

De algemene inleiding tracht het belang van door DME en DEE verbeterde oliewinning in het kader van de activiteiten betreffende verbeterde oliewinning te definiëren. Elk hoofdstuk behandelt verschillende aspecten van oliewinning met behulp van wederzijds oplosbare oplosmiddelen, die kan helpen bij de kwantificering van de winningsverbetering. Hoofdstuk 2 bestudeert de verdelingscoëfficiënt van diëthylether (DEE) in pekel/olie en water/olie systemen. Om te kunnen vergelijkingen hebben wij ook de verdelingscoëfficiënt van tetrahydrofuraan (THF) in pekel/olie en water/olie systemen gemeten. De metingen omvatten het effect van de aanwezigheid van zout, de concentratie van het oplosmiddel en het modelolietype (hexadekaan, Ondina 919 en Ondina 933) op de verdelingscoëfficiënt van THF en DEE tussen de waterige en olieachtige fasen. De resultaten van deze metingen werden maakten een schatting van de orde van grootte van de verdelingscoëfficiënt mogelijk en werden gebruikt in de simulaties van hoofdstuk 3 om de DEE/pekel spontane imbibitie experimenten te duiden. Het experimentele gedeelte van hoofdstuk 3 is relevant voor de matrix/breuk wisselwerking bij gebruik van de DEE/pekel oplossingen. De experimenten kunnen bij atmosferische druk worden uitgevoerd. De experimenten werden in AMOTT cellen uitgevoerd, waarbij zowel met olie verzadigde gemengd-bevochtigend (verouderd) en water bevochtigend Berea kernen en met olie verzadigde gemengd-bevochtigende dolomietkernen werden blootgesteld aan pekel met en zonder DEE. Bovendien hebben wij massabehoud en de wet van Darcy gecombineerd met een vereenvoudigd (constante verdelingscoëfficiënt) fase gedrag van het DEE pekel/ruwe oliesysteem om een numeriek model te ontwikkelen voor spontane imbibitie van DEE/pekel. Een vergelijking tussen de experimentele en numerieke resultaten laat zien welke mechanismen verantwoordelijk zijn voor de oliewinning. Gebaseerd op de numerieke resultaten van dit hoofdstuk hebben wij de experimentele en numerieke studies voor hoofdstuk 4 gedefinieerd, waar de DEE werd vervangen door DME. We hebben een AMOTT cel die bij hogedruk kan werken en worden toegepast op DME/pekel imbibitie testen.

We hebben tweetraps spontane imbibitie experimenten uitgevoerd met pekel en DME/pekel mengsels in waterbevochtigende en gemengd-bevochtigende kernen. Wij hebben ons numerieke model voor DEE/pekel spontane imbibitie aangepast om de spontane DME/pekel imbibitie experimenten te duiden. In aanvulling op de spontane imbibitie experimenten die relevant zijn voor gebroken media hebben wij ook experimenten uitgevoerd die relevant zijn voor niet-gebroken zandsteen media zoals beschreven in hoofdstuk 5. In deze verdringingsexperimenten, is het doel om het verbeteringseffect van DME/water verdringing van olie met een gemiddelde viscositeit en de verbetering ten gevolge van gehydrolyzeerd polyacrylamide (HPAM) te kwantificeren. Voor deze experimenten hebben wij een opeenvolging van injectie condities gebruikt. We begonnen met co-injectie van een mengsel van DME/pekel or DME/polymeer. Vervolgens verdrongen wij de DME slug door een polymeer opdrijf-slug of pekel opdrijfslug en bepaalden de olieverdringingsverbeteringen. De verbeteringen omvatten niet alleen de mobiliteitsbeheeersingseffecten maar ook de verbeterde oploseffecten. Het proefschrift sluit af met een samenvatting van de belangrijkste conclusies in hoofdstuk 6.

In het algemeen is er aangetoond dat de wederzijds oplosbare oplosmiddelen de oliewinning verbeteren zowel in lineaire verdringingsexperimenten in Bentheimer zandsteen als in imbibitie-experimenten gebroken reservoirs. De verbetering profiteert van gedeeltelijke oplosbaarheid in pekel en volledige oplosbaarheid in olie. De resultaten kunnen grotendeels worden geduid door een vergelijk tussen experimentele resultaten met numerieke modellering. De voornaamste mechanismen zijn (1) zwelling (verdunning), (2) exces volume expansie, (3) viscositeitsreductie en (4) mobiliteits-verhouding verbetering door de aanwezigheid van polymeer.

بسمه تعالی

چکیده

روش‌های ازدیاد برداشت نفت از مخازن به منظور تولید نفت پسماند در مخزن مورد استفاده قرار می-گیرد. پس از برداشت ابتدایی (با نیروهای طبیعی مخزن) یا برداشت مرحله دوم (با پروسه‌های نگهداشت فشار) از مخزن، به طور میانگین ۳۰ تا ۵۰ درصد نفت درجای مخزن تولید می‌گردد. بنابراین ۵۰ تا ۷۰ درصد نفت درجای مخزن توسط نیروهای مویئنه به تله افتاده ویا به دلیل عدم وجود بازدهی جابجایی مناسب و یا بازدهی جاروب‌زنی ضعیف و ناقص در مخزن باقی می‌ماند. بازده جابجایی تابع نیروهای مویینه، چگال و گرانرو بوده و بازده جاروبزنی تابع نیروهای گرانرو و چگال می باشد. علاوه بر این زمانی که نسبت تحرک پذیری فازها (تحرک پذیری فاز آبی تقسیم بر تحرک پذیری فاز نفتی) بالا باشد، در بخشی هایی از مخزن، نفت خارج از دسترسِ فاز آبی باقی مانده و باعث افزایش نفت پسماند مخزن می-شود. در پروسه‌های ازدیاد برداشت که با نام برداشت مرحله سوم (ثالثیه) از مخزن شناخته‌می شود، پروسه‌های نظیر کاهش کشش سطحی آب-نفت، کاهش گرانروی نفت، افزایش گرانروی آب، بهبود تحرک پذیری نسبی فازها و غیره به‌کار برده می شود تا بخشی از نفت پسماند در مخزن تولید شود.

نمونه هایی از روش های ازدیاد برداشت عبارت است از تزریق سیال‌هایی نظیر گاز امتزاجی، پلیمر، مواد فعال کننده سطحی، بخار، حلال و غیره.

موضوع پژوهش حاضر استفاده از حلال های محلول در آب و نفت (به عنوان مثال دی متیل اتر و دی اتیل اتر) برای ازدیاد برداشت از مخازن نفتی بوده و تمرکز اصلی بر استفاده از دی متیل اتر می‌باشد. دی متیل اتر به عنوان یکی از مهمترین حلال‌های محلول در آب ونفت، در سال‌های اخیر به عنوان سوختی تمیز و نیز گزینه‌ای برای جایگزینی سوخت‌های موجود مورد توجه قرار گرفته است. دی متیل اتر در شرایط اتمسفری به صورت فاز گاز بوده و در فشار بالاتر از ۵,۱ بار در دمای محیط و یا دماهای پایین تر از ۲۵- درجه سانتی گراد در فشار اتمسفری به مایع تبدیل می شود. دی متیل اتر (دی ام ای) در حالت مایع دارای چگالی و گرانروی پایینی بوده و حلالیت نسبتا بالایی در آب دارد. علاوه بر این اثرهای مخرب زیست‌محیطی کمتری نسبت به بسیاری از موارد شیمیایی دارد. به عنوان مثال در صورت آلوده شدن زمین یا محیط به دی متیل اتر به دلیل سرعت بالای تبخیر آن، ریسک آلودگی بسیار کمی متوجه زمین یا محیط خواهد بود. همچنین اثر تخریبی پایینی بر لایه اوزون داشته و نیز دارای ضریب پتانسیل گرمایش زمین (که نسبت به دی اکسید کربن به عنوان گاز مبدا سنجیده می شود) بسیار پایینی (در حدود ۰,۱) می‌باشد. علاوه براین دی متیل اتر از منابع مختلف قابل تولید بوده و در بخش های مختلف صنعت نیز استفاده می‌شود. به دلیل همین ویژگی‌ها و نیز افزایش روزافزون تولید دی متیل اتر، این حلال را می توان به عنوان یک پتانسیل برای مقاصد ازدیاد برداشت در نظر گرفت.

نفت پسماند به صورت تجمع گلبول‌های نفتی ناپیوسته و یا به صورت نفت جاروب‌نشده در برخی نواحی مخزن باقی می ماند. با تزریق حلال (دی اتیل اتر یا دی متیل اتر) به مخزن و با اولین تماس فاز آبی با نفت، حلال از طریق سطح مشترک فازها، بین دو فاز آبی و نفتی توزیع می شود. دو حلال اشاره‌شده تمایل بیشتری به انحلال در فاز نفتی نسبت به فاز آبی دارند به طوری که نسبت توزیع حلال بین فازها معمولا از عدد یک بزرگ تر است. نسبت توزیع حلال بین فازها به صورت نسبت غلظت حلال در فاز نفتی به غلظت حلال در فاز آبی پس از برقراری تعادل بین فازها تعریف می‌گردد. با حل شدن حلال در نفت، حجم نفت در محیط متخلخل افزایش یافته و گلبول‌های نفت به هم پیوسته و بانک نفتی تشکیل می‌شود. افزایش حجم نفت در محیط متخلخل به معنای افزایش تراوایی نسبی فاز نفتی بوده و بنابراین باعث افزایش نسبی تحرک‌پذیری فاز نفتی در مخزن می‌شود. علاوه بر این، پس از فرآیند تزریق حلال، فاز نفتی باقی‌مانده در مخزن شامل هر دو جزء نفت و حلال بوده که به معنای کاهش بیشتر نفت

پسماند در مخزن است. همچنین در فرآیند حل شدن حلال در نفت، گرانروی نفت کاهش یافته و بنابراین تحرک‌پذیری فاز نفتی افزایش می‌یابد. این مکانیسم در مخازن دارای نفت با گرانروی متوسط یا بالا موثرتر است.

در مخازن شکافدار طبیعی که توده‌سنگ (ماتریس) با شکاف احاطه شده‌است کنش متقابل ماتریس و شکاف تعیین‌کننده‌ترین عامل در ازدیاد برداشت نفت از توده‌سنگ می‌باشد. پس از انتقال فاز آبی به شبکه شکاف و فراگرفتن مرزهای توده‌سنگ آب‌دوست، فرآیند آشام خودبخودی مهم‌ترین مکانیسم ازدیاد برداشت از توده‌سنگ خواهد بود. پدیده آشام خودبخودی عمدتا توسط نیروهای موئینه کنترل شده و موثرترین مکانیسم تولیدی بنابراین عبارت است از نفوذ مویینگی. میزان نفوذ مویینگی فاز آبی در سنگ توسط ضریب نفوذ مویینه (capillary diffusion coefficient) کنترل می‌شود. ضریب نفوذ مویینه به صورت حاصل‌ضرب تحرک پذیری فاز نفتی در جریان جزیی فاز آبی ضرب‌در مشتق تابع فشار مویینه نسبت به اشباع آب تعریف می‌شود. پارامترهای موثر بر آشام خودبخودی و نیز عوامل موثر بر برهم‌کنش توده‌سنگ و شکاف، ازدیاد برداشت نفت از توده سنگ را تحت تاثیر قرار می‌دهند. در مخازن شکافدار، در حضور عوامل زیر مکانیسم آشام خودبخودی ضعیف بوده و بنابراین برداشت نفت به صورت ناقص انجام شده و بخش زیادی از نفت در توده‌سنگ باقی می‌ماند: ۱- تراوایی پایین توده‌سنگ، ۲- ناهمگونی بالای توده‌سنگ، ۳- نفت با گرانروی بالا و یا ۴- توده‌سنگ آب‌گریز. افزودن حلال به فاز آبی باعث بهینه‌تر شدن آشام خودبخودی گردیده و بنابراین نفت پسماند در توده‌سنگ کاهش می‌یابد. در این صورت مکانیسم‌های افزایش حجم فاز نفتی و نیز کاهش گرانروی فاز نفتی باعث ازدیاد برداشت نهایی نفت و نیز افزایش سرعت آشام فاز آبی در سنگ شده و در نتیجه باعث کاهش نفت پسماند در توده‌سنگ می‌گردد.

در فرآیند تزریق دی متیل اتر به مخازن غیرشکافدارِ دارای نفت با گرانروی میانه یا بالا، معمولا تفاوت زیادی بین تحرک پذیری فازهای آبی و نفتی وجود دارد. بنابراین فاز آبی سریع‌تر به سمت چاه تولیدی حرکت کرده و بنابراین بخش هایی از نفت مخزن به صورت جاروب نشده باقی می‌ماند. دراین شرایط با کنترل تحرک‌پذیری فاز آبی، ضریب جابجایی و ضریب جاروب زنی افزایش می‌یابد. یکی از راه‌های کنترل تحرک‌پذیری فاز آبی افزودن پلیمرهای محلول در آب (به عنوان مثال پلی اکریل آمید هیدورلیز شده) می‌باشد. گرانروی فاز آبی با افزودن مقادیر بالاتر پلیمر ویا باافزودن پلیمر با وزن مولکولی بالاتر افزایش می‌یابد. گرانروی محلول پلیمر تابع شوری آب و نوع یون‌های موجود در آب نیز می‌باشد. بنابراین

با تزریق همزمان پلیمر و دی‌متیل‌اتر به عنوان فاز آبی مکانیسم‌های تولید شامل موارد زیر می‌باشد: ۱- کاهش تحرک‌پذیری فاز آبی باعث افزایش بازده جاروب‌زنی مخزن ونیز جابجایی موثرتر فازآبی در مخزن می‌گردد، ۲- در اثر انحلال حلال در فاز نفتی، حجم نفت افزایش یافته و گرانروی آن کاهش می‌یابد.

هدف اساسی پژوهش حاضر بررسی نقش حلال‌های محلول در آب و نفت (به طور ویژه دی متیل اتر) در پروسه ازدیاد برداشت از مخازن شکافدار و غیرشکافدار می‌باشد. مهمترین سوال این پژوهش عبارت است از اینکه مکانیسم‌های ازدیاد برداشت نفت از مخازن شکافدار و غیرشکافدار با حلال‌های محلول در آب و نفت چیست؟

به منظور پاسخ به سوال بنیادین این پژوهش، مطالعه‌های گسترده آزمایشگاهی در داخل و خارج محیط متخلل انجام گرفته و برخی نتایج آزمایشگاهی نیز مدل‌سازی گردیده‌است. در این پژوهش، امکان‌سنجی استفاده از حلال‌های محلول در آب و نفت (مخصوصا دی متیل اتر) به عنوان یک روش جدید ازدیاد برداشت از مخازن شکافدار و غیرشکافدار در مقیاس آزمایشگاهی مورد بررسی و مطالعه قرار گرفته‌است. همچنین نتایج آزمایشگاهی ازدیاد برداشت نفت از مخازن شکافدار با استفاده از دی متیل اتر و دی اتیل اتر مدل‌سازی شده است. این امر باعث شناخت بهتری از شرایط بهینه برای ازدیاد برداشت نفت از مخازن شکافدار و نیز درک بهتری از مهمترین مکانیسم‌های ازدیاد برداشت گردید. همچنین طراحی و امکان‌سنجی آزمایشگاهی کنترل تحرک‌پذیری فاز تزریقی با تزریق همزمان پلیمر و دی‌متیل‌اتر و سپس جابجایی آن با تزریق فاز پلیمری مورد بررسی قرارگرفته‌است. اهداف این مطالعه به شرح زیر می‌باشد:

- تعیین مقادیر آزمایشگاهی ضریب توزیع حلال های محلول در آب و نفت در حضور نمک در فاز آبی، و نیز بررسی اثر غلظت اولیه سیال، نوع نفت و نوع حلال بر ضریب توزیع حلال بین فازهای آبی و نفتی مختلف.
- نشان دادن پتانسیل دی متیل اتر و دی اتیل اتر در ازدیاد برداشت از سنگ‌های ماسه‌ای و کربناته، و نیز پیدا کردن شواهد آزمایشگاهی برای پاسخ به این سوال که آیا حلال پروسه آشام خودبخودی را نیز بهبود می‌دهد؟
- به کارگیری مدل‌سازی عددی به منظور فهم، توصیف و تفسیر بهتر مکانیسم‌های ازدیاد برداشت با استفاده از روش آشام خودبخودی محلول دی اتیل اتر در آب نمک یا محلول دی متیل اتر در آب نمک از سنگ‌های اشباع شده با نفت.

- طراحی و توسعه روش آزمایشگاهی کنترل تحرک‌پذیری فاز تزریقی با افزودن دی‌متیل‌اتر به محلول پلیمر (پلی اکریل‌آمید هیدرولیز شده) در آب‌نمک (به عنوان فاز آبی) با هدف ازدیاد برداشت نفت از سنگ مایه ای بن‌تایمر، و نیز بررسی اثر نسبت تحرک‌پذیری مناسب بر افزایش برداشت نفت.

پایان‌نامه حاضر بر مبنای چهار مقاله تحقیقات آزمایشگاهی و مدل‌سازی درباره کاربرد حلال‌های محلول در آب و نفت برای ازدیاد برداشت تهیه گردیده است. علاوه بر این، پایان‌نامه حاضر شامل فصل‌های مقدمه و نتیجه‌گیری نیز می‌باشد. مطالعات مورد نیاز برای این پایان‌نامه در دانشگاه دلفت انجام شده و طرح کلی پایان نامه به شرح زیر می‌باشد:

فصل اول مقدمه کلی پایان‌نامه شامل اهمیت و کاربرد روش ازدیاد برداشت نفت با استفاده از دی متیل اتر و دی اتیل اتر می‌باشد. در فصل دوم روش آزمایش و نتایج اندازه‌گیری ضریب توزیع دی اتیل اتر و تتراهیدروفوران بین فازهای آبی و نفتی بررسی گردیده و اثرهای حضور نمک در فاز آبی، غلظت اولیه حلال در فاز آبی و نوع نفت بر ضریب توزیع حلال‌های اشاره‌شده در سیستم های آب/نفت یا آب-نمک/نفت بررسی شده است. نتایج این بخش به منظور تخمین تقریبی ضریب توزیع دی‌اتیل‌اتر به عنوان یکی از داده‌های ورودی برای شبیه‌سازی و تفسیر نتایج آزمایشگاهی ازدیاد برداشت با روش آشام خودبخودی آب‌نمک و دی اتیل اتر در مخازن شکافدار (که در فصل سوم بحث شده است) مورد استفاده قرار گرفته است. آزمایش‌های آشام در محفظه آموت شیشه‌ای و در شرایط اتمسفری انجام گردیده است. در این مطالعه مغزه‌های کاملا آب‌دوست (ماسه‌سنگ) و مغزه‌های با ترشوندگی میانه (ماسه‌سنگ و دولومیت) مورد آزمایش آشام قرار گرفته و ازدیاد برداشت و سرعت تولید نفت در طول آزمایش جمع‌آوری گردیده است. سپس به منظور توسعه مدل ریاضی فرآیند، معادلات بقای جرم هر ماده شیمیایی حاضر در فرآیند با معادله دارسی و رفتار فازی ساده شده اتر-آب-نفت ترکیب و سپس مدل عددی حاصل‌شده با نرم افزار کامسول حل و نتایج برخی آزمایش های شبیه سازی گردیده است. با استفاده از نتایج این فصل، آزمایش های فصل چهارم طراحی شده است. در فصل چهارم ازدیاد برداشت نفت با استفاده از آشام خودبخودی محلول دی متیل اتر در نفت در ماسه‌سنگ نسبتا آب‌دوست و نیز سنگ‌آهک نسبتا آب‌گریز مطالعه و بررسی شده است. ابتدا سلول آزمایش آموت برای فشار حدود ده بار طراحی و ساخته شد. سپس به ترتیب آزمایش های آشام خودبخودی آب‌نمک و آشام خودبخودی محلول ده درصد مولی دی متیل اتر در آب‌نمک انجام گردیده است. در هر مرحله، میزان نفت تولیدی

نسبت به زمان و نیز نمودار تولید بر حسب زمان جمع آوری گردیده است. در آزمایش‌های آشام در سنگ‌های نسبتا آب‌دوست اثر شرایط مرزی بر آشام نیز بررسی‌شده است. در آزمایش‌های آشام در سنگ‌های نسبتا آب‌گریز (ترشوندگی میانه) نیز اثر حضور اشباع آب همزاد بررسی شده است. سپس مدل عددی استفاده شده در فصل سوم برای فرآیند آشام برای دی‌متیل‌اتر نیز گسترش داده شد و نتایج آزمایشگاهی شبیه‌سازی گردید. آزمایش‌ها و نتایج مدل‌سازی عددی انجام شده در این فصل ایده‌هایی درباره نحوه طراحی، استفاده از مواد مناسب در دستگاه آزمایشگاهی و نیز انجام مطالعات آزمایشگاهی کنترل تحرک‌پذیری فاز تزریقی در فصل پنجم به ما داد. هدف از آزمایش‌های فصل پنجم بررسی اثر سیلاب‌زنی همزمان پلیمر و دی‌متیل‌اتر در مغزه بر بهبود ازدیاد برداشت نفتِ باگرانروی میانه از مخازن غیرشکافدار می‌باشد. در این فصل ابتدا فاز آبی شامل دی متیل اتر در آب‌نمک یا محلول دی متیل اتر و پلیمر به صورت کسری از حجم محیط متخلخل تزریق گردیده و سپس توسط آب‌نمک یا محلول پلیمر در آب‌نمک جابجا گردید. در ادامه اثر استفاده از سناریوهای مختلف تزریقی بر افزایش ضریب برداشت نفت بررسی و مطالعه گردید. پایان‌نامه درانتها با ارائه چکیده نتایج در فصل ششم جمع بندی شده است.

در این پایان نامه برای نخستین بار نشان داده شد که استفاده از دی متیل اتر و دی اتیل اتر در فرآیند آشام، باعث ازدیاد برداشت نفت از مخازن شکافدار می‌گردد. همچنین برای نخستین بار پتانسیل تزریق همزمان دی متیل اتر و پلیمر به عنوان یک روش نوین آزمایشگاهی برای ازدیاد برداشت نفت از مخازن غیر شکافدار نشان داده شد. مزیت حلال‌های فوق حل شوندگی جزیی در فاز آب و انحلال کامل در فاز نفت می‌باشد. نتایج آزمایشگاهی با کمک مدل‌سازی عددی قابل تفسیر می‌باشد. مکانیسم های تولیدی شامل موارد زیر می‌باشد: ۱- افزایش حجم فاز نفتی (رقیق سازی فاز نفتی)، ۲- افزایش حجم نهایی فازها پس از انتقال حلال از فاز آبی به فاز نفتی، ۳- کاهش گرانروی فاز نفتی، و ۴- بهبود نسبت تحرک‌پذیری با استفاده از پلیمر.

محمد چهاردولی

بهمن‌ماه ۱۳۹۴ خورشیدی

دلفت ـ هلند

Nomenclature

Greek Symbols

$\omega(t)$	Time dependant ramp function
γ	Activity coefficient of MSS in the aqueous or oleic phase
μ	The ionic strength of the solution
ϕ_w	The association parameter of water
ϕ_h	The association parameter of oil
μ_α	The viscosity of phase α
ρ_α	The density of phase α
ρ_{dme}	The density of pure liquid DME
ρ_W	The density of pure brine
ρ_H	The density of pure oil
γ	Fitting parameter for the capillary pressure curve
σ	Interfacial tension
φ	Porosity of the rock
λ	Sorting factor
μ_W	The viscosity of pure brine
μ_H	The viscosity of pure oil
μ_S	The viscosity of pure solvent
θ	The contact angle

Roman Symbols

A_i	The area open to imbibition
C_a	Capillary number
c_s^o	The concentration of the solvent in the oleic phase
c_s^a	The concentration of the solvent in the aqueous phase
c_{DEE}^a	The mole fraction of DEE in the aqueous phase
ΔC	The uncertainty in the estimation of concentration

	from the refractive index measurements
D	Darcy
D_{sa}	The molecular diffusion of the solvent in the aqueous phase
D_{so}	The molecular diffusion of the solvent in the oleic phase
D_{mol}	The molecular diffusion coefficeint
g	Gravitational acceleration
I	The ionic strength
K	Absolute permeability
$k_{r\alpha}$	Relative permeability of the phase α
k_{ra}^{e}	The end-point relative permeability of the aqueous phase
k_{ro}^{e}	The end-point relative permeability of the oleic phase
k_{r}^{e}	Relative permeability at the end of solvent imbibition
k_{r}^{b}	Relative permeability at the beginning of solvent imbibition
K_s	The salting out coefficient (Setchenow coefficient)
K_{og}^{H}	Henry's constant in oil-gas system
K_{ag}^{H}	Henry's constant in water-gas system
K_{oa}^{P}	The partition coefficient between oleic and aqueous phase
K_{oa}	Partition coefficient
$\log_{10} K_{ow}^{DEE}$	The logarithm (with base 10) of partition coefficient of diethyl ether between the aqueous phase and the oleic phase
$\log_{10} K_{ow}^{THF}$	The logarithm (with base 10) of partition coefficient of tetrahydrofuran between the aqueous phase and the oleic ph
$\log_{10} K_{ob}^{DEE}$	The logarithm of the partition coefficient of diethyl ether between brine and hexadecane
$\log_{10} K_{ow}^{DEE}$	The logarithm of the partition coefficient of diethyl ether between demi-water and hexadecane
L_H	The height of the block
L_c	The characteristics length, which is defined by 4.22
L_i	The distance from A_i to the center of the matrix block
m	Molality of MSS in the aqueous or oleic phase
M_w	The molecular weight of water
M_h	The molecular weight of oil
n_{DEE}^{o}	The number of moles of DEE in the oleic phase
n_{h}^{i}	The number of moles of the oil
n_{DEE}^{i}	The initial number of moles of DEE in the aqueous phase
n_{w}^{i}	The number of mole of the make-up water
n_{a}^{i}	The number of moles of component i in the aqueous phase
Δn	The uncertainty in the measurement of refractive index by refractometer

P_α	The pressure of the phase α
P_c	Capillary pressure function
P_c^b	Capillary pressure at the beginning of solvent imbibition
P_c^e	Capillary pressure at the end of solvent imbibition
S_α	The saturation of the phase α
S_{wc}	Connate water saturation
S_{or}	Residual oil saturation
S_a	The saturation of the aqueous phase
S_e	The effective saturation of the aqueous phase
T	Temperature in Kelvin
t_{Dc}	The characteristics capillary times
t_{Dg}	The characteristics gravity times
t_{Dv}	The characteristics viscous time
t_{Dd}	The characteristics molecular diffusion time
u_α	The Darcy velocity of the phase α
$V_{\alpha c}$	The volume fraction of the component c in the phase α
V_{aw}	The volume fraction of water in the aqueous phase α
V_{as}	The volume fraction of solvent c in the aqueous phase α
V_{oh}	The volume fraction of oil c in the oleic phase α
V_{os}	The volume fraction of solvent c in the oleic phase α
V_{od}	The volume fraction of DME in the oleic phase
V_{ad}	The volume fraction of DME in the aqueous phase
V_s	Molar volume of the solvent, in cm^3/mol
V_b	The bulk volume of the matrix
$\hat{V}_{dme}$	Molar volume of DME in cm^3/mol that is defined as the volume of a mole of DME at its normal boiling point
$\partial_n f(n)$	The first order derivation of the tuned polynomial to the reference curves with respect to refractive index
x	The concentration of MSS in the oleic phase
Δx	The uncertainty in the concentration of MSS in the oleic phase
y	The concentration of MSS in the aqueous phase
Δy	The uncertainty in the concentration of MSS in the aqueous phase
z_i	Valency of ion
z	The upward vertical distance from the bottom of the core

Abbreviations

ABO	All boundaries open to imbibition
BC	Boundary conditions
BEO	Bottom end open to imbibition
$BRCW$	Water-wet Berea sandstone saturated with crude oil
$BRHW$	Water-wet Berea sandstone saturated with hexadecane
$BROW$	Water-wet Berea sandstone saturated with Ondina 033
BRS	Berea sandstone
$BRSM$	Mixed-wet Berea sandstone
$BTCW$	Water-wet Bentheimer sandstone saturated with crude oil
$BTHW$	Water-wet Bentheimer sandstone saturated with hexadecane
$BTOW$	Water-wet Bentheimer sandstone saturated with Ondina 933
BTS	Bentheimer sandstone
$C16$	Hexadecane
COA	Crude oil A
COB	Crude oil B
CW	Carbonated water
DEE	Diethyl ether
DME	Dimethyl ether
$DMEB$	DME/brine
$DMEP$	DME/polymer
EOR	Enhanced oil recovery
EOS	Equation of state
GWP	Global warming potential
$HPAM$	Hydrolyzed polyacrylamide
IC	Initial conditions
IFT	interfacial tension
IPA	Isopropyl alcohol
MW	Mixed-wet
NB	Bond number
$O19$	Ondina 919
$O33$	Ondina 933
$OIIP$	Oil Initially In-Place
PV	Pore volume
RI	Refractive index
RF	Recovery factor
$RFCW$	Water-wet Red Felser sandstone saturated with crude oil
$RFHW$	Water-wet Red Felser sandstone saturated with hexadecane
$RFOW$	Water-wet Red Felser sandstone saturated with Ondina 933
RFS	Red Felser sandstone
ROS	Residual oil saturation
$SLDM$	Mixed-wet Silurian dolomite

SPE	Society of Petroleum Engineers
TEO	Top end open to imbibition
$TEsO$	Two ends open to imbibition
THF	Tetrahydrofuran
UR	Ultimate recovery
WW	Water-wet

Subscripts

a	Aqueous phase
b	Bulk
h	Hydrocarbon component
o	Oleic phase
s	Solvent component
w	Water component
α	Phase α

List of Figures

List of Tables

Acknowledgments

In the Name of Allah the Merciful the Clement. "Praise belongs to Allah, who chose for us the good qualities of creation, granted us the agreeable things of provision, and appointed for us excellence through domination over all creation" (As-Sahifa Al-Sajjadiyya, Dua 1). Then to Him belongs praise, in place of His every favour upon me, praise equal to the praise of His close angels, and His prophets.
I would like to express my appreciation to all those who have contributed directly or indirectly to the accomplishment of this research work.
I would like, first, to express my sincere gratitude to my promoter, Professor Hans Bruining for his excellent guidance and encouragements. Hans, I have enormously benefited from your invaluable scientific support, advice and continuous encouragement. I am always inspired by your perseverance, not giving up, and by your dedication. My genuine gratitude goes to my co-promoter Dr. Rouhi Farajzadeh for his guidance, advice and initiating me into the world of the mutually soluble solvents. Rouhi, you brought the idea of the use of dimethyl ether for oil recovery to the TU Delft, thank you for all things I learned about solvents. Many thanks for all the time Hans and you took and all the discussions we had.
Besides my promoter and co-promoter, I am extremely grateful to reading committee members: Prof. Krastev, Prof. Rossen, Prof. Zitha, Prof. Slob, Dr. Boersma and Dr. Mahani, thank you for all your efforts.
I gratefully acknowledge the Iran Ministry of Science, Research and Technology and the National Iranian Oil Company (NIOC) for awarding me the PhD scholarship. I also acknowledge Shell Global Solutions International for sponsoring part of my PhD research. I am thankful to Hassan Mahani and Niels Brussee for preparing the mixed-wet core samples. I wish to appreciate Shehadeh Masalmeh and Cor van Kruijsdijk for their valuable comments on chapter 4 of this thesis. I am also grateful to Paul te Riele and John van Wunnik for valuable comments on chapter 5 of this thesis. I also thank Alexander Chernetsky and Efraim Keijzer for their technical advice and support for the DME experiments. I would also like to thank

the MSc students that I supervised during my PhD study; Almagul Zholdybayeva, for the great work we did together, which enriched chapter 3 of this thesis and Annas Hassan, for his contribution to chapter 2 of this thesis.
During my PhD, I also had a great opportunity to work as a visiting researcher in the bioorganic chemistry and analytics department at the Natural and Medical Sciences Institute (NMI) at the University of Tbingen, Germany. I would like to thank Prof. Krastev for inviting me as well as for the many fruitful discussions we had together and for his support during my stay in Germany. I would like to thank Markus Herma and Elsa Arefaine for their technical support. Ingrid has helped me to have a pleasant time in the lab, "gracias" Ingrid. My dear friend Kia has helped me to have a nice time far from my home and family, thank you so much Kia. I would like to thank the other friends, who supported me in NMI, who are not mentioned here.
The experimental part of this thesis would not have been possible without the professional assistance and support of the technicians at the Dietz Laboratory at the TU Delft. I would like to thank Henk van Asten and Michiel Slob for their support in the development of the experimental set-ups and for their assistance with the experiments. My appreciation also goes to the technical support of Dirk, Gerard, Ellen, Jolanda, Marck, Karel, Paul, Wim, Joost, and Jan. A special thank goes to the support staff of the Geoscience and Engineering department, Anke, Hannie, Ralf, Marlijn, Lydia, Margot, Claudia and especially Marja. Marja, all of us missed you; I hope you recover very soon, "beterschap!" I would also like to thank Mariette van Tilburg for reading this thesis very carefully. I am thankful to Theda Olsder and staff of the International Office for the arrangement of visa and accommodation.
In addition, I had the enriching opportunity to work within a large group of colleagues and fellow PhD's in the department of Geoscience and Engineering. In particular, I wish to thank Seyyed Mojtaba Hosseini Nasab, Ehsan Eftekhari, Elham Ashoori, Amin Ameri, Rouzbeh Khosrokhavar, Negar Khoshnevis, Huajan Fan, Narjes Shojaei Kaveh, Siavash Kahrobaei, Anna Peksa, Amin Fatemi, Faisal Al Saadi, Nikita Lenchenkov, Eduardo Dias de Barros, Bander Alquaimi, Shirishkumar Baviskar, Jiakun Gong, Matteo Cusini, Ahmed Hussain, Durgesh Kawale, Christian Kosack, Jakolien van der Meer, Rafael Morae, Rodrigo Salazar, Swej Shah, Jinyu Tang, Guanqun Yu, Matei Tene, Rahul Fonseka, Sin Jones, Leon Kapetas, Alex Kirichek and Sohei Minato. My special thanks go to Seyyed Mojtaba Hosseini Nasab for the so many fruitful discussions that we have had together. I deeply appreciate Mohammad Simjoo for his strong support and for the many good times that we spent together.
I wish to thank all my dear neighbours at the fourth floor of the Civil Engineering faculty, especially Rahul Thorat and Ralph Feld for the great working atmosphere that we have had. I would also like to express my gratitude to my Iranian friends; without their support my life in the Netherlands would have been quite difficult.

I would like to thank all Iranian friends who have organized so many wonderful gatherings and fun activities, Jalase Quran (reciting the Holly Quran every Friday evening), Hey'at-e Mohebban Al-Mahdi (religious gatherings) and Kolbeye Andishe (knowledge sharing). I am afraid I cannot mention them one by one here. Among many, I would like to especially thank the families Mehrara, Derakshani, Alemi, Najafi, Latifi, Shahbazi, Madadi, Bornaee, Bakhshandeh, Mirzaei, Boroomandzadeh, Ahmadimehr, Ghaeminia, Abbasi, Tohidian, Kavian, Fasihi, Saeedi, Rahimi, Hesan, Ghafarian, Tunk, Lotfi, Mohammadi, Mianabadi, Abouhamzeh, Ahmadi, Yazadanpanah and Behdani: Thank you all! I would also like to express my appreciation to Mohammad Azim, Shahab, Seyyed Ahmad Reza, Mohammad Bashir, Hamed, Alireza, Mohammad Mahdi, Amin, Nader, Mohammad Reza and Morteza for good times and friendly conversations, with my apologies for all others who I have forgotten to mention.

I am indebted to my former teachers at primary school, secondary school, Petroleum University of Technology and Sahand University of Technology for their support and encouragement during my educational life. I wish to thank them all.

During my PhD studies, my newborn nephews (Mobin and Matin), my uncle (Daei Rajab), my cousin (Akbar), and my friend (Hassan) have passed away. I miss you! My God bless your soul.

Most importantly, I express my deepest appreciation to my family. I am extremely grateful of my wonderful parents for their unconditional love and kindness, long-life support and their patience in these years. In fact, it is beyond my ability to compensate even a small part of your support. You are the best parents anybody can ever imagine, I am really proud of you. My special and loving gratitude goes to my brothers and my sisters. You are the best brothers and sisters in the world. Thank you so much for your support, love, kindness and encouragements. I am sure that I would not have gotten here without you and I have missed you a lot when I moved to the Netherlands. I also want to thank my parents in-law, brothers- and sisters in-law for their love always backing me. Last, but certainly not least, comes my lovely wife and my beloved daughter. My dear and lovely wife, you are my inspiration and, of course, my best friend. I would like to express the deepest gratitude to you for your everlasting love, infinite support, encouragement and motivation. I really appreciate your understanding and patience during the hard times of the Ph.D studies, especially the last year of my Ph.D. I am very grateful to my beloved baby daughter, Zahra Jan. You are the source of inspiration and motivation to us. Zahra Jan, thank you for teaching us the way of exploring a new world.

Mohammad Chahardowli
Delft, March 2016

Scientific publications

Journal papers

1. **M. Chahardowli**, R. Farajzadeh, and J. Bruining "Experimental Investigation of the Use of the Dimethyl Ether/Polymer Hybrid as a Novel Enhanced Oil Recovery Method", accepted for publication in Journal of Industrial and Engineering Chemistry, doi:10.1016/j.jiec.2016.04.008.

2. **M. Chahardowli**, R. Farajzadeh, S. Masalmeh, and J. Bruining "Dimethyl Ether Technology for Oil Recovery: Mechanisms of Oil Recovery by DME/Brine Spontaneous Imbibition from Water-Wet and Mixed-Wet Rocks", will be submitted to Energy Fuels.

3. **M. Chahardowli**, A. Zholdybayeva, R. Farajzadeh, and J. Bruining "Numerical and Experimental Evaluation of Diethyl Ether-Enhanced Spontaneous Imbibition in Water-Wet and Mixed-Wet Rocks", will be submitted to Journal of Industrial Engineering Chemistry Research.

4. **M. Chahardowli**, R. Farajzadeh, R. Krastev, and J. Bruining "Measurement of partition coefficient of diethyl ether and tetrahydrofuran in oil / water + NaCl systems", will be submitted to Journal of Colloid and Interface Science.

Journal papers in preparation

1. "Numerical Simulation of Hybrid DME/Polymer for Enhancing Oil Recovery", in preparation for the Journal of Fuel.

2. "The Effect of Polymer on the Partition Coefficient of Diethyl Ether and Tetrahydrofuran in Oil / Water + Polymer + NaCl Systems", in preparation for the Journal of Colloid and Interface Science.

3. "Numerical Simulation of Non-Equilibrium Effects in Imbibition of Surfactant Solutions", in preparation for Journal of Petroleum Science and Engineering.

Conference papers

1. **M. Chahardowli**, R. Farajzadeh, S. Masalmeh, and J. Bruining "A Novel Enhanced Oil Recovery Technology in Fractured Reservoirs: Spontaneous Imbibition of Dimethyl Ether/Brine in Water-Wet Sandstone and Mixed-Wet Limestone Rocks", SPE-181340, accepted at the SPE Annual Technical Conference and Exhibition to be held 26 - 28 September 2016 in Dubai, U.A.E., doi:10.2118/179850-MS.

2. **M. Chahardowli**, R. Farajzadeh, and J. Bruining " Experimental investigation of Dimethyl Ether/Polymer Hybrid as an Enhanced Oil Recovery Method", SPE-179850, SPE EOR Conference at Oil and Gas West Asia, 21-23 March, Muscat, Oman 2016.

3. S.M. Hosseini Nasab, **M. Chahardowli**, and P. Zitha, "Simplified Numerical Model for simulation of Surfactant/Polymer (SP) Flooding Process for Enhanced Oil Recovery", accepted at the 78th EAGE Conference Exhibition 2016, to be held 30 May-2 June 2016, Vienna, Austria.

4. **M. Chahardowli**, R. Farajzadeh, and J. Bruining "Numerical Simulation of Mutually Soluble Solvent-Aided Spontaneous Imbibition in Fractured Reservoirs", 14th European Conference on the Mathematics of Oil Recovery, ECMOR XIV, 8th-11th September 2014, Catania, Sicily, Italy, doi:10.3997/2214-4609.20141854.

5. **M. Chahardowli**, and J. Bruining "Modeling of Wettability Alteration during Spontaneous Imbibition of Mutually Soluble Solvents in Mixed-Wet Fractured Reservoirs", COMSOL Multiphysics Conference, September 17 - 19th 2014, Churchill College, Cambridge, UK.

6. **M. Chahardowli**, R. Farajzadeh, and R. Krastev "Measurement of Partition Coefficient of a Mutually Soluble Solvent between Oil and Mixture of Polymer + Salt + Water", in the Booklet of the International Colloid and Surface Science Symposium, UK Colloids 2014, p. 225, abstract no. P12, 6 - 9th July 2014, London, United Kingdom.

7. **M. Chahardowli**, and J. Bruining "Modelling of Non-equilibrium Effects in the Solvent-Enhanced Spontaneous Imbibition in Fractured Reservoirs", COMSOL Multiphysics Conference, 23 - 25th October 2013, Rotterdam, The Netherlands.

8. **M. Chahardowli**, A. Zholdybayeva, R. Farajzadeh, and J. Bruining "Solvent Enhanced Spontaneous Imbibition in Fractured Reservoirs", SPE 164908, 13th EuroPEC Conference and Exhibition, 10-13th June 2013, London, UK, doi:10.2118/164908-MS.

9. **M. Chahardowli**, and J. Bruining "Modelling of Non-equilibrium Effects in the Gravity Driven Countercurrent Imbibition", COMSOL Multiphysics Conference, 11-13th October 2012, Milan, Italy.

About the Author

Mohammad Chahardowli was born in Malayer, Iran. He obtained his B.Sc. degree from Petroleum University of Technology (Iran) in 2003 and his M.Sc. degree (with honour) from Sahand University of Technology (Iran) in 2007, both in reservoir engineering, before enrolling at Delft University of Technology in the winter of 2010. He worked as a reservoir engineer at NISOC, Iran, from 2004 to 2005, and as an academic staff at Sahand University of Technology (Iran) from 2008 to 2010. He accomplished his Ph.D in the spring of 2016. During his Ph.D, he worked on experimental work and numerical modeling of enhanced oil recovery from conventional and fractured reservoirs by the use of mutually soluble solvents. The most interesting results of this research are described in this thesis. Currently, he is a member of the Department of Chemical Engineering at Sahand University of Technology, Iran.

Contact information:
Petroleum Engineering Faculty
Sahand University of Technology
P.O. Box: 51335-1996
Sahand New Town, Tabriz, Iran
Phone: +98 412 3459152
Fax: +98 412 3444355
Email: chahardowli@sut.ac.ir